Analysis of ultimate capacity of the structural elements of single hull VLCC subject to corrosion

Rachid DAMI

Master Thesis
Presented in partial fulfillment
of the requirements for the double degree:
“Advanced Master in Naval Architecture” conferred by University of Liege
"Master of Sciences in Applied Mechanics, specialization in Hydrodynamics, Energetic and Propulsion” conferred by Ecole Centrale de Nantes

developed at West Pomeranian University of Technology, Szczecin
in the framework of the

“EMSHIP”
Erasmus Mundus Master Course
in “Integrated Advanced Ship Design”

Ref. 159652-1-2009-1-BE-ERA MUNDUS-EMMC

Supervisor: Dr.Maciej Taczala, West Pomeranian University of Technology, Szczecin

Reviewer: Dr.Eng. Patrick Kaeding, University Rostock

Szczecin, February 2012

ABSTRACT

During the last few decades, the emphasis in structural design has been moving from the allowable stress design to the limit state design, because the latter approach has many more advantages. A limit state is formally defined as a condition for which a particular structural member or an entire structure fails to perform the function that it has been designed for.

In order to ensure critical for economy and safe design of a ship's hull, it is necessary to accurately evaluate the capacity of the hull girder considering extreme loads.

The objective of this project is to perform the strength analysis for tank structures, according to the Det Norske Veritas (DNV) Rules and Regulations; following the IACS Common Structural Rules (CSR).

The general plan and methodology of the project are presented in the report (dissertation). The project is focused on the analysis of the structural strength of the hull and the ultimate capacity of structural elements and the hull girder of the single hull VLCC, taking into account the influence of the uniform and atmospheric corrosion.

Based on the model that describes the phenomenon of the corrosion, a model (2) (see Chapter 4) has been introduced. This model is based on the approach which was taken from (Shengping Qin and Weicheng, 2002); it was used to develop a methodology to predict reduction of thickness of structural elements due to corrosion. The results obtained using the prediction methods were verified against the experimental results.

The effect of the corrosion on the section modulus and the variation of the section area of the cargo deck were investigated, as a function of the time and the exponential depth of the corrosion. It was to get the relationship between weight and the ratio of the section modulus during 25 years the service of the tanker.

The results of the calculations as a comparison between different models which determine the ultimate stress for the plate and rigid panels, including the results received using the PULS software (the theory of nonlinear plate) are presented in the dissertation. Based on the study of the parameters influencing the reduction in ultimate capacity of the plate, the effect of the corrosion on the reduction of the ultimate capacity was investigated for various regions of the tanker (bottom, deck, side, and longitudinal bulkhead).

The analysis of the progressive collapse of the hull girder, based on the computation for the two candidate models, the Rahman code and the results of the Nauticus Hull (using the procedure of CSR) was carried out to evaluate the ultimate bending moment after 25 years of

service. At the end of the work, the results of finite elements (using engineering software), the methodology to create the model, the mesh, the boundary conditions and loading conditions will all be presented and discussed. The results show the maximum displacement of three tankers and the distribution of the von Mises stresses in the critical area, during 25 years of ship service; due to the global loading conditions (full load in sagging condition).The dissertation is completed with conclusions from the analyses and recommendations.

RESUME

L'objectif de ce projet c'est de faire une analyse de résistance de la structure de tanker, selon la norme et les règles de classification DNV ainsi que CSR.

A cet effet ce rapport montre le plan général à suivre pour étudier le projet ainsi la méthodologie et les étapes à suivre pour finaliser l'étude de la résistance de la structure en prennent en considération l'effet de la corrosion générale (la corrosion atmosphérique uniforme).

En se basant sur le model qui décrit le phénomène de la corrosion, on introduit un nouveau model (model(2) voir chapitre 4) basant sur l'approche de (Shengping Qin and Weicheng, 2002); pour trouver une bonne prédiction entre les résultats expérimental et celle de nouveau model.

A cet effet on regarde l'effet de la corrosion sur le module de section ainsi la variation de la section du pont en fonction du temps et de la variation exponentiel de la corrosion.

La détermination de la variation de module de section du pont permettra de déduire la variation du poids du pont.

Ce rapport discutera une comparaison entre différente model qui détermine la contrainte ultime pour la plaque et les panneaux rigide ,avec les résultats soustraite de logiciel PULS (la théorie de non linéaire plaque) .en effet basant sur l'étude des paramètres qui influencent sur la réduction de ultime capacité de plaque et l'effet de la corrosion général on définie les raisons de l'écart de réduction de ultime contraintes de différente zone géométrique de Tanker (le pont, les murailles).

L'analyse de l'effondrement progressif de la poutre-coque se base a compare le programme de Rahman et celle de Nauticus Hull (utilisant la procédure de CSR), a la fin de déterminer l'évolution de l'axe neutre ainsi de ultime moment après 25 ans de service.

A la fin du travail, on présent les résultats des éléments finie (utilisant Génie software), la méthodologie de création de modèle, de maillage, les conditions aux limite ainsi les conditions de chargement .Ces résultats montrent le maximum déplacement de trois tanker et la distribution du contraintes de von Mises après 25 ans de service pour une condition de globale chargement.

Le rapport est complété par les conclusions des analyses et des recommandations.

CONTENTS

LIST OF FIGURES

LIST OF TABLES

NOMENCLATURE

a	Length of stiffened plate between two adjacent transverse frames
b	Breadth of plating, spacing between adjacent longitudinal stiffeners
B	Breadth of the stiffened panel, spacing between two adjacent longitudinal girders
t	Thickness of plating
b_e	Effective width of the plating corresponding to breadth b
I_y	Moment of inertia with respect to horizontal neutral axis
RSM	Ratio the section modulus
RSA	Ratio the section area
β	Reduced slenderness ratio of the plating
λ	Slenderness ratio of stiffener with attached effective plating
E	Young's modulus
υ	Poisson's ratio
σ_Y	Yield stress
σ_{oeq}	Equivalent yield stress of the entire stiffened panel
A_o	initial deflection of the plate
C_o	Sideway initial deflection amplitude of stiffener
B_o	The maximum amplitude Out from plane of stiffener
W_{po}	Initial deflection of plating
W_{os}	The initial deflection of the stiffeners
υ_{0s}	The initial deflection of the stiffeners
P	Lateral pressure on panel
σ_x	Stress in x-direction (longitudinal stress)
σ_y	Stress in y-direction (transverse stress)
Φ	Curvature
σ_U	Ultimate compressive stress of stiffened panel
M_P	Plastic collapse moment for hull girder under vertical bending
M_S	Characteristic still water bending moment based on actual cargo and ballast conditions
M_W	Characteristic wave bending moment based on an annual probability of exceedance of $10^{-2.}$

M_U	Characteristic bending moment resistance of the hull girder
γ_S	Load factor for still water loads (permanent + variable functional loads)
γ_W	Environmental load factor
γ_m	Safety factor material
Q_S	Characteristic still water shear force based on actual cargo and ballast conditions
Q_W	Characteristic wave shear force based on an annual probability of exceedance of 10^{-2}
Q_U	Characteristic shear resistance of the hull girder
σ_v	Nominal vertical hull girder bending stress
σ_h	Nominal horizontal hull girder bending stress
σ_t	Nominal torsion stress in hull girder
σ_a	Nominal axial stresses due to hull girder end pressure
σ_{ve}	Nominal vertical hull girder bending stress due to end pressure
σ_2	Nominal secondary bending stress in double bottom or double side
σ_{v2}	Nominal secondary vertical hull girder bending stress due to lateral pressure on transverse bulkheads
σ_{a2}	Nominal secondary axial stress due to lateral pressure on transverse bulkheads
Z	Section modulus at the considered transverse section (i)
F_{as}	Characteristic still water axial force due to hull end pressure
F_{aw}	Characteristic wave axial force based on an annual probability of exceedance of 10^{-2}(100 years)
SA_i	section area based on gross thickness at the considered transverse section (i)
τ_{global}	Total nominal design shear stress from global shear force
τ_{local}	Total nominal design shear stress from local effects
Q_S	Characteristic design still water shear force based on actual cargo and ballast conditions
Q_W	Characteristic wave shear force based on an annual probability of exceedance of 10^2 (100 years)
A_B	Total sectional area of outer bottom
A'_B	Total sectional area of inner bottom
A_D	Total sectional area of deck

A_S	Half sectional area of all sides (including longitudinal bulkheads and inner sides)
D	Hull depth
D_B	Height of double bottom
g	Neutral axis position above the baseline in sagging condition or bellow the deck in hogging condition
H	Depth of hull section in linear elastic state
M_{US}, M_{UH}	Ultimate bending moment in sagging or hogging condition, respectively
$\sigma_{YB}, \sigma'_{YB}$	Yield stress of outer bottom or inner bottom, respectively
$\sigma_{YD}, \sigma'_{YD}$	Yield stress of deck side, respectively
$\sigma_{UD}, \sigma'_{UD}$	Ultimate buckling stress of deck or side shell, respectively
$\sigma_{UB}, \sigma'_{UB}$	Ultimate buckling stress of outer bottom or inner bottom, respectively
Ψ_U	Ratio of the ultimate stress

Declaration of Authorship

I declare that this thesis and the work presented in it are my own and have been generated by me as the result of my own original research.

Where I have consulted the published work of others, this is always clearly attributed.

Where I have quoted from the work of others, the source is always given. With the exception of such quotations, this thesis is entirely my own work.

I have acknowledged all main sources of help.

Where the thesis is based on work done by myself jointly with others, I have made clear exactly what was done by others and what I have contributed myself.

This thesis contains no material that has been submitted previously, in whole or in part, for the award of any other academic degree or diploma.

I cede copyright of the thesis in favor of the West Pomeranian University of Technology in Szczecin.

Date: 15 of January of 2012 Signature: 

1. INTRODUCTION

1.1 Background

During the last few decades, the emphasis in structural design has been moving from the allowable stress design to the limit state design, because the latter approach has many more advantages. A limit state is formally defined as a condition for which a particular structural member or an entire structure fails to perform the function that it has been designed for.

Four types of limit states are considered, namely:

• Serviceability limit state (SLS): conventionally represents failures under normal operations due to deterioration of less vital functions such as, local damage, unacceptable deformations and excessive vibration.

• Ultimate limit state (ULS): also referred to as ultimate strength, represents the collapse of the structure due to the loss of structural stiffness and strength

• Fatigue limit state (FLS): Represents fatigue crack occurrence in structural details due to stress concentration and crack damage accumulation under the action of repeated loading.

• Accidental limit state (ALS): Represents excessive structural damage as consequence of accidents, e.g., collisions, grounding, explosion and fire, which affect the safety of the structure and the environment.

The structural design criteria against the ULS are based on plastic collapse. The design of many types of structures including merchant ships has in the past tended to rely on estimates of the strength and buckling of components. In order to ensure critical for economy and safe design of a ship's hull, it is necessary to accurately evaluate the capacity of the hull girder considering extreme loads.

There are four methods used to analyze the progressive collapse of hull girder. Those methods are: the conventional nonlinear finite element method (NFEM), the idealized structural unit method (ISUM), the plastic node method, and the simplified method (SM).

Among these four methods, the simplified method based on the Smith algorithm of the hull cross-section has proved its simplicity and efficiency.

The safety condition the ship hull structure is to applied loads smaller than the design loads, in fact to avoid the damage or buckling collapse of the structure. Wherever knowing the loads applied in the hull girder we can may the scantling of midsection of the ship. Therefore the structure is checked employing the DNV Rules and Common Structural Rules.

The structure members of the hull will buckle in compression and yield in tension, and the most highly compressed member will collapse first and the stiffness of the overall hull decrease gradually (JEOM K.Paik and Alaa, E.Mansour, 1995).

Finally when the structural safety of a ship's is considered, the ultimate overall hull strength should be evaluated. By considering the life service of the ship we include the effect of the corrosion (general or atmospheric corrosion), such as this phenomena can be produce many cracks, and destroy the structure, for that reason the model to check the speed the corrosion during the year's service describing.

1.2 Objectives

The overall objective of this present thesis is to analyze and evaluate the gap of the reduction the ultimate strength of Tanker vessel hull girder (single hull VLCC), subject to the general corrosion. This will help the designer to decide the true ultimate strength that the hull girder can withstand. According to this ultimate strength, the designer will be able to set a reasonable safety factor.

In achieving the main objective is to follow many points to estimated the gap the reduction of the ultimate capacity of the Tanker ship, according to the DNV rules, and selected the candidates models to assess the ULS, to made computation to compare and to verify the accuracy of the results, between the candidate model and as with getting by software DNV and the CSR, since to get the optimum margin error.

In the beginning, the procedure is to build the single hull VLCC tanker in the Nauticus hull software, to check the scantlings, and to make the analysis of the ultimate strength of the ship. Following the verification of the post buckling and ULS capacity based to the non-linear plate theory (using PULS software).

According to the data received, the aim is to discuss various parameters influencing the ultimate capacity of plates, considering effect of the stiffeners spacing, plate slenderness, imperfections, and the lateral pressure.

Considering the influence of these parameters helps us to understand and to interpret the efficiency of scantling, when the strength of the ship becomes lower.

Second subject including effect of the corrosion, we develop different models of the corrosion with assumption data, and we try to develop the new model adapted with experimental data, to get good prediction.

Regarding to model (2) developed (see Chapter 4), we defined the reduction gap of the section modulus and the section area of the ship tanker, to obtain good relationship between weight versus ratio of the section modulus.

Finally, we discuss the progressive collapse of the hull girder, by comparing the candidate models with the results received by the DNV software and CSR rules, to define the gap of the reduction of the ultimate vertical bending moment, subject to the effect of the corrosion, in the present thesis the period of the ship service considered is 25 years.

1.3 Outline of the Thesis

This thesis is organized as follows:

Chapter two gives brief introduction of the methodology and the rules to assess the ULS of the tanker ship.

Chapter three illustrates various parameters influencing the reduce of the ultimate strength of plates, considering the boundary condition, the stiffeners spacing, the plate slenderness, the imperfection, and lateral pressure.

Chapter four discusses a new model for evaluating the evolution of the depth of the general corrosion (atmospheric corrosion) versus time.

Comparing a model (2) (see Chapter 4) with the existing models, and the assumed data to defined the gap of the reduction of the ratio of the section modulus and section area of the

cargo deck after 25 years in service. The relationship between weight and the ratio of the section modulus of the cargo deck is also derived.

Chapter five illustrates the application case: ultimate strength of the single hull VLCC tanker.

Discussing the reduction of the ULS of the tanker ship after 25 years services comparing the results obtained by the candidate’s models and CSR , and we present interesting results reached by finite element method, to define the maximum displacement, and the distribution of the von Mises stress in the hull girder in the sagging condition.

2. DNV RULES AND COMMON STRUCTURAL RULES TO CHECK THE ULS CAPACITY OF THE TANKER SHIP

2.1. DNV Rules to Design Loading of Offshore Ships

The ultimate limit state assessment comprises yield and buckling capacity checks of the structure according to the LRFD format as described in DNV-OS-C101 - Design of Steel Structure. Ultimate hydrodynamic loads from the hydrodynamic analysis are to be combined with static loads in the yield and buckling checks. All relevant load conditions should be examined to ensure that all dimensioning loads are correctly included (Recommended Practice DNV-RP-C102, 2002).

Following the Principe of the DNV Rules to assess the hull girder (typical cargo); is to evaluate the capacity of the hull governed by buckling and yield capacity of the bottom and deck.

To verify the hull girder capacity strength is to check the hull girder bending capacity (Eq.2.1) and the hull girder shear capacity (Eq.2.2).

$$\gamma_s M_s + \gamma_W M_W \leq \frac{M_U}{\gamma_m} \quad (2.1)$$

$$\gamma_s Q_s + \gamma_W Q_W \leq \frac{Q_U}{\gamma_m} \quad (2.2)$$

where:

M_s: Characteristic still water bending moment based on actual cargo and ballast conditions.

M_W: Characteristic wave bending moment based on an annual probability of exceedance of 10^{-2}.

M_U: Characteristic bending moment resistance of the hull girder.

γ_S: Load factor for still water loads (permanent + variable functional loads).

γ_W: Environmental load factor.

γ_m: Material factor.

Q_S: Characteristic still water shear force based on actual cargo and ballast conditions.

Q_W: Characteristic wave shear force based on an annual probability of exceedance of 10^{-2}.

Q_U: Characteristic shear resistance of the hull girder.

To define the hull girder ULS, we check the design moment and shear forces, using the partial load factors given in Table 2.1:

Table2.1 Partial coefficient for the Ultimate Limit State

Load combination	Load category	
	still water loads	**Environnemental loads**
(1)	**1.2**	**0.7**
(2)	**1**	**1.15**

It should be noted that the use of partial load factor 1.2, for combination (1) assumes that the permanent loads can be determined with high accuracy like tank loads with known geometry.

2.2 .Governing Ultimate Limit State Combination

Following the DNV Rules to assess the ultimate strength of the hull girder, we use the partial coefficient for ULS, and we defined the still water moments for unrestricted operations are:

$$M_S = -0.065\, C_W\, L^2 B\, (C_B + 0.7)\, (kNm)\ in\ sagging \quad (2.3)$$

$$M_S = C_W L^2\, B\, (0.1225 - 0.015\, C_B)\, (kNm)\ in\ hogging \quad (2.4)$$

Where:

$C_{WU} = C_W$ for unrestricted service

$=0.0792$ L for L ≤ 100

$=10.75 - [(300 - L) / 100]^{3/2}$ for $100 < L < 300$

$=10.75$ for $300 \leq L \leq 350$

$=10.75 - [(L - 350) / 150]^{3/2}$ for $350 < L$

The Rule wave bending moments for seagoing conditions are:

$$M_{WS} = -0.11\, C_W\, L^2\, B\, (C_B + 0.7)\, (kNm)\ in\ sagging \quad (2.5)$$

$$M_{WH} = 0.19\, C_W\, L^2\, B\, C_B\, (kNm)\ in\ hogging \quad (2.6)$$

By dividing the $\frac{M_{WS}}{MS}$, we get the ratio between the bending moment in sagging and as the still water; the same for the bending moment in hogging.

The values of the both of the ratio are:

$$\frac{M_{WS}}{MS} = 1.69 \text{ in sagging (2.7)}$$

$$\frac{M_{WH}}{MS} = 1.57 \text{ in hogging (2.8)}$$

Hence, by design of wave, we defined the response the ship and the amplitude of wave, to get the different forces impact in the hull or in the platform.

Wherever, discussing the cases of loading, the internal and external forces are acting in the hull; we made three levels of assessment of the structural capacity.

2.2.1. The First Level: Ultimate Bending Moment, M_U of the Global Structure

By following the moment –curvature curve ($M - \phi$) as shown in Fig.2.1;we made analyzes of the strength of the ship , if the deck is in compression the maximum stress is ultimate stress, in fact in the bottom we verify the yielding stress because the bottom is in tensile (Philippe Rigo and Enriso Rizzuto, 2003)..

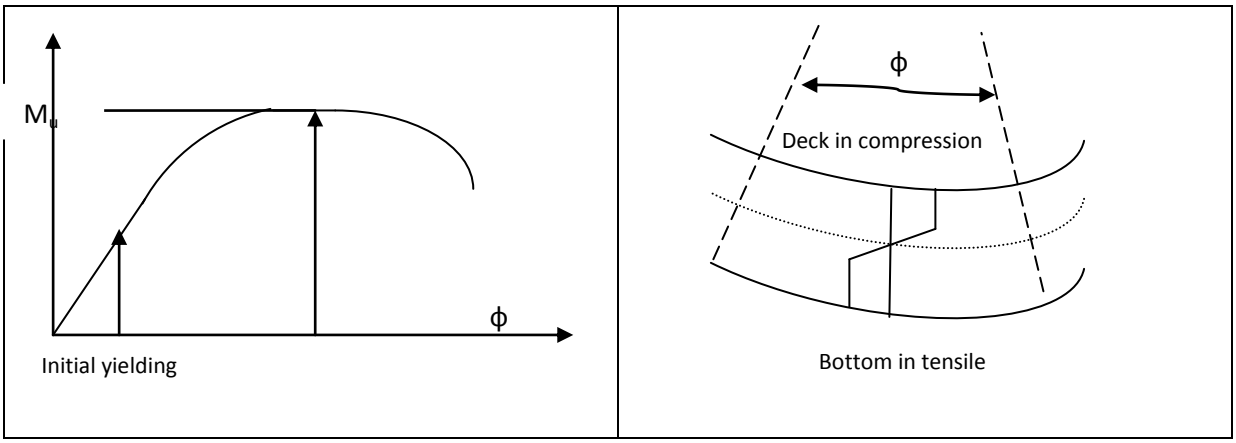

Figure.2.1. The moment –curvature curve ($M - \phi$), (Philippe Rigo and Enriso Rizzuto, 2003).

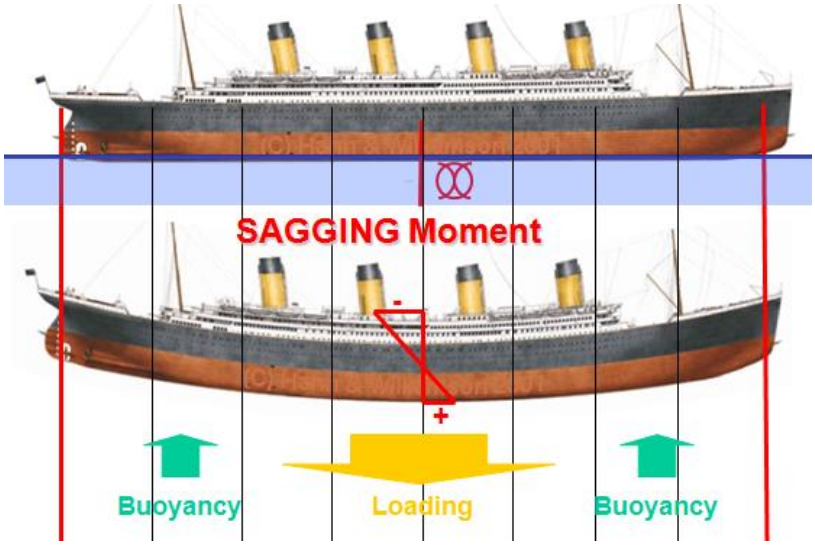

Figure.2.2. The sagging loading.

By considering the first level; the ship is a beam theory, to assess the primary response.

In the case of still water and sagging loading the ship will be bend (cf. Fig.2.2), create the negative bending moment and the ship react follow, the deck will be in compression in this case we care about buckling, even tripping and the limit of strength is ultimate stress .In the other way the bottom is in tensile the yielding stress limit is checking.

In hogging, the deck is in tensile and the bottom is in compression (cf. Fig.2.3).

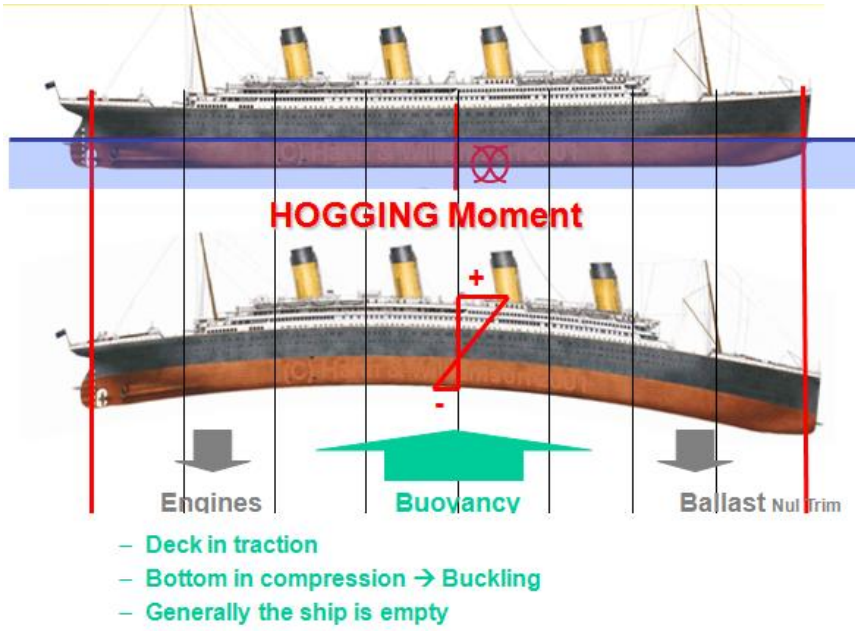

Figure.2.3. The hogging loading.

The methodology is to assess at different various loading the shear forces, induced by bending, the torsion induced by diagonally swell (cf. Table 2.2).

Table.2.2 .The shear forces and torsion level ship beam ship

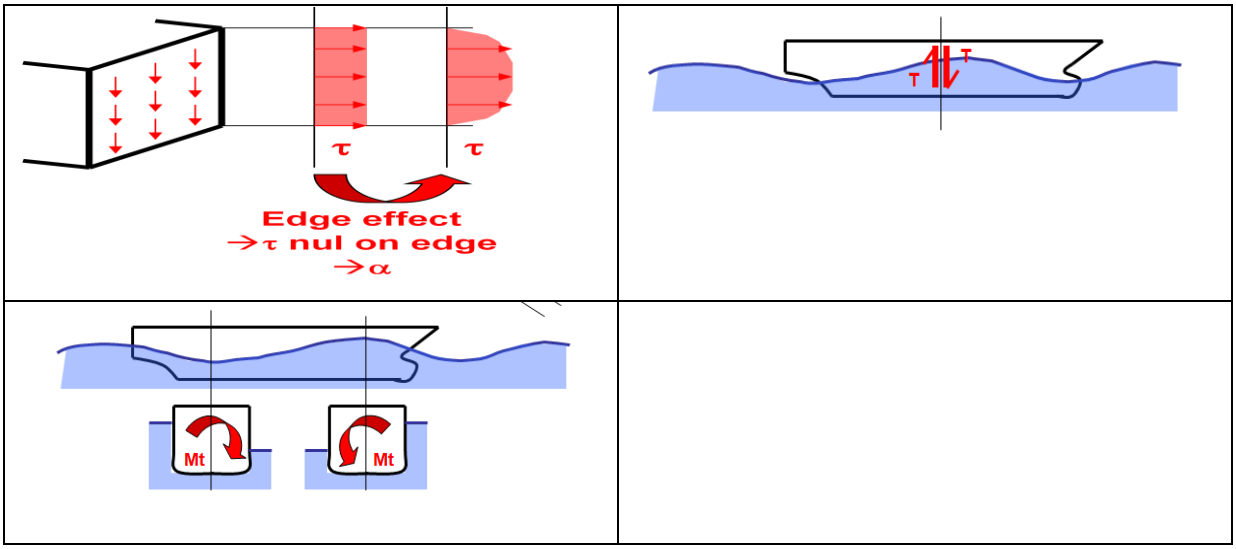

Finally, we evaluated the first response considering the global structure cargo hold/tank compartment (structure between two bulkheads).

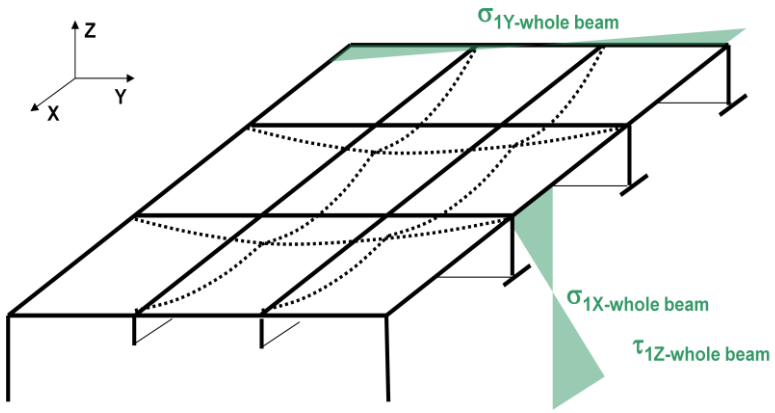

Figure.2.4. The first response considering ship as beam.

2.2.2. The Second Level: Ultimate Strength of Compressed Orthotropic Stiffened Panel (σ_U)

In the second level, the ultimate stresses follow the formula:

$$\sigma_U = \min[\sigma_u(modei)]$$

where *i*=1 to 6, and the 6 considered failure modes.

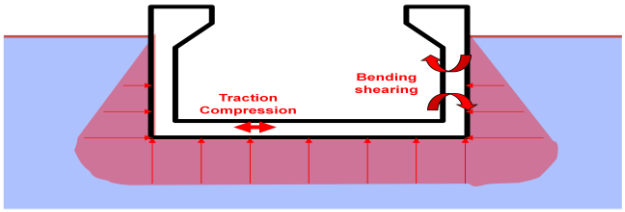

Figure.2.5.External forces acting in the hull ship.

In this level we defined the external forces acting in the hull like hydrostatic pressure.

More important type of failure that may occur in ship structure is the pillars, and basically in case the compression the risk the rupture can be caused by buckling phenomena.

In case the tensile the ruptures occur at the ends of the ships.

According to the DNV Rules we have two loads conditions as show in Figs.2.6; 2.7.

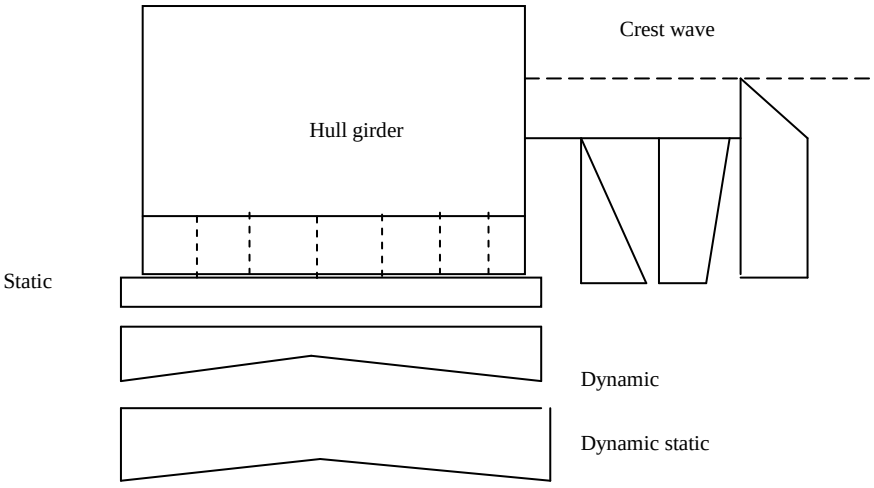

Figure.2.6.Lateral pressure distribution load condition (1), (Recommended Practice DNV-RP-C102, 2002).

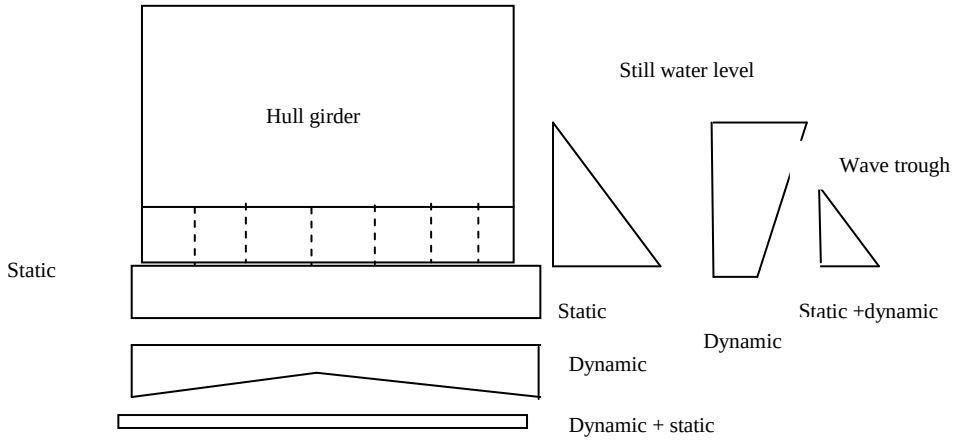

Figure.2.7.Lateral pressure distribution load condition (2), (Recommended Practice DNV-RP-C102, 2002).

We assess the second response in the panel following the action in the next Fig.2.8.

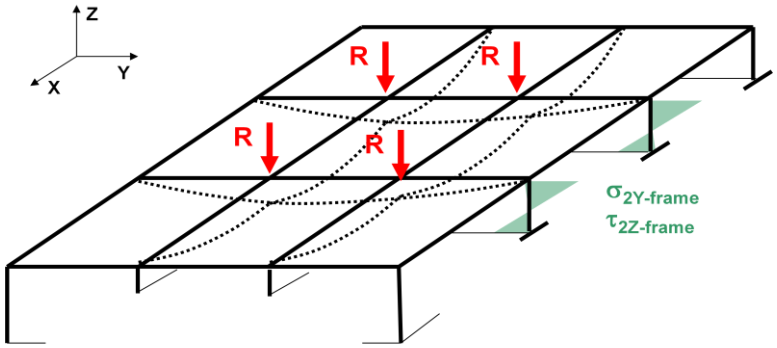

Figure.2.8. The second response considering lateral and local pressure in the panel.

2.2.3. The Third Level

The third level is presented by five mode, the first is overall buckling, second is the plate/ stiffeners yielding, third is flexural buckling of stiffeners include plating, four and five is Lateral-torsion buckling of stiffeners (tripping), and elastic buckling of plating between stiffeners.

- ✓ Mode 1: overall buckling collapse

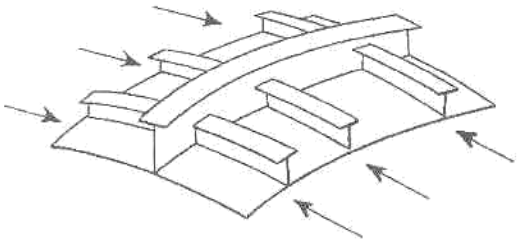

Figure.2.9. Overall stiffened panel buckling (Grillage or Gross buckling-Mode 1), (Philippe Rigo and Enriso Rizzuto, 2003).

- ✓ Mode2: plate/stiffener yielding
- ✓ Mode3: σ_U of interframe panels with a plate-stiffener combination (Fig.2.10) using a beam-column model or an orthotropic model, considering:
  - ➢ Plate induced failure (buckling)
  - ➢ Stiffener induced failure (buckling or yielding)

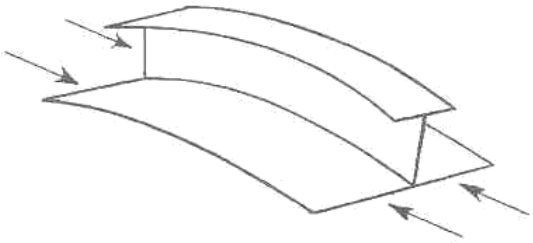

Figure.2.10. Flexural buckling of stiffeners includes plating (beam column), (Philippe Rigo and Enriso Rizzuto, 2003).

- ✓ Mode 4 and 5: instability of stiffeners (local buckling, tripping-fatigue-Fig.2.11)

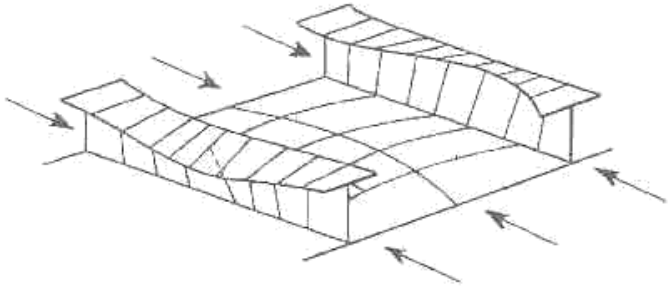

Figure.2.11. Lateral-torsion buckling of stiffeners (tripping), (Philippe Rigo and Enriso Rizzuto, 2003).

✓ Mode 4: Gross yielding buckling collapse of unstiffened plate (Fig.2.12).

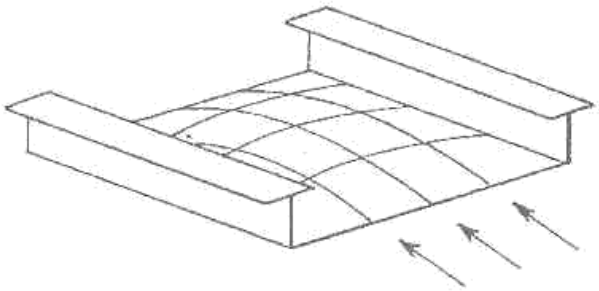

Figure.2.12.Elastic buckling of plating between stiffeners, (Philippe Rigo and Enriso Rizzuto, 2003).

At this level we assess third response in the plate and longitudinal stiffeners (see Fig.2.13);

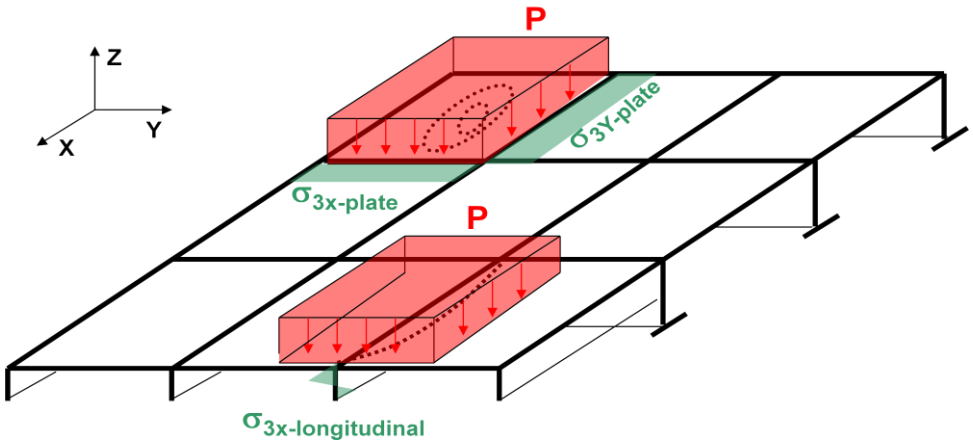

Figure.2.13. The third response in the plate and longitudinal stiffeners.

The more important point must be avoided in the scantling is the shear lag phenomenon.

In the case the shear lag, we get the non-linear normal stress distribution caused by the presence of shear stresses (cf. Fig2.14).

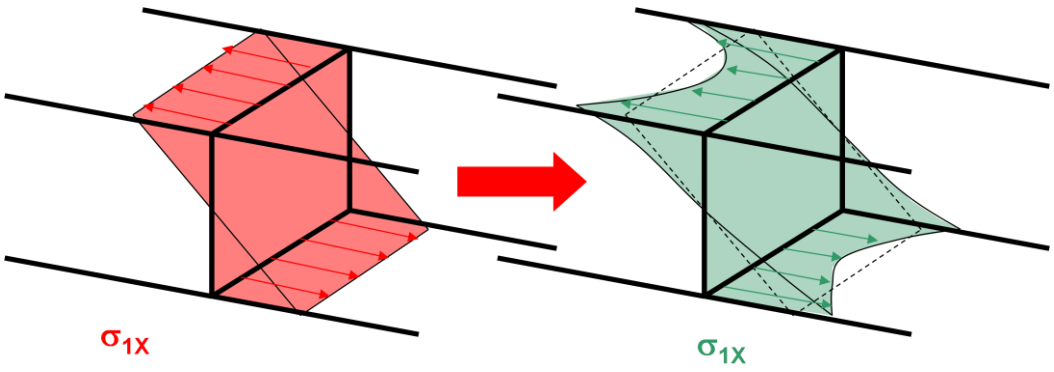

Figure.2.14. The shear lag phenomena.

Therefore, to take the shear lag into consideration, we introduce the concept of effective breadth (cf. Fig2.15).

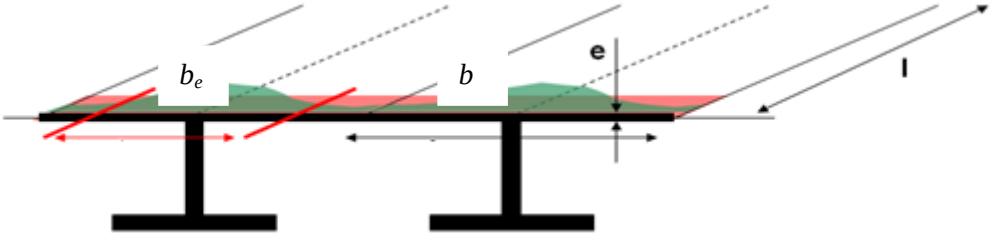

Figure.2.15. The effective breadth of the plate (b_e).

An analytical model has been developed to obtained first approach to assess the ultimate strength of the element the structure, and for accuracy the results we the finite element analysis is performed using the DNV software.

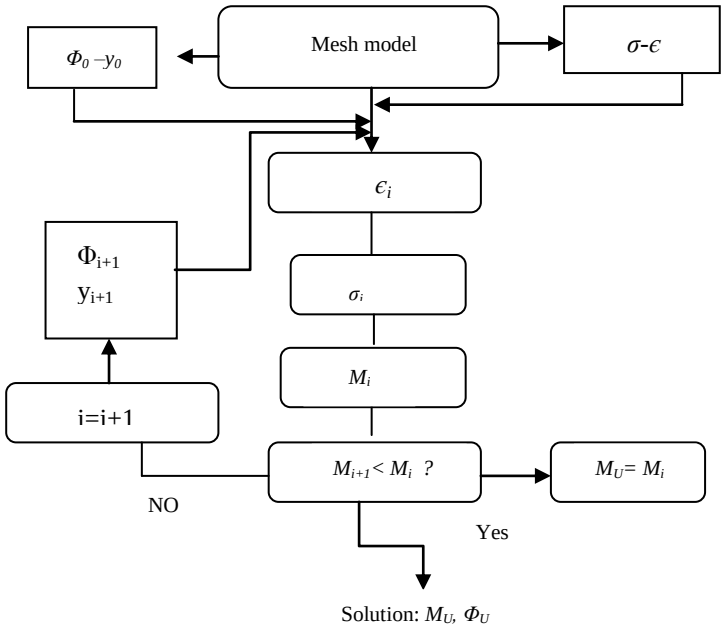

Figure.2.16. The algorithm of the Smith (Philippe Rigo and Enriso Rizzuto, 2003).

2.2.4. The Progressive Collapse of the Hull Girder

The optimum way is to start by the candidates models (the models taken in this work were those developed by Paik, Hughes, Rahman, Faulkner/Sadden, Valsgaard/Steen, Modified Caldwell, Frize/Lin, and Vinner).The aim to start by the candidates models is to avoid to made long calculations FEM, and to get first approach for the results.

2.2.4.1. The Paik and Mansour Model

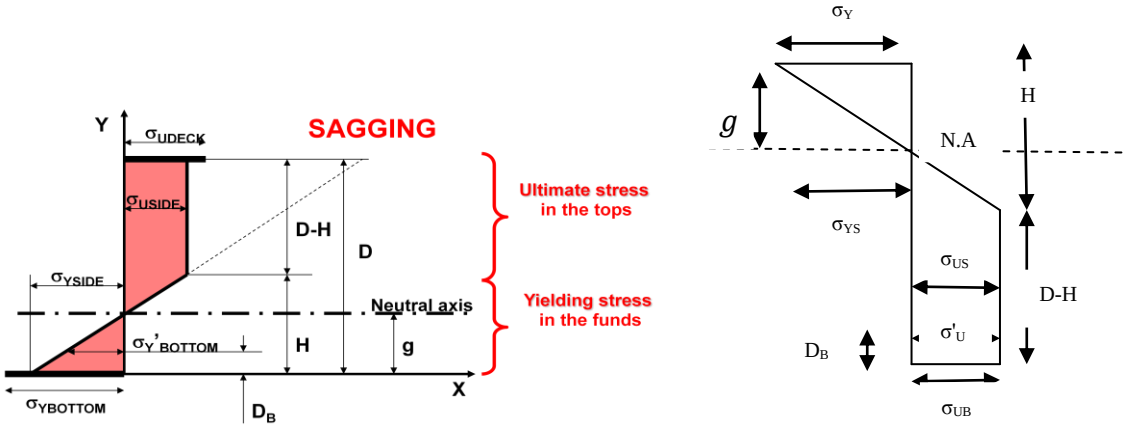

Figure.2.17. Assumed distribution of longitudinal stresses in a hull cross section at the overall collapse state. Sagging condition is shown on the left; and hogging is shown on the right (Mansour, Alaa, Liu, Donnald, 2008).

Paik and Mansour developed the semi-analytical model to describe the ultimate strength for single and double hull ships under vertical bending moment.

The model presents, the ultimate limit state reached when a part of the cross section under tension reaches the yield strength; in fact the part under compression is buckled.

Since, when the stresses change from tension to compression the side keeps linear stress, and the position of the neutral axis as well as the depth at which the stress distribution starts to become linear were determined from the condition that the axial force must be zero (Mansour, Alaa, Liu, Donnald, 2008).

The resulting sagging and hogging ultimate bending moments are given by:

$$M_{US} = -A_D(D-g)\sigma_{UD} - \frac{A_S}{D}(D-H)(D+H-2g)\sigma_{US} - A_B g\sigma_{YB} + \frac{A_B}{H}(g-D_B)[D_B\sigma_{US} - (H-D_B)\sigma_{YS}] - \frac{A_S H}{3D}[(2H-3g)\sigma_{US} - (H-3g)\sigma_{YS}] \quad (2.9)$$

and

$$M_{UH} = A_D g\sigma_{YD} + A_B(D-g)\sigma_{UB} + A_B{}'(d-g-D_B)\sigma'_{UB} + \frac{A_S}{D}(D-H)(D+H-2g)\sigma_{US} + \frac{A_S H}{3D}[(2H-3g)\sigma_{US} - (H-3g)\sigma_{YS}] \quad (2.10)$$

H and g in the equations here are defined by:

$$H = D\,\frac{A_B\sigma_{UB} + A_B{}'\sigma'_{UB} + 2A_S\sigma_{US} - A_D\sigma_{YD}}{A_S(\sigma_{US}+\sigma_{YS})} \quad (2.11)$$

$$g = D\frac{A_B\sigma_{UB}\sigma_{YS}+A_B{}'\sigma'_{UB}\sigma_{YS}+2A_s\sigma_{US}\sigma_{YS}-A_D\sigma_{YD}\sigma_{YS}}{A_s(\sigma_{US}+\sigma_{YS})^2} \quad (2.12)$$

2.2.4.2. The Modified Caldwell Model

In the beginning Caldwell formula is based on the assumption that the yield stress of all structural members is the same. In fact, the Caldwell formula cannot be useful to assess the ultimate limit state of the double hull ship (JEOM K.Paik and Alaa, E.Mansour, 1995).

For that reason the authors have modified the Caldwell original formula by including the effects of different materials and double-hull cross sections.

The procedure of modification as shown in the Fig.2.25, where the yield strengths of the tension flange and side material under tension are not necessarily the same. Even the ultimate buckling strength of the compression flange is not necessarily the same as the side shell buckling strength (Mansour, Alaa, Liu, Donnald, 2008).

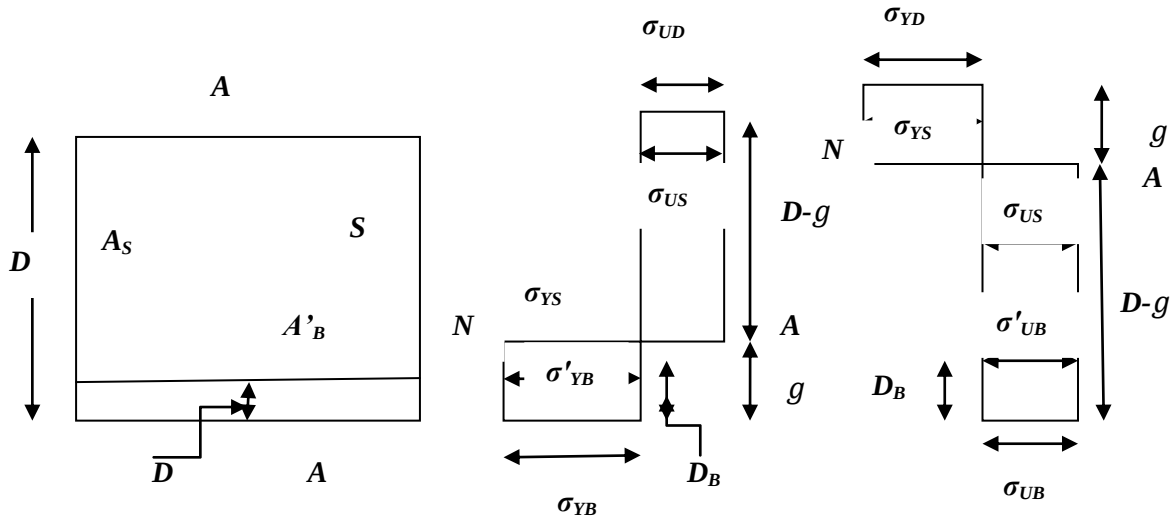

Figure.2.18.The Modified Caldwell in the left equivalent double hull, the center the stress distribution in sagging, and in the right the stress distribution in hogging, (JEOM K.Paik and Alaa, E.Mansour, 1995).

The ultimate buckling capacity of the hull section in sagging condition in this work for single hull tanker VLCC:

$$M_{US} = -A_D(D-g)\sigma_{uD} - A_B g\sigma_{YB} - \frac{A_D}{D}[(D-g)^2\sigma_{uS} + g^2\sigma_{YS}] \quad (2.13)$$

$$M_{UH} = A_D g\sigma_{YD} + A_B(D-g)\sigma_{UB} + \frac{A_S}{D}[(D-g)^2\sigma_{uS} + g^2\sigma_{YS}] \quad (2.14)$$

where in sagging:

$$g = D\,\frac{A_D\sigma_{uD}+2A_S\sigma_{US}-A_B\sigma_{YB}}{2A_S(\sigma_{uS}+\sigma_{YS})} \quad (2.15)$$

While in hogging:

$$g = D\,\frac{A_B\sigma_{uB}+2A_S\sigma_{US}-A_D\sigma_{YD}}{2A_S(\sigma_{uS}+\sigma_{YS})} \quad (2.16)$$

2.2.4.3. The Frieze/Lin Model

The Frieze/Lin expressed a normalized ultimate moment capacity of the hull as function a normalized ultimate strength of the compression flange using the quadratic equation, such as the ultimate collapse strength of ship's hull under a vertical bending moment correlated with the ultimate strength of the compression flange (JEOM K.Paik and Alaa, E.Mansour, 1995).

The Frieze/Lin model follows the quadratic equation:

$$\frac{M_U}{M_P} = d_1 + d_2\frac{\sigma_U}{\sigma_Y} + d_3\left(\frac{\sigma_U}{\sigma_Y}\right)^2 \quad (2.17)$$

In fact using the least squares method to the data in sagging and hogging conditions separately we calculated:

$$d_1 = -0.172\,, d_2 = 1.548, d_3 = -0.368 \text{ in sagging}$$

$$d_1 = -0.003\,, d_2 = 1.459, d_3 = -0.461 \text{ in hogging}$$

where M_P is the plastic bending moment, evaluated according to the following expression :

$$\frac{M_P}{\sigma_Y} = A_D\gamma_D + A_B D(\gamma^2 + 1 - \gamma) + A_S(1-\gamma^2)^2 \quad (2.18)$$

where:

$$\gamma = \frac{2A_D+A_B-A_D}{4A_S} \quad (2.19)$$

2.2.4.4. The Vinner Model

The Vinner assumed that elastic behavior is maintained up to the point where the longitudinal of the compression flange collapses and that causes immediate hull collapse (JEOM K.Paik and Alaa, E.Mansour, 1995).

For this reason he derived another model:

$$M_U = \alpha Z \sigma_U \quad (2.20)$$

where Z is the section modulus, since to describe the ultimate bending moment in sagging we use the section modulus of the deck, in fact if we study ultimate bending moment in hogging we take account of the bottom section modulus.

The mean of value of $\alpha \epsilon [0.92 - 1.05]$ is taken which is $\bar{\alpha} = 0.985$.

2.2.4.5. The Faulkner/Sadden Model

The Faulkner and Sadden by taking account of the systematic errors associated with the yield strength, ultimate compressive strength, and section effects, suggested the model expressed by the following formula (JEOM K.Paik and Alaa, E.Mansour, 1995):

$$M_U = 1.15 Z \sigma_Y \left[-0.1 + 1.4465 \frac{\sigma_U}{\sigma_Y} - 0.3465 \left(\frac{\sigma_U}{\sigma_Y} \right)^2 \right] \quad (2.21)$$

2.2.4.6. The Valsgaard/Steen Model

The Valsgaard/Steen models describe the effect of the hull section, since it includes the strength reserve beyond the onset of collapse of the compression flange (JEOM K.Paik and Alaa, E.Mansour, 1995).For this reason they introduce the concept of the hull section strength margin following parameter B_c .

The suggested formula by the model is:

$$M_U = B_c Z \sigma_U \quad (2.22)$$

where B_c is varied with actual shape of the hull cross section, in the present work for single hull tanker VLCC the mean value of the $B_c = 1.127$ in hogging.

Finally, to evaluate the results ,we check the next algorithm (Fig.2.19); to define the ultimate limit state of the structure, in fact to compare different results received by different candidate models as with the CSR (multistep procedure Nauticus Hull software).

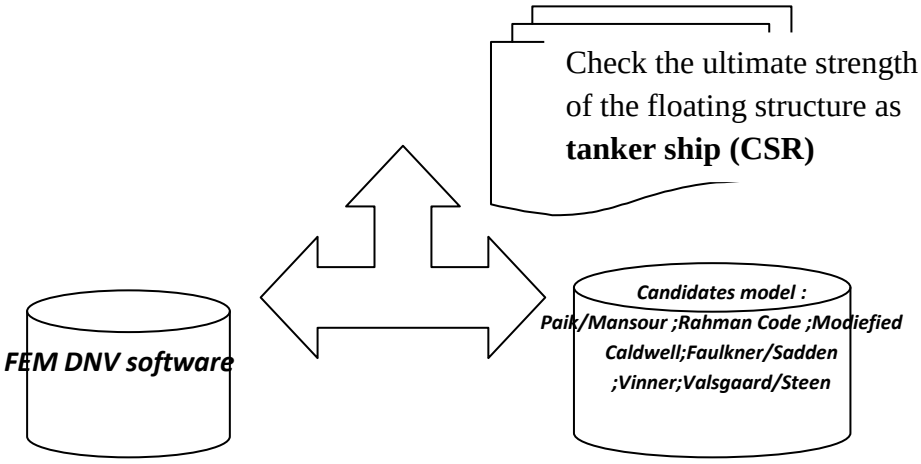

Figure.2.19.The algorithm to check the ultimate strength capacity the tanker ship.

2.3. Combination of Stresses

According to the DNV Rules, in order to carry out the ULS moment capacity checks, both global stresses must be combined.

Generally, the total longitudinal design stress may be derived as:

$$\sigma_{x,total} = \sigma_{x,global} + \sigma_{x,local} \quad (2.23)$$

Total transverse design stress:

$$\sigma_{y,total} = \sigma_{y,global} + \sigma_{y,local} \quad (2.24)$$

Total design shear stress:

$$\tau_{x,total} = \tau_{x,global} + \tau_{x,local} \quad (2.25)$$

Note that the global and local stresses must be calculated for static and dynamic loads separately in order to include the ULS partial load factors in the calculation of design stresses.

2.3.1. Longitudinal Stresses

The nominal longitudinal stresses derived from the analysis will be a combination of the stress components shown in Fig.2.27. The following stress components for the total longitudinal design stress are discussed:

$$\sigma_{x,\,Total} = (\sigma_v + \sigma_h + \sigma_t + \sigma_a + \sigma_{ve})_{x,\,global} + (\sigma_2 + \sigma_{v2} + \sigma_{a2})_{\,x,\,local} \quad (2.26)$$

σ_v = Nominal vertical hull girder bending stress.

σ_h = Nominal horizontal hull girder bending stress.

σ_t = Nominal torsion stress in hull girder.

σ_a = Nominal axial stresses due to hull girder end pressure.

σ_{ve} = Nominal vertical hull girder bending stress due to end pressure.

σ_2 = Nominal secondary bending stress in double bottom or double side.

σ_{v2}= Nominal secondary vertical hull girder bending stress due to lateral pressure on transverse bulkheads.

$\sigma_{a2=}$Nominal secondary axial stress due to lateral pressure on transverse bulkheads.

σ_v = nominal vertical hull girder bending stress.

$$\sigma v = \frac{\gamma_S M_S + \gamma_W M_W}{Z_i} \quad (2.27)$$

where:

M_S = Characteristic still water bending moment based on actual cargo and ballast conditions.

M_W = Characteristic wave bending moment based on an annual probability of exceedance of 10^{-2}(100 years).

γ_s = Load factor for still water loads.

γ_w = Environmental load factor.

Z_i = section modulus at the considered transverse section (i).

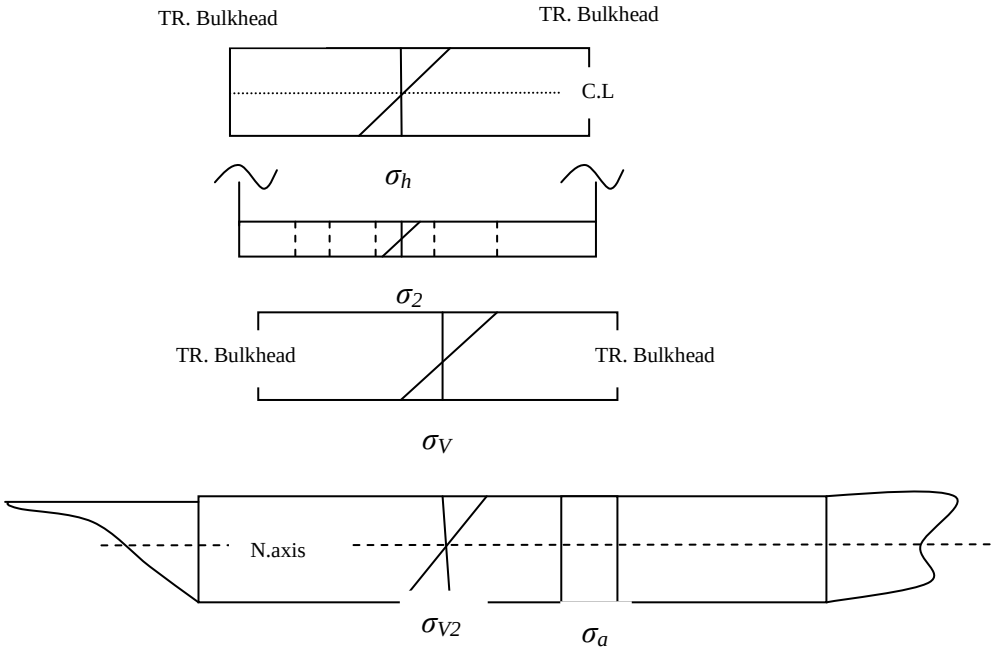

Figure.2.20.Longitudinal stress components, (Recommended Practice DNV-RP-C102, 2002).

where: σ_h - nominal horizontal hull girder bending stress.

The nominal horizontal bending stress should be considered, and the horizontal bending stress is caused by wave loads only. The stress σ_h can be calculated as:

$$\sigma_h = \frac{\gamma_w M_w}{Z_i} \quad (2.28)$$

The symbol definition is the same as for vertical bending stress above.

where: σ_a nominal axial stresses due to hull girder end pressure the hull girder, axial stress due to the static and dynamic end pressure can be considered to act uniformly on the complete cross section within the cargo area. The design stress can be calculated according to the following formulae:

$$\sigma_a = \frac{\gamma_s F_{as} + \gamma_w F_{aw}}{A_i} \quad (2.29)$$

where:

F_{as} = characteristic still water axial force due to hull end pressure.

F_{aw} = Characteristic wave axial force based on an annual probability of exceedance of 10^{-2}(100 years).

γ_s = Load factor for still water loads.

γ_w = Environmental load factor.

A_i = Cross section area based on gross thickness at the considered transverse section (i).

2.3.2. The Shear Stress

The wave shear forces derived from direct calculations for worldwide operation has proved to be much higher (30 - 80%) than the unified IACS requirement. From experience the hull shear capacity at the "¼ lengths" of the hull must be considered early in the design, and the effect of topside loads must be included. The main reasons for this are:

- ✓ The still water shear forces and wave shear forces are usually maximum at the ends of the cargo area.
- ✓ The scantlings of the longitudinal bulkheads/sides are also often reduced in these regions or terminate completely.
- ✓ The hull girder wave bending moment and wave shear force are almost in phase
- ✓ The shear stresses and vertical stresses from the topside loads are often higher than in the amidships area due to pitch accelerations.

The following shear stress components should be considered for the total shear stress:

$$\tau_{Total} = \tau_{Global} + \tau_{Local} \quad (2.30)$$

where :

τ_{Global}= total nominal design shear stress from global shear force

τ_{Local}= total nominal design shear stress from local effects

The global design shear force (τ_{Global}) in side, inner side, longitudinal bulkheads and other global shear carrying elements is normally obtain by the following formula:

$$\tau_{Global} = \frac{\gamma_S . Q_S + \gamma_W . Q_W}{t} . q(Fz1) \quad (2.31)$$

where:

Q_S = Characteristic design still water shear force based on actual cargo and ballast conditions

Q_W = Characteristic wave shear force based on an annual probability of exceedance of 10^{-2} (100 years)

γ_s= Load factor for still water loads

γ_W = Environmental load factor

t = Plate thickness of considered panel

q (Fz1) = Shear flow factor [N/mm] given by the shear flow analysis (eg. In Nauticus) due to a unit vertical shear force (Fz = 1 N).

The nominal shear stresses from local effects (τ_{Total}) are normally derived from the cargo hold finite element analysis.

However, the global hull girder loads may be included in a cargo hold model by using the method as described in Classification Notes 31.3 - Strength Analysis of Hull Structure in tankers, Appendix A. The total shear stress may then be determined directly from the cargo hold analysis.

3. Various Parameters Influencing the Ultimate Strength of Plates

3.1. Introduction

Before the ULS analysis of the plate and panel, we check in the beginning effect of the some parameters reducing the ultimate strength in the plate.

The ultimate strength of stiffened panel affected by the following parameter:

- Length/width ratio of the panel
- Stiffener geometry and spacing
- Aspect ratio for plate between stiffeners
- Plate slenderness
- Residual stresses
- Initial distortions
- Boundary conditions
- Type of loading

To define the effect of these parameters, to reduce the ULS of the plate, we follow the next procedure.

Using the non-linear plate theory (PULS software), we fixe in the beginning the stiffeners spacing, and we look of the effect of the plate slenderness, without considering the lateral pressure. Thus, we introduce the quality of the imperfection, such as this parameter is related to the thickness of the plate, and the stiffeners spacing.

Second step, we fix the thickness of the plate, and we look to the effect of the stiffeners spacing.

At the end we apply the lateral pressure at the area of the different plate has been different thickness, and we defined the relationship between the ultimate stress and the lateral pressure.

3.2. Effect the Boundary Condition to Assess the Ultimate Strength of the Plate

To define the effect of the boundary condition to assess the ULS capacity of the plate, we follow the bellow steps:

- ✓ The working stress is $\sigma_x = 332.4\ MPa\ \ and\ \ \sigma_y = 99.72\ MPa$.

- ✓ We apply, the biaxial compression, and we take for boundary condition two cases; the plate clamped in the four edges and in the second case the simple supports.

Using the PULS code, we get the summary results checking the buckling of the plate, at the different value of the slenderness locale plates, in two cases of supports: clamped and simple, the Fig.3.1 show the dimension the plate considering.

Such as, the initial deflection of the plate taking by PULS software was 4.35 mm as defaults value. Wherever we compare in these summary results, the effect of the boundary condition to check the buckling phenomena, and to assess the ultimate capacity.

As we can conclude, the plate buckled if we have simple supports, and the load higher .For all the interpretation presenting in this chapter, according to the results presented in below Table 3.1.

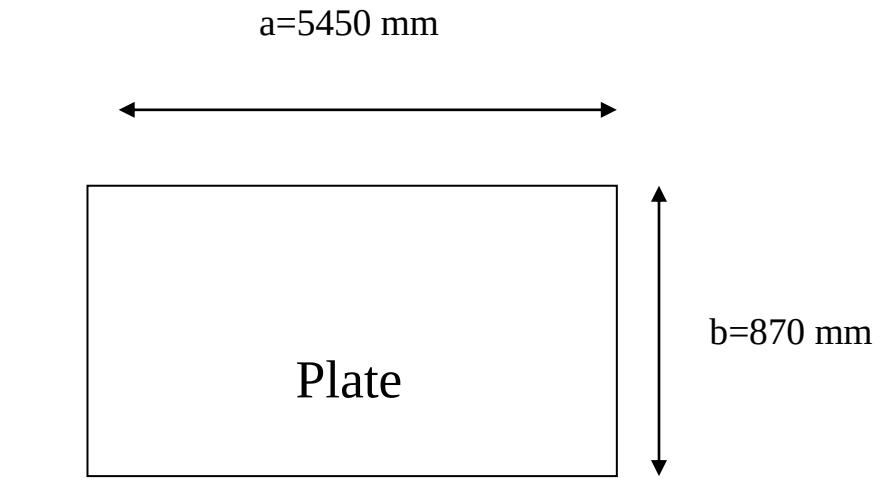

Figure.3.1.The dimensions of the plate.

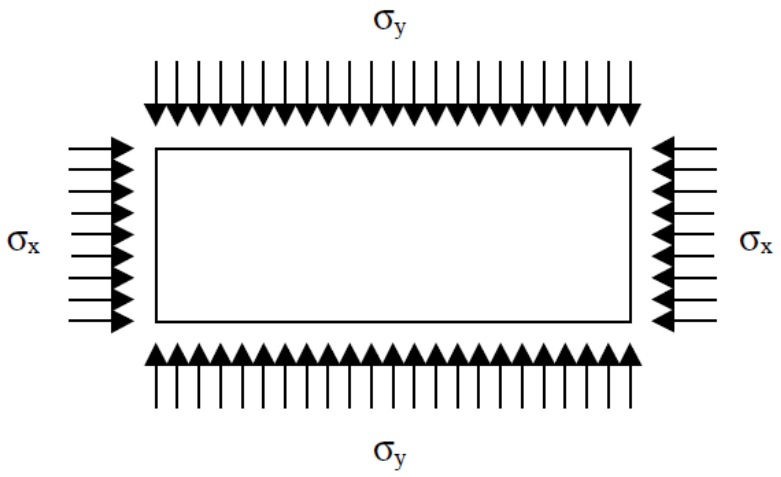

Figure.3.2.The plate under biaxial compression.

The plates are collapsed with the ratio between average stresses in longitudinal and transverse direction kept constant; ensuring so called proportional loading.

$$\sigma_y = k\,\sigma_x \quad (3.1)$$

Such as *k* is the proportionality constant, can be expressed as: $k = \tan(\Phi)$.

Table.3.1. Summary results to check the buckling and ULS plate results

						plate			BUCKLING		ALLOWABLE USAGE FACTOR
Clamped supports	Thickness =22mm	β=1,38	σ_{Ux} (MPa)	243	269	276	239	144	0,98	**OK**	1
			σ_{Uy}(MPa)	0	75	168	256	278			
			σ_{Ux} / σ_Y	0,95	1,05	1,08	0,94	0,56			
			σ_{Uy}/ σ_Y	0,00	0,29	0,66	1,00	1,09			
	24mm	β =1,26	σ_{Ux} (MPa)	246	272	280	241	147	0,96	**OK**	1
			σ_{Uy} (MPa)	0	76	170	258	283			
			σ_{Ux}/ σ_Y	0,96	1,07	1,10	0,95	0,58			
			σ_{Uy} / σ_Y	0,00	0,30	0,67	1,01	1,11			
	20mm	β =1,52	σ_{Ux} (MPa)	240	264	270	235	140	1	**OK**	1
			σ_{Uy} (MPa)	0	74	164	251	270			
			σ_{Ux} / σ_Y	0,94	1,04	1,06	0,92	0,55			
			σ_{Uy} / σ_Y	0,00	0,29	0,64	0,98	1,06			
	19mm	β =1,6	σ_{Ux} (MPa)	238	260	266	232	137	1,01	**NOT OK**	1
			σ_{Uy} (MPa)	0	73	162	248	265			
			σ_{Ux} / σ_Y	0,93	1,02	1,04	0,91	0,54			
			σ_{Uy} / σ_Y	0,00	0,29	0,64	0,97	1,04			

Simple supports	Thickness =22mm	β =1,38	σ_{Ux} (MPa)	235	245	200	120	67	27	1,19	**NOT OK**	1
			σ_{Uy} (MPa)	0	69	122	129	130	129			
			σ_{Ux} /σ_Y	0,92	0,96	0,78	0,47	0,26	0,11			
			σ_{Uy} / σ_Y	0,00	0,27	0,48	0,51	0,51	0,51			
	24mm	β =1,26	σ_{Ux}(MPa)	240	256	226	138	77	30	1,12	**NOT OK**	1
			σ_{Uy} (MPa)	0	72	138	148	148	147			
			σ_{Ux} / σ_Y	0,94	1,00	0,89	0,54	0,30	0,12			
			σ_{Uy} /σ_Y	0,00	0,28	0,54	0,58	0,58	0,58			
	20mm	β =1,52	σ_{Ux} (MPa)	227	230	174	104	58	23	1,33	**NOT OK**	1
			σ_{Uy} (MPa)	0	64	106	111	112	112			
			σ_{Ux} / σ_Y	0,89	0,90	0,68	0,41	0,23	0,09			
			σ_{Uy} / σ_Y	0,00	0,25	0,42	0,44	0,44	0,44			
	19mm	β =1,6	σ_{Ux} (MPa)	222	221	161	96	53	21	1,5	**NOT OK**	1
			σ_{Uy} (MPa)	0	62	98	102	103	103			
			σ_{Ux} / σ_Y	0,87	0,87	0,63	0,38	0,21	0,08			
			σ_{Uy}/ σ_Y	0,00	0,24	0,38	0,40	0,40	0,40			

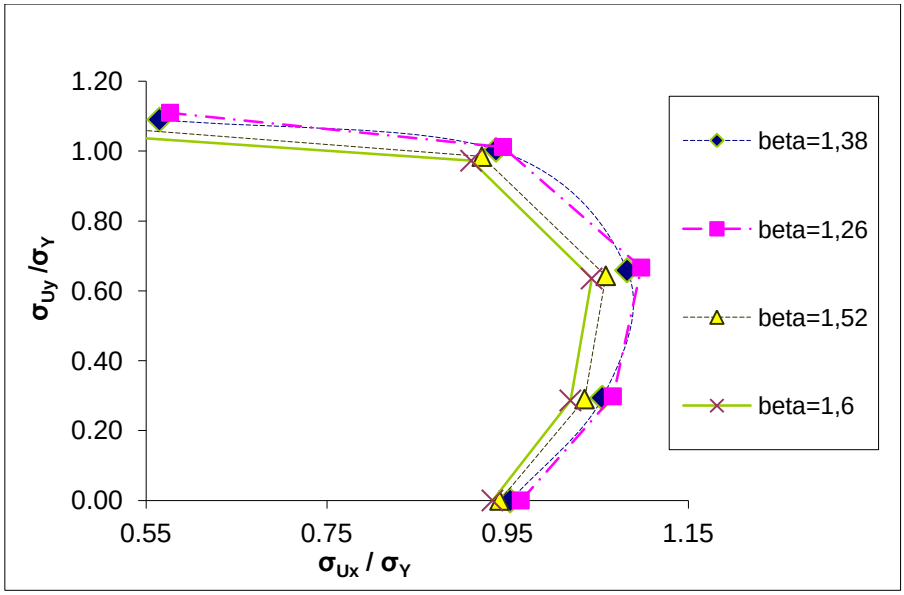

Figure.3.3.The plate at clamped supports with lateral pressure P=0.16 MPa, $\frac{a}{b} = 6.26$.

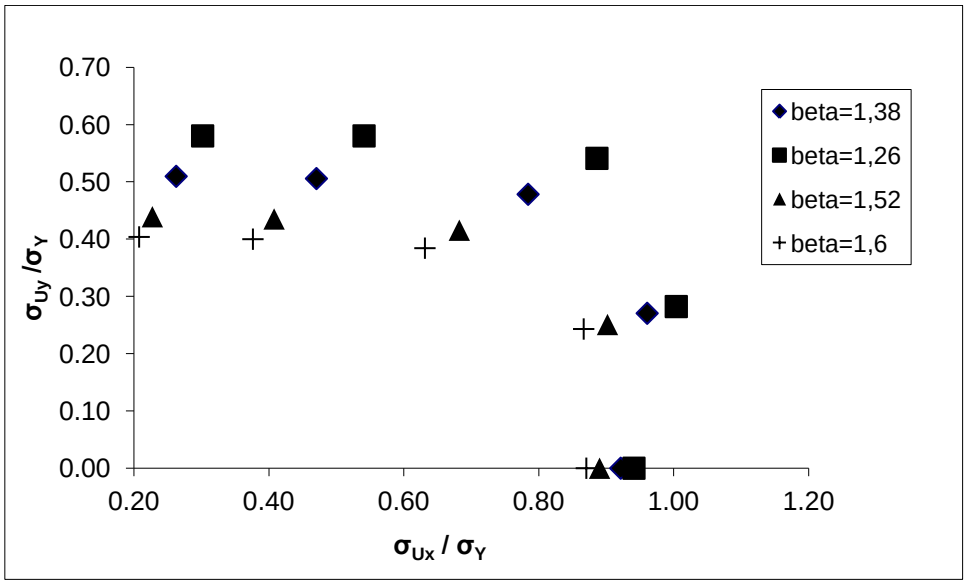

Figure.3.4.The plate at simple supports with lateral pressure P=0.16 MPa, $\frac{a}{b} = 6.26$.

Two types of the boundary conditions were considered in the benchmark study; the panel edges parallel to the stiffeners (longitudinal edges) were either simply supported or clamped. Figs.3.4, 3.3, shows a comparison of ultimate strength for both boundary conditions. Apparently, the boundary conditions on longitudinal edges have only a minor influence on panel strength, but when the edges are clamped the panel strength increases slightly

The buckling test in the case the clamped supports is ok ,all the thickness plate will be acceptable without effect of the buckling , contrariwise for simple supports all the plate will be buckled.

In two curves (Figs.3.3, 3.4) above the effect of the slenderness plate is understanding, by increase the load applied, the ultimate strength of small slenderness plate have high ultimate stress, in fact the plate had the small thickness the ultimate stress will be lower.

Second things, take the simple support, the axial compression have not big effect as the transversal compression. Indeed, in the case of clamped plate, we observe even if we increase the applied load the ultimate strength is closer for the different value of slenderness plates.

3.3. Effect the Initial Deflection to Assess the Ultimate Strength

The plating is usually continuously welded along the plate-stiffener intersection and it is well established that the welding process introduces in the plate and stiffener a residual stress field and both plating and stiffeners have initial deflection due fabrication from post-weld. Accordingly, there are three types of initial imperfection, as illustrated in Fig.3.5, are accounted for, namely Plate out-of-plane displacement, W_{p0}Stiffener out-of-straightness relative to the plate plane, W_{0s} sideways sway of the stiffener, and the initial deflection of the top the stiffeners υ_{0s}.

The effect of imperfections on the ultimate strength depends strongly on their shape. In the most theoretical studies, initial deflections have been assumed to have the same shape as the buckling mode which gives a reduction in ultimate stress.

The maximum amplitude for initial imperfection (i.e, initial deflection and residual stress) related to fabrication, it's implementing in the critical buckling mode shape for plate (out-of-plane shape) and for longitudinal stiffener (lateral-torsional shape) which obtains from eigenvalue analysis is taken according to the tolerance limit for fabrication given by DNV (CN30.1):

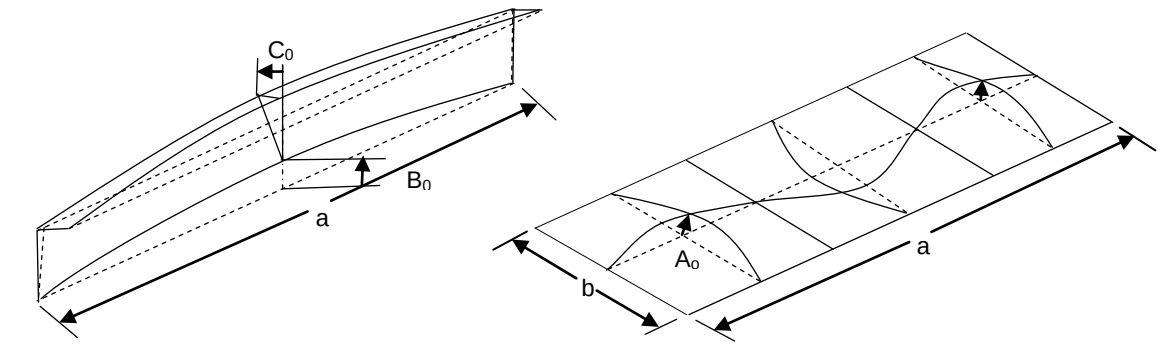

(b) Stiffener (a) Panel

Figure.3.5. Assumed initial deflections in stiffened plates where A_o, B_o, C_o is the maximum amplitude for plate out from plane, stiffener out from straight and sideway sway of stiffener respectively (Yao T. et al, 2000).

From the reference (Yao T. et al, 2000); we define the initial deflection as follow the next formula:

The initial deflection of the plate:

$$W_{p0} = \delta_{p0}\sin\left(\frac{m\pi x}{a}\right) cos\left(\frac{\pi y}{b}\right) \quad (3.3)$$

The initial deflection of the stiffeners:

$$W_{0s} = B_0\sin\left(\frac{\pi x}{a}\right) \quad (3.4)$$

The initial deflection of the top the stiffeners:

$$\upsilon_{0s} = C_0\sin\left(\frac{\pi x}{a}\right) \quad (3.5)$$

where δ_{p0} is the average level of the maximum initial panel deflection, according to the smith et al (Yao T. et al, 2000) is given by:

$\delta_{p0} = 0.1\beta^2 t$, such as $\beta = \frac{b}{t}\left(\frac{\sigma_Y}{E}\right)^{0.5}$ and $m = \frac{1}{2}H$,where m is the half of the wave height.

As we considered, the plate is clamped and we apply the work stress (biaxial stress), to check the buckling and the ultimate capacity of the plate.

According to the new value of the deflection of the plate presented in Table.3.2, we describe the new analysis of the ultimate strength capacity of the plate by applying the working stress $\sigma_x = 332.4\ MPa\ \ and\ \ \sigma_y = 99.72\ MPa$.

Table.3.2. The initial imperfection of the plate

β	1.26	1.38	1.52	1.6
δ_{p0} (mm)	3.49	4.18	5.08	5.63
W_{p0} (mm)	1.23	1.48	1.8	1.99

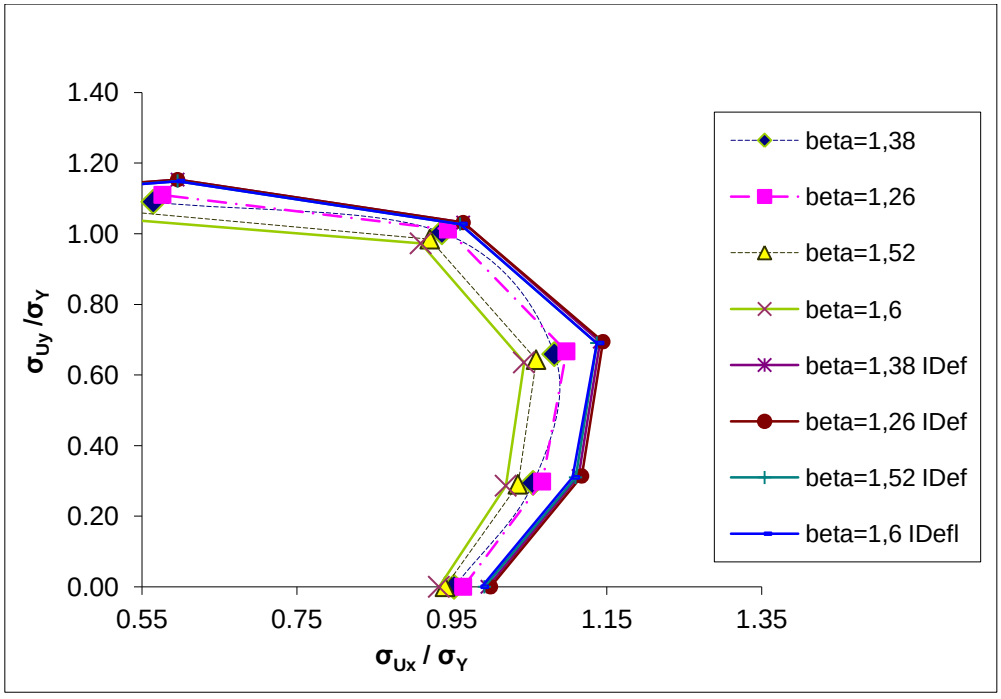

Figure.3.6. The plate at clamped supports with applying the lateral pressure P=0.16 MPa with effect the imperfection. IDef: calculation of the initial imperfection using Smith et al equation (Eq.3.3).

From the curve above (cf. Fig3.6), we obtain the effect of the initial deflection to reduce the ultimate strength capacity of the plate.

By comparing the level the ultimate strength of the plate the initial imperfection is considered, the DNV PULS consider by defaults the initial deflection the sum of the local and the global mode, and the plate initial deflection equal b/200, the column type initial of stiffener equal a/1000, and the sideways initial deflection of stiffener equal a/1000. In fact, using the above formula (Eq.3.3), the new estimation of the initial deflection of the plate is calculated.

As we observe in Fig.3.6, the DNV PULS receive the lower ultimate strength region of the plate, using the defaults value of the initial imperfection.

Wherever, increasing the applied load, and the plate had large initial deflection as the DNV PULS consider in the first running, the plate can be buckled faster under the transversal compression, on the contrary if we consider the lower initial imperfection, we get more large ultimate capacity. The much higher deflections at the mid part of the plate create a much higher out of plane curvature with much more abrupt geometry changes between the different parts of the plates, taking into account the fact that most of the load carrying takes place towards the longitudinal edges of the plate, an effective transfer of the longitudinal stresses is prevented by the abrupt geometry changes. The higher out of plane curvature also results in higher bending moments at the mid part of the plate with reduced capability to carry longitudinal stresses.

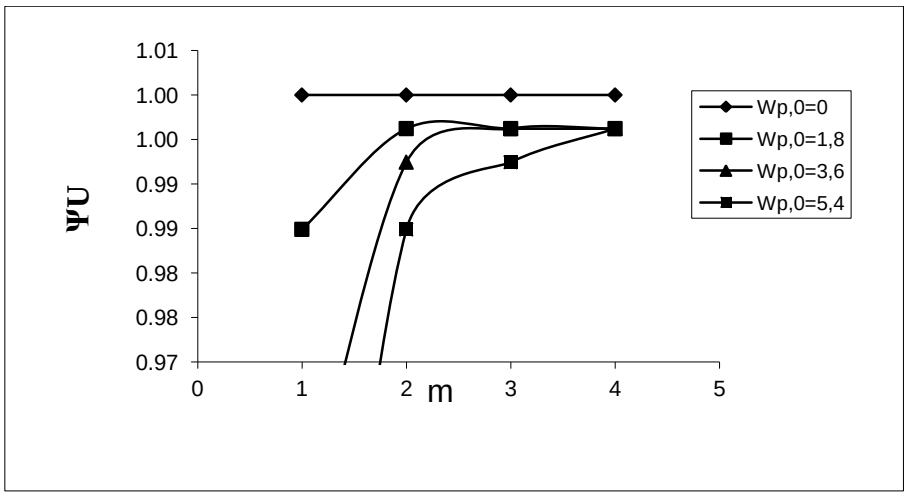

Figure.3.7. Effect of initial deflection shape on the ultimate strength.

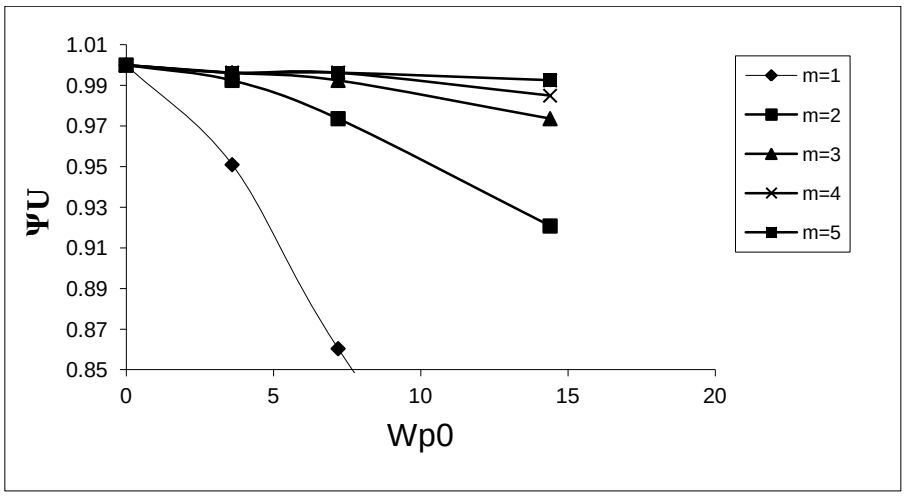

Figure.3.8. Effect of initial deflection amplitude on the ultimate strength.

Cui and Mansour's formula (Cui WC, Mansour AE, 1998) is used to express the relation calculate the initial deflection shape and amplitude: $W_{P0} = W_{0,max}\frac{0.756}{i^{1.565}}$. (3.6)

In Figs.3.7, 3.8 it can be said that as *i* increases W_{P0} will decrease, that is, when the initial deflection component number *i* is high, the corresponding amplitude will be small. Therefore, we need to establish reasonable relation between W_{P0} and *i* based on practical measurements.

3.4. Effect the Plate Slenderness and the Stiffeners Spacing

Before discuss the effects of the general corrosion on the ultimate strength, it would be quite interesting to know the ultimate strength of a perfect plate. By perfect plate we mean that both residual stresses and initial deflection are zero. Therefore, the only parameters which might affect the ultimate strength are β and λ. The results are shown in Fig.3.9 it can be seen that λ has negligible effect on ultimate stress and therefore only β is the significant parameter for defining the ultimate strength of an unstiffened perfect plate. This is consistent with the current literature (Faulkner D. A, 1975), and the (Eq.3.7) present the Cui/Mansour formula to express the relation between ultimate stress and the slenderness plate.

$$\Psi_U = \begin{cases} 1 \; if \; \beta < 1.9 \\ 0.08 + \frac{1.09}{\beta} + \frac{1.26}{\beta^2} \quad if \; \beta > 1.9 \end{cases} \quad (3.7)$$

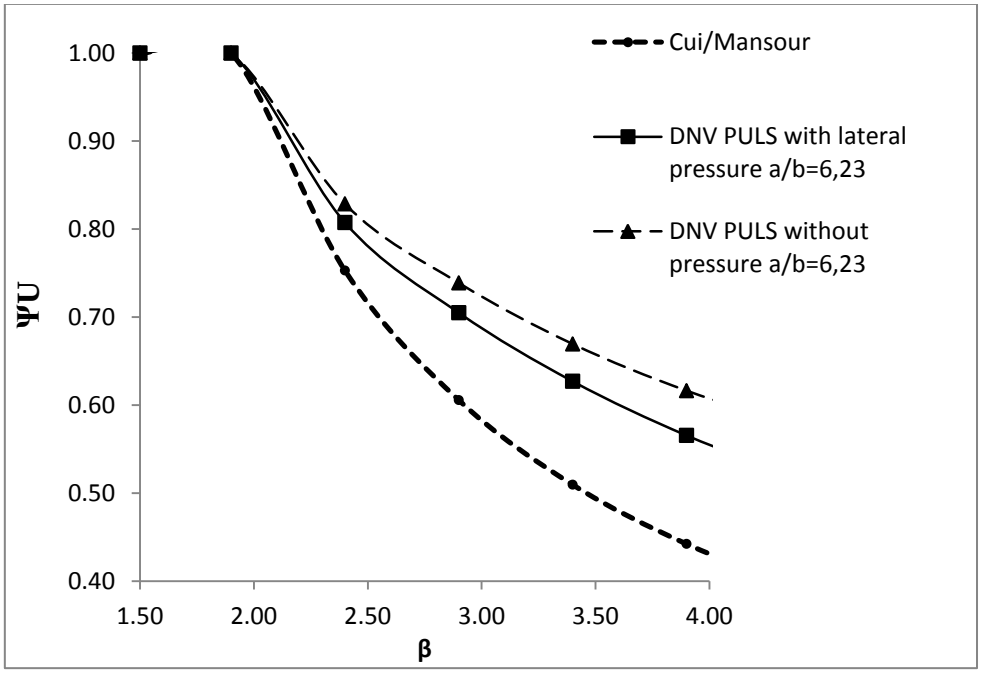

Figure.3.9. A comparison of the Cui and Mansour Formula (Eq.3.7) with DNV PULS.

Table.3.3. The characteristics of the plate to study ULS (b=870 mm; P=0MPa; $\frac{a}{b} = 6.26$)

Plate	Thickness(mm)	β	W_{P0} (mm)
1	12	2.53	2.71
2	14	2.12	2.22
3	19.5	1.52	1.59

Table.3.4. The characteristics of the plate to study ULS (t=18 mm; P=0MPa)

Plate	b (mm)	β	W_{P0} (mm)	$\frac{a}{b}$
4	500	0.97	0.6	10.9
5	850	1.65	1.72	6.41
6	950	1.84	2.15	5.73

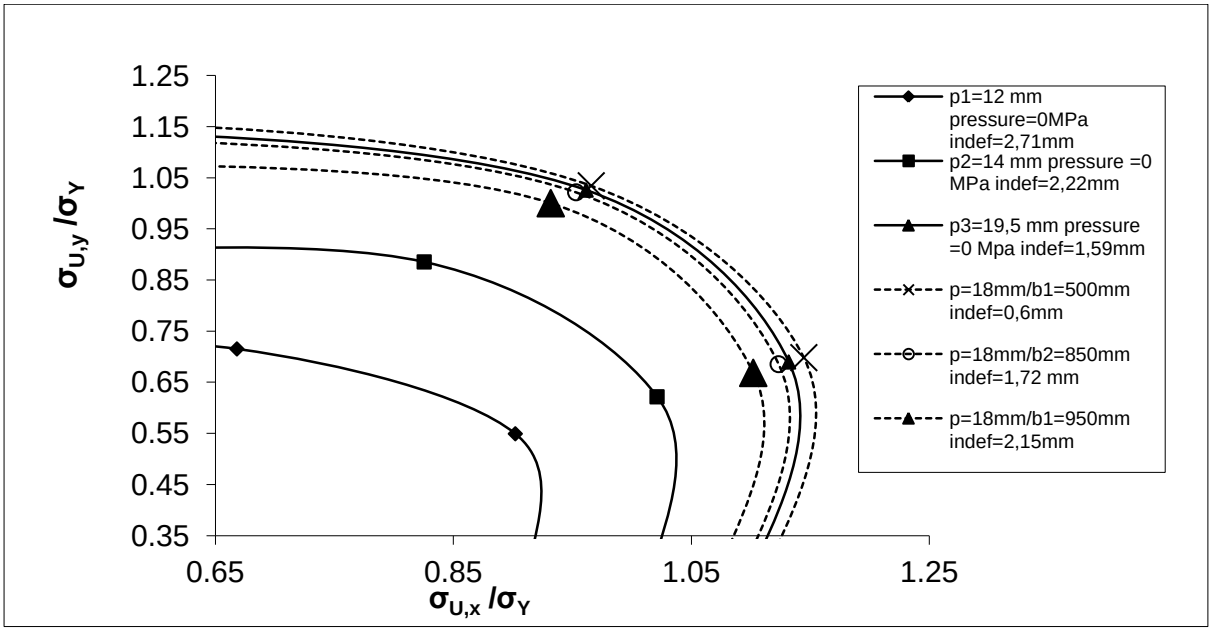

Figure.3.10. Ultimate strength interaction relationships of plates under biaxial compression without lateral pressure.

In Fig.3.9, we conclude if β less than 1.9 the ultimate stress of plate not change, but if higher than 1.9 the decay of the ultimate stress starts to be faster and the slope is higher.

Two correlations are obtained to define the ultimate stress as function the plate slenderness, by solving two linear systems presented as follow:

- Ignoring lateral pressure

$$\begin{cases} 1 = 0.58 + \frac{b}{1.9} + \frac{c}{1.9^2} \\ 0.67 = 0.58 + \frac{b}{3.9} + \frac{c}{3.9^2} \end{cases} \quad (3.8)$$

Then the formula of ultimate stress function the plate slenderness is obtained:

$$\Psi_U = \begin{cases} 1 \; if \; \beta < 1.9 \\ 0.58 + \frac{1.27}{\beta} - \frac{0.9}{\beta^2} \quad if \; \beta > 1.9 \end{cases} \quad (3.9)$$

- Considering lateral pressure

$$\begin{cases} 1 = 0.52 + \frac{b}{1.9} + \frac{c}{1.9^2} \\ 0.7 = 0.52 + \frac{b}{2.9} + \frac{c}{2.9^2} \end{cases} \quad (3.10)$$

The expression of the ultimate stress becomes:

$$\Psi_{U,P} = \begin{cases} 1 \; if \; \beta < 1.9 \\ 0.52 - \frac{0.26}{\beta} + \frac{2.23}{\beta^2} \quad if \; \beta > 1.9 \end{cases} \quad (3.11)$$

In the other ways, Fig.3.10 show if we decrease the slenderness plate and the stiffeners spacing the ultimate capacity of the plate becomes higher.

3.5. Effect the Lateral Pressure to Reduce the ULS Capacity of the Plate

The benchmark results presented in Fig.3.11 indicate that lateral pressure is a significant parameter in the design and modeling of stiffened panels, and clearly affects safe range of in-plane loads. Lateral pressure of 0.4 MPa resulted in a drop of ultimate strength by 5-10%. This imposes bending in stiffeners and increased membrane forces in the plate. Thus, the drop in strength is greater when the longitudinal in-plane load (along stiffeners) is predominant, because in this case panel strength depends more on the stiffeners.

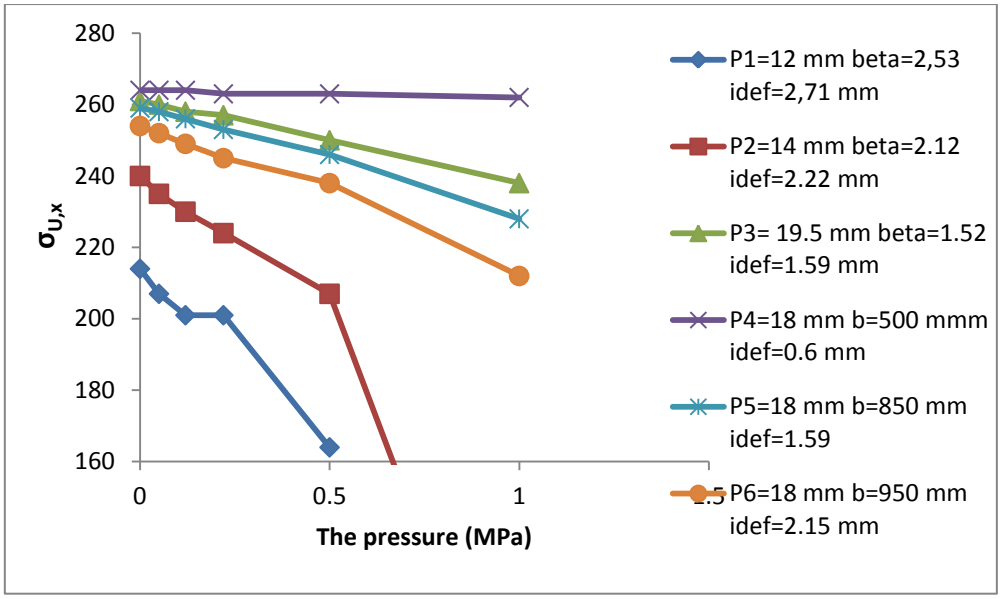

Figure.3.11.Ultimate strength of the plates under biaxial compression with lateral pressure.

4. THE NEW CORROSION MODEL COMPARING WITH OTHERS CANDIDATES MODELS AND THE ASSUMED DATA

4.1. Introduction

The marine environment is one of the aggressive parameters to deteriorate the steel material, such as the steel considers the allowable material using in shipbuilding for the reason economic.

Statistics, by effect of the corrosion for ship hulls show that around 90% of ship failures are attributed to corrosion, including corrosion fatigue (Emi H, Yuasa M, Kumano A, Arima T, Yamamoto N, Umino M, 1993).

In this chapter, we discuss various models the corrosion of the ship structure, following the basic equation the evolution the depth of the corrosion versus the time.

This equation based to the weibull distribution, and using the least squares method we get the first assumption of the parameters, at the end we compare the solution with data as the reference ABS (Offshore Technology Conference, 5 May-8May 2003).

From the first solution of the Weibull distribution using the LSM method, we go to compare the assumed Data as have the reference of the paper (Shengping Qin and Weicheng, 2002), since we get the large gap between the data and the proposal solution of the distribution.

In fact, we develop a new model based to the approach of the Paik/al model, developing the basic equation at second order of the Taylor series, finally we analyse the result by comparing the new model to the others candidate models present in this chapter: Melchers, Guedes Soares/Garbatov, and Paik/al.

Before touch all this points, we start to present short view, discussing type of the corrosion, and the hard condition of the marine environment.

Since, we discuss different existing models, and the methodology to extract the new model.

To validate the models, and to make computation between the existing models and a new model, we present the assumed data as have been reference ,in fact to get good relationship between reduction the ratio of the section modulus and the area of the deck cargo versus time. Effectively, to determine the relationship between weight and ratio of the section modulus.

4.2. The Marine Corrosion

Year upon year the cost of marine corrosion has increased until it is estimated today at 4 % of the Gross National Product. An enlightened approach to materials selection, protection and corrosion control is needed to reduce this burden of wasted materials, wasted energy and wasted money. These notes have been compiled by Members of the Marine Corrosion Forum to help marine designers, engineers, and equipment users, understand the causes of marine corrosion and the way in which protective systems and more resistant materials can be used to reduce or entirely eliminate sea water corrosion problems.

Many different types of destructive attack can occur to structures, ships and other equipment used in sea water service. The term "aqueous corrosion" describes the majority of the most troublesome problems encountered in contact with sea water, but atmospheric corrosion of metals exposed on or near coastlines, and hot salt corrosion in engines operating at sea or taking in salt-laden air are equally problematical and like aqueous corrosion require a systematic approach to eliminate or manage them.

Corrosion by sea water, aqueous corrosion, is an electrochemical process, and all metals and alloys when in contact with sea water have a specific electrical potential (or corrosion potential) at a specific level of sea water acidity or alkalinity the pH .

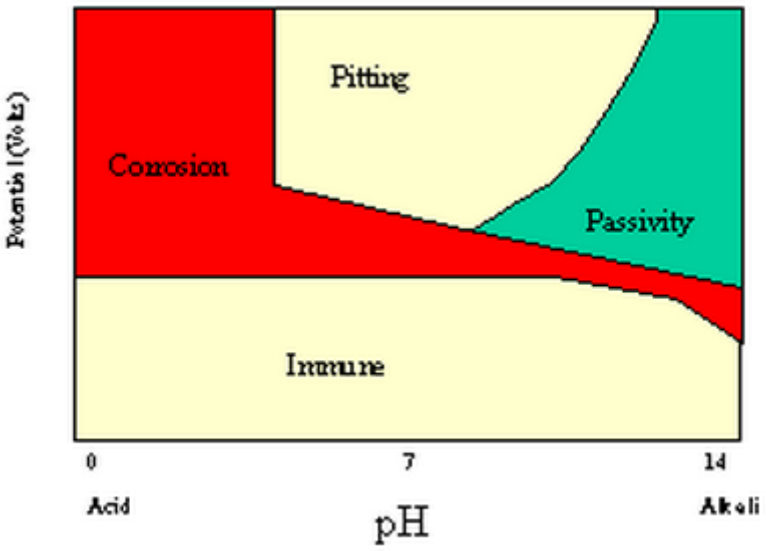

Figure.4.1. The diagram potential versus PH for aqueous corrosion. Available from http://www.marinecorrosionforum.org/explain.htm.

This typical diagram (cf. Fig.4.1), shows the regions where the metal will freely corrode; the region of passivation where stable oxide or other films form and the corrosion process is

stifled; the region of pitting corrosion where the corrosion potential of the metal exceeds that of its oxide; and the region of immunity where the metal is normally fully safe to use. More resistant alloys mean less corrosion, metals like gold platinum and tantalum can resist virtually all corrosion, but for marine service the final choice will always be a compromise with cost.

Most corrosion resistant metals rely on an oxide film to provide protection against corrosion. If the oxide is tightly adherent, stable and self healing, as on many stainless steels and titanium, then the metal will be highly resistant or immune to corrosion. If the film is loose, powdery, easily damaged and non self repairing, such as rust on steel, then corrosion will continue unchecked. Even so, the most stable oxides may be attacked when aggressive concentrations of hydrochloric acid are formed in chloride environments (From http://www.marinecorrosionforum.org/explain.htm). As we can understand the mechanism of the progressive corrosion, and the evolution of the speed of the corrosion, then we look to the statistical data, to defined the more critical area attacked by corrosion for Tanker ship.

According to the Fig.4.2 we can see the mains principal factor affecting hull structural failure is the corrosion. In the others ways, following the circular diagram (Fig.4.3), the critical area attacked by corrosion is the deck plating.

For that reason, this chapter, present how to define the new model to describe the speed of the corrosion the plating deck cargo. To show the effect of the corrosion to decrease the sections area and the section modulus.

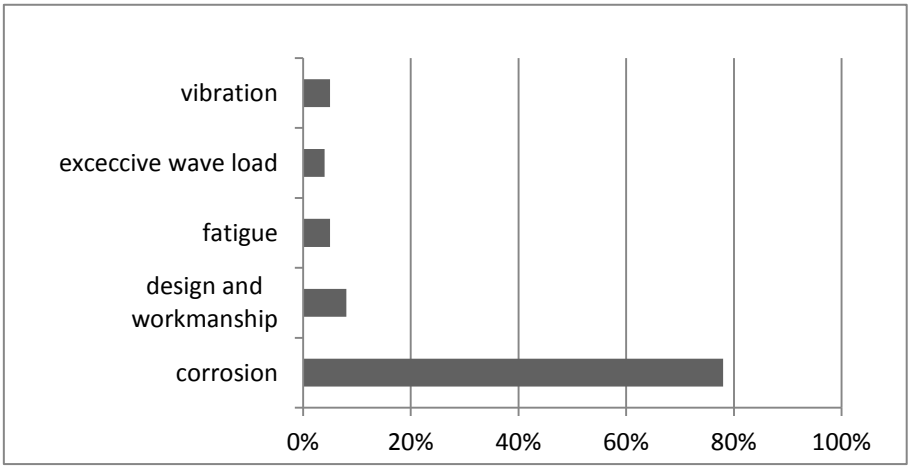

Figure.4.2.The mains factor affecting hull structural failure (M.A.Shama, 2005).

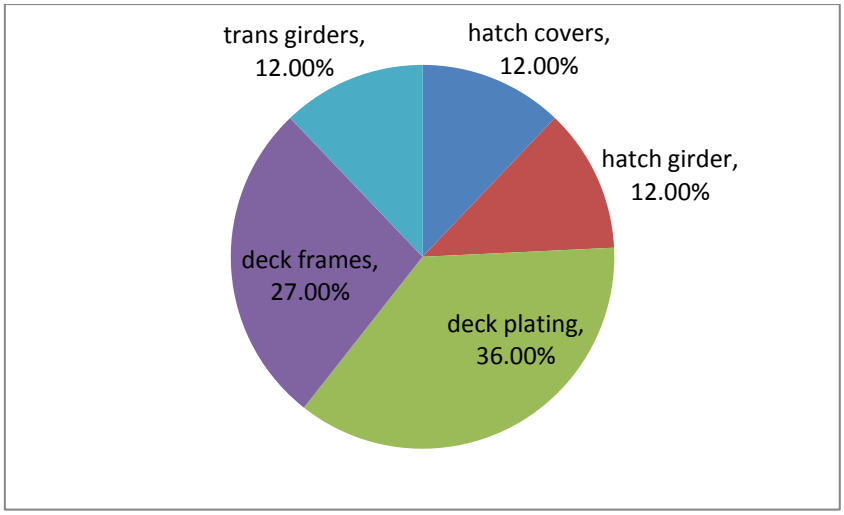

Figure.4.3. Corrosion failures of deck structure (M.A.Shama, 2005).

4.3. Existing Models

In this moment, more research topic focus about the evolution of the corrosion. Since the most of the study, on time dependent the reliability of ship structure, in the beginning, the authors observe the linear decrease of plate thickness with time, considering the constant rate versus time.

However, the experimental data reported by some authors, they look for non-linear model is more appropriate. Therefore, the whole corrosion process can be divided into three stages:

- ✓ The first stage is no corrosion when the time is less than the life coating, since t $\epsilon[0,T_{st}]$,where T_{st} is the life coating .
- ✓ The second stage is the corrosion accelerating, and is produce by pitting corrosion, such as t ϵ $[T_{st}, T_A]$.
- ✓ The third stage is the corrosion decelerating t ϵ $[T_A,T_L]$, where T_L is the life of the structure or the time at which repair and maintenance action takes place.

The wear of thickness due to the corrosion can be calculated by definition [13]:

If t > T_{st}

$$d(t) = d_{\infty}\left[1 - \exp\left(-\left(\frac{t-T_{st}}{\eta}\right)^{\beta}\right)\right] \quad (4.1)$$

In fact, if β=1 then we get the Guedes Soares/Garbatov model:

$$d(t) = d_{\infty}\left[1 - \exp\left(-\left(\frac{t-T_{st}}{\eta}\right)\right)\right] \quad (4.2)$$

In the others way, If we take η=1, using the Taylor series, we keep the first term linear we obtained the Paik /al model:

$$d(t) = d_{\infty}(t - T_{st})^{\beta} \quad (4.3)$$

Finally if β=0.6257, and T_{st} =0 we received Melcher model.

$$d(t) = 0.1207t^{0.6257} \quad (4.4)$$

4.4. A New Model

Discussing the concept of the basic equation of the evolution the depth the corrosion versus time, we can present different way of the evolution, regarding to the parameters β, η, T_{st}, and d_{∞}.

In this present thesis, I follow the next procedure to define the two models the corrosion.

The first procedure, we use the least squares method, and we solve the basic equation .Since to get the parameter β, and η, with fix $d_{\infty} = 3.3\ \text{mm}$, and Tst=5 years, according to the reference data.

So, we solve the basic equation as following the next steps:

$$\frac{1}{1-\frac{d(t)}{d_{\infty}}} = e\exp\left(\left(\frac{t-T_{st}}{\eta}\right)^{\beta}\right)$$

$$\text{lnln}\left[\frac{1}{1-f(t)}\right] = \beta\ln(t-T_{st}) - \beta\ln(\eta)$$

$$\bar{x} = \frac{1}{n}\sum_{i=1}^{n}\text{LnLn}\left[\frac{1}{1-\frac{i}{n+1}}\right]$$

$$\bar{y} = \frac{1}{n}\sum_{i=1}^{n}\ln(t_i)$$

Then, we substitute the estimation of the two parameter β, and η :

$$\hat{\beta} = \frac{\left\{n\sum_{i=1}^{n}\text{Ln}(t_i)\text{LnLn}\left[\frac{1}{1-\frac{i}{n+1}}\right]\right\} - \left\{\sum_{i=1}^{n}\text{LnLn}\left[\frac{1}{1-\frac{i}{n+1}}\right]\sum_{i=1}^{n}\text{Ln}(t_i)\right\}}{\left\{n\sum_{i=1}^{n}(\text{Ln}(t_i))^2\right\} - \left\{\sum_{i=1}^{n}\text{Ln}(t_i)\right\}^2}$$

$$\hat{\eta} = \exp\left(\bar{y} - \frac{\bar{x}}{\hat{\beta}}\right)$$

Finally, we define the model (1) by the formula:

$$d(t) = d_{\infty}\left[1 - \exp\left\{-\left(\frac{t-T_{st}}{26}\right)^{0.2}\right\}\right] \quad (4.5)$$

The second method is to follow the same approach of the Paik/al model, and we developed the basic equation of the corrosion at the second order, using the Taylor series.

Then we get the model (2) as follow the next formula:

$$d(t) = d_{\infty}\left[\left(\frac{t-T_{st}}{\eta}\right)^{\beta} - \frac{1}{2}\left(\frac{t-T_{st}}{\eta}\right)^{2\beta}\right] \quad (4.6)$$

At the end two models are defined; the next step is to get the parameter β, and η, for the model (2).

However, we start to compare the model (2) with Paik/al model keeping for η=1 and we play with different value of β, to reach the target to compare the agreement between model Paik/al and model (2) regarding to the experimental data.

4.5. The Assumed Data and the Description of the Geometry

To start the computation between the candidate models, and the model (1) and (2), we follow the next reference data.

The first data is based to some inspection report of the American Bureau shipping (Offshore Technology Conference, 5 May-8May 2003, see Table.4.1), the second data is presented in Table 4.2.

Table.4.1.The experience data for FPSO structural design (Offshore Technology Conference, 5 May-8May 2003)

		Data (Offshore Technology Conference, 5 May-8May 2003)					
		d(t) evolution the thickness of corrosion (mm)					
	Time (years)	6	10	15	20	25	34
Deck plating	Cargo	0.40	0.66	0.99	1.32	1.65	2.24
	Ballast	0.33	0.55	0.83	1.10	1.38	1.87
side shell	Cargo	0.26	0.44	0.66	0.88	1.10	1.50
	Ballast	0.26	0.43	0.65	0.86	1.08	1.46
Bottom shell	Cargo	0.51	0.85	1.28	1.70	2.13	2.89
	Ballast	0.29	0.49	0.74	0.98	1.23	1.67
Long bulkhead plating	Cargo	0.29	0.49	0.74	0.98	1.23	1.67
	Ballast	0.31	0.51	0.77	1.02	1.28	1.73

Table.4.2. The assumed data (Shengping Qin and Weicheng, 2002)

	Data assumed	Model (2)
Time(year)	d(mm)	d(mm)
1	0	0.00
2	0	0.00
3	0	0.00
4	0	0.00
5	0	0.00
6	0.37	0.39
7	0.53	0.61
8	0.69	0.77
9	0.85	0.91
10	0.99	1.03
11	1.13	1.14
12	1.25	1.22
13	1.35	1.30
14	1.42	1.37
15	1.49	1.43
16	1.53	1.48
17	1.56	1.52
18	1.59	1.55
19	1.6	1.58
20	1.61	1.61
21	1.62	1.63
22	1.62	1.64
23	1.62	1.65
24	1.63	1.65
25	1.63	1.65

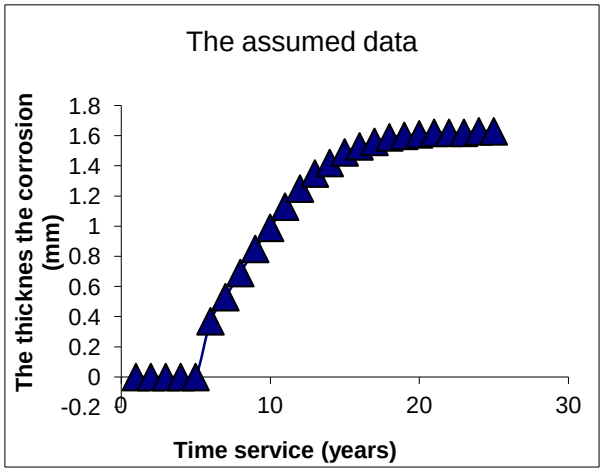

Figure.4.4.The evolution the depth of the corrosion the assumed data (Shengping Qin and Weicheng, 2002).

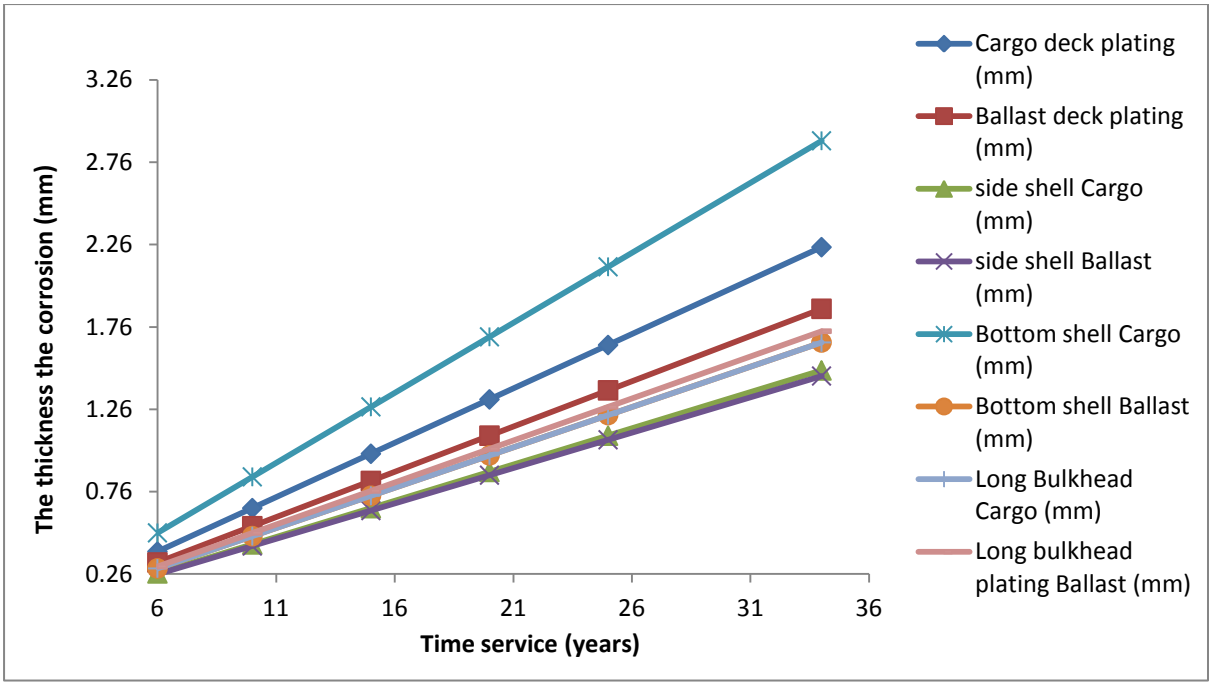

Figure.4.5. The evolution the depth of the corrosion (Offshore Technology Conference, 5 May-8May 2003).

The infinite depth due to corrosion equal to the 3.3 mm for deck section area, and we treat the evolution the uniform corrosion of the section cargo deck (cf. Fig.4.6).

The methodology of the computation, based in the beginning to check the model (2), with the model Paik/al, because we are describing this model regarding to the same method to obtaine the Paik/al model.

Hence, keep $\eta=1$ and we play with the parameter β, to compare the assumed data, and the Paik/al model regarding to the model (2).

Second task, is to study the flexibility of the rate function, for goal to define the relationship between η and β, to estimate these parameters of the model (2), to receive at the end good prediction with the assumed data.

Third task is to compare the candidate models, with model (1), and model (2), regarding to the assumed data.

Finally, we study the variation of the mean section, and the ratio the section modulus of the cargo deck, versus time, subject to the corrosion.

Defining the model of the evolution the section area, and the section modulus of the cargo deck, we can substitute the relationship between weight and the ratio of the section area.

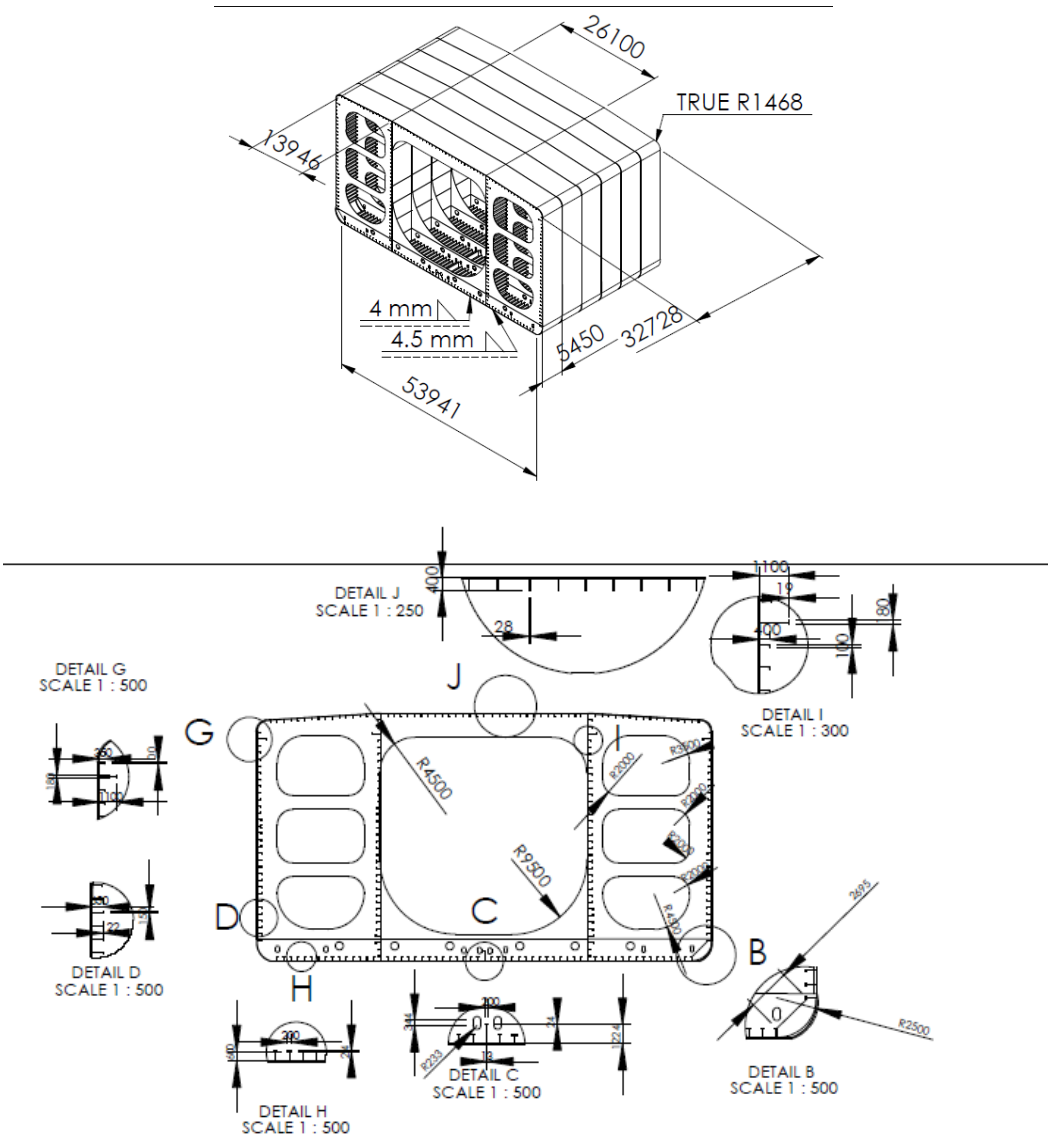

Figure.4.6. The description geometric of the amidships section, for corrosion we focus about section (J).

4.6. The Comparison of the Models

The first, we present the comparison between Paik/al model, and model (2), keeping η=1. Following the results presented in Fig.4.7, we get the Paik/al model far way to the assumed data, in fact the shape of the evolution the corrosion is exponential ,but the long term rate of the corrosion the data very small than the Paik/al model, since the gap is 3.37 mm .

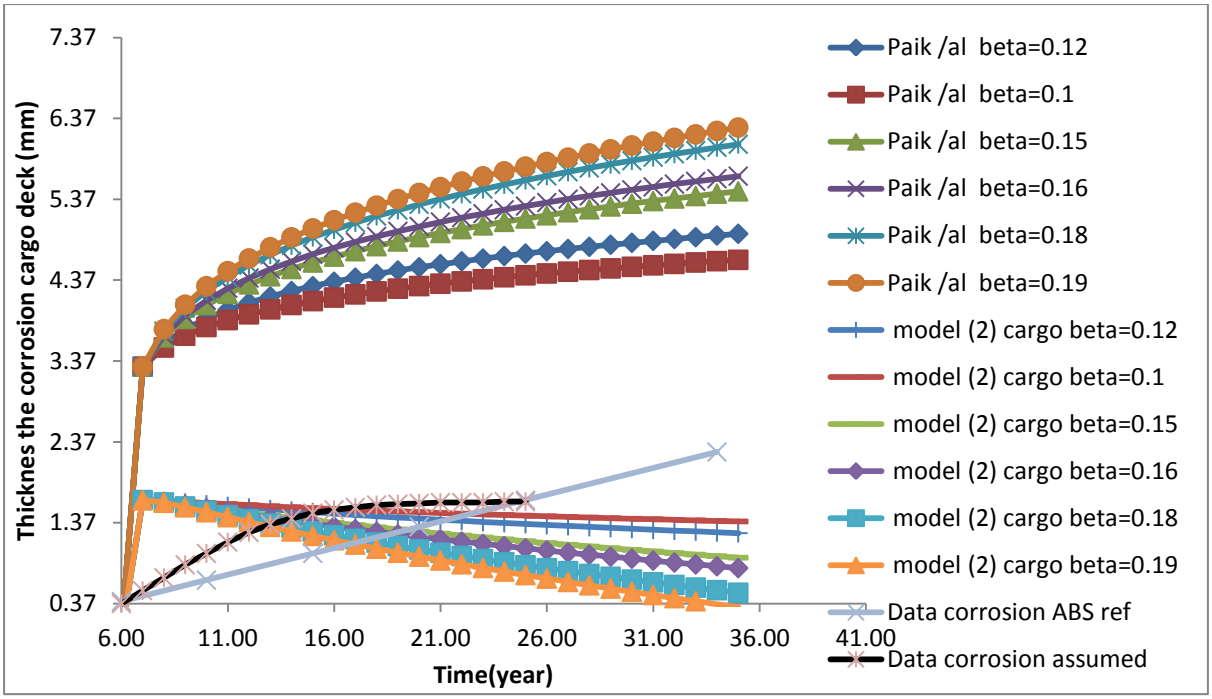

Figure.4.7. Comparison the model (2), the Paik/al model, and the assumed data.

Discussing the agreement of the model (2), and the data assumed ,we find at β=0.1 the long term rate of the model (2) close to the assumed data, in the opposite way the shape of the model(2), after 5 years when the life coating was expired, not save the exponential evolution. For that reason, we need to go deeper to define the true value of the parameters η, and β.

Wherever, we compare model (1), model (2), and candidate models, regarding to the assumed data (cf. Fig.s4.7, 4.8) for cargo and ballast. The Soares model start to be close to the assumed data until 10 years, after that the evolution of the Soares model goes up faster .The model (1) keeps the exponential shape, but the gap very large regarding to the assumed data. The Melcher model had bad prediction to the assumed data.

Finally, the model (2) between 5 and 15 years the evolution of the depth corrosion had bad shape, and that caused by keeping in the second order of Taylor series the value of η=1,so the second term of the model (2) decrease the depth of the corrosion .

In fact from 15 years to infinity, we are close to the same long term rate of assumed data.

However, we analyze the flexibility of the basic equation of the depth corrosion, according to the distribution of the speed the corrosion, to describe the effect of the parameters η, and β.

For aim to keep the model (2), as the perfect model to obtain the good prediction with the assumed data we define the parameters η, and β, following the analysis of the flexibility of the rate function.

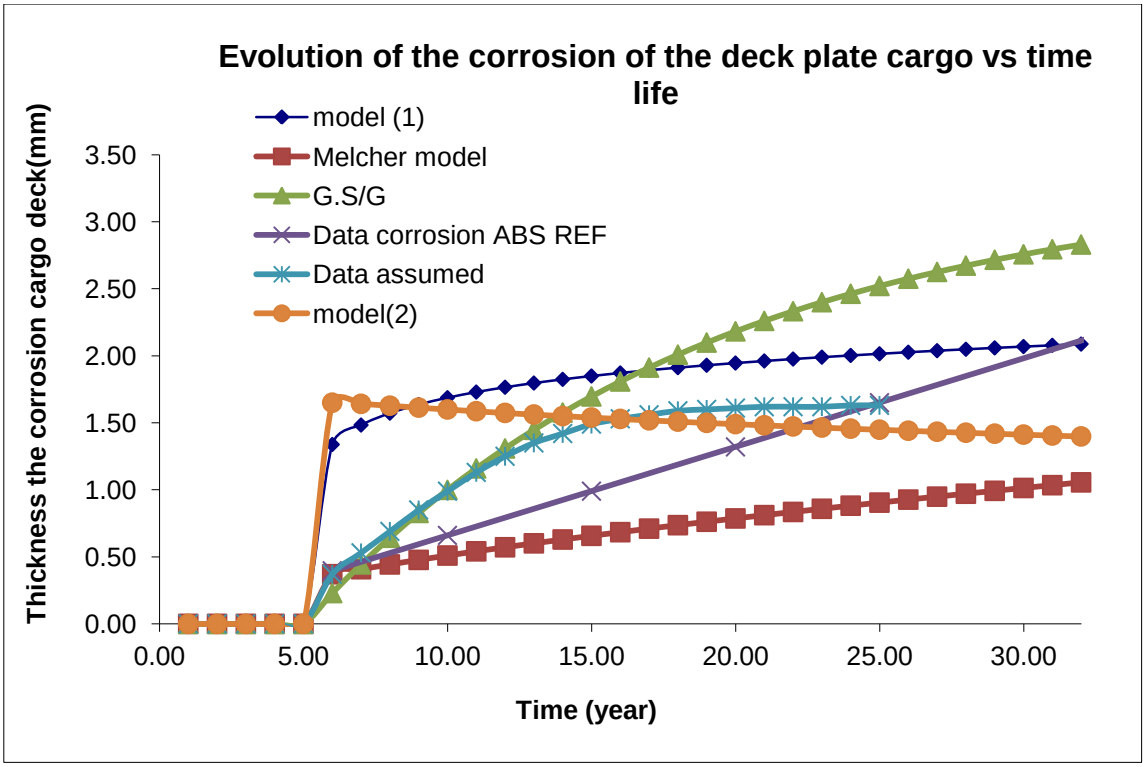

Figure.4.8. Comparison the assumed data, candidate models, model (1), and model (2) for evolution the depth the corrosion of the cargo deck.

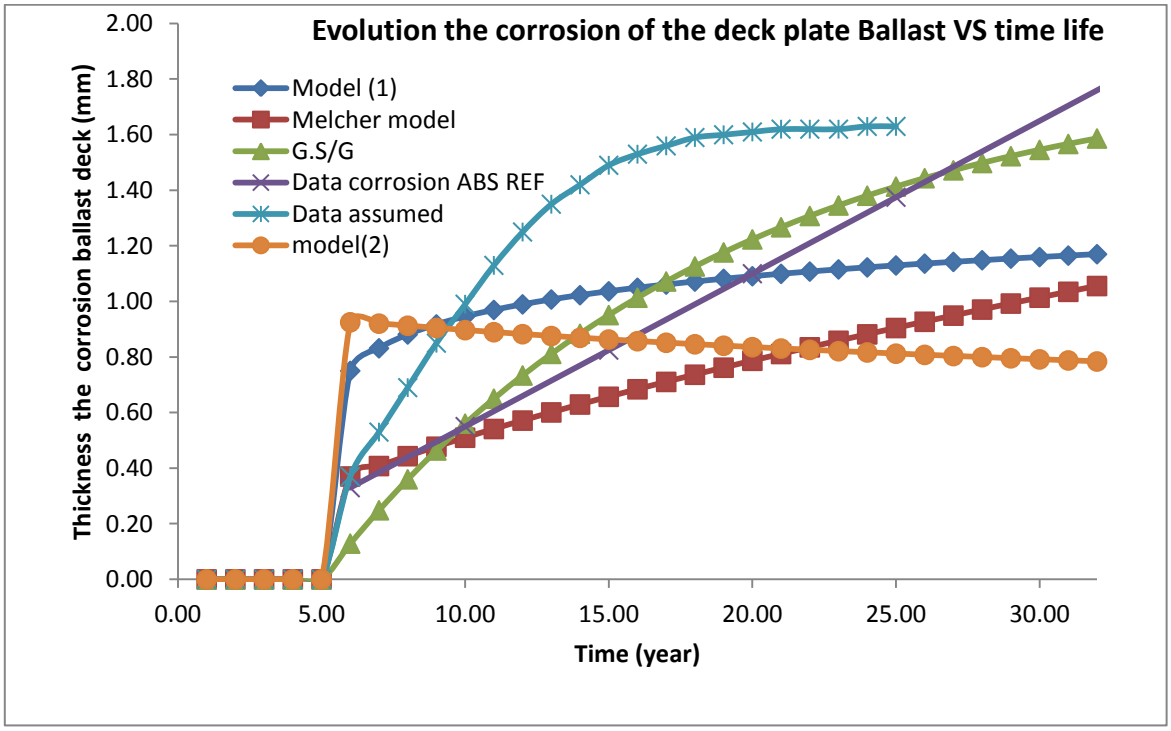

Figure.4.9. Comparison the data assumed data, candidate models, model (1), and model (2) for evolution the depth the corrosion of the ballast deck.

The speed of corrosion is defined as the derivative of the depth versus time.

The speed the corrosion is defined by formula:

$$r(t) = \frac{\mathrm{d}(d(t))}{\mathrm{d}t}$$

$$r(t) = \frac{\mathrm{d}(d(t))}{\mathrm{d}t} = \frac{\mathrm{d}\left(d_\infty \left[1 - \exp\left(-\left(\frac{t-T_{st}}{\eta}\right)^\beta\right)\right]\right)}{\mathrm{d}t}$$

$$r(t) = \begin{cases} 0 \quad if\ t < T_{st} \\ d_\infty \frac{\beta}{\eta}\left(\frac{t-T_{st}}{\eta}\right)^{\beta-1} \exp\left[-\left(\frac{t-T_{st}}{\eta}\right)^\beta\right] \end{cases} \qquad t > T_{st} \quad (4.7)$$

To analyze the flexibility of the rate function, the parameter η is fixed, and β is varied. In the opposite way, fixe β and η varied to reach the relationship between those parameters.

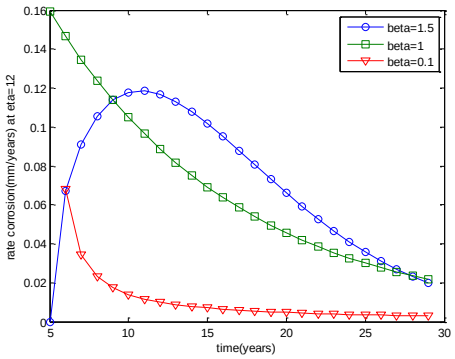

Figure.4.10. The flexibility of the basic equation, fixing η=12.

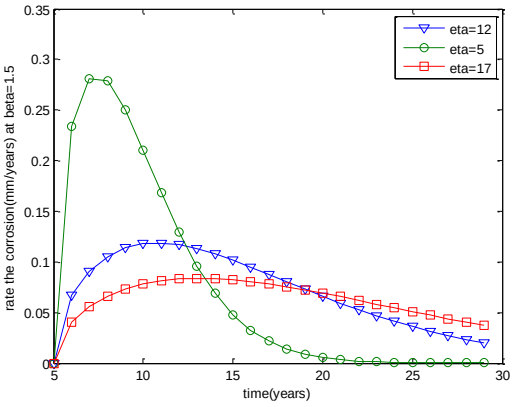

Figure.4.11. The flexibility of the basic equation, fixing β=1.5.

From the analysis the two curves the flexibility of the rate corrosion; we observe two very important points (cf. Figs.4.10, 4.11).

By fixing the parameter η (cf. Fig.4.10), if we increase β the distribution of the rate shifted to be more uniform and to have parabolic shape.

In fact, we fixe β, as we can see in Fig.4.11, increasing η the distribution shifted down, and the pick the rate function goes down, since to get the large distribution.

As we can understand to define the parameters β, and η for the model (2), we run different scenario to receive good agreement with assumed data, and to define the relationship between β, and η. At the end the simulation, we obtain the important results:

Table.4.3.The results of the simulation to get relationship between β, and η

Parameters	β	η	d_{∞}
Run 1	0.62	20	3.3
Run 2	0.7	19.3	3.3

For β= [0.62, 0.7] we describe the ratio between the parameters β and η equal to:

$$\frac{\eta}{\beta} = 30$$

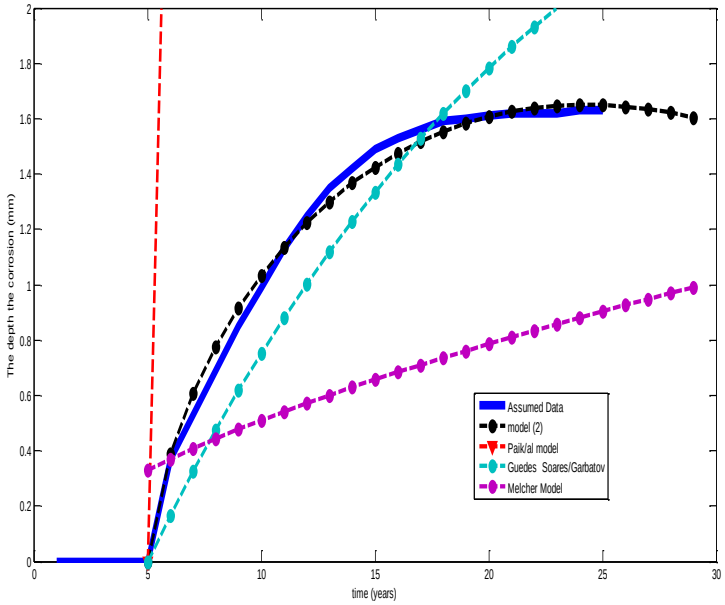

Figure.4.12.The comparison the results between model (2), Soares, Paik/al, Melcher, and the assumed data.

As we can observe, following the Fig.4.12 the model (2) is more close to the evolution of the assumed data. In the opposite way, the Melcher, Paik/al, and the Soares model far way to the assumed data.

Finally, by keeping the second order of the Taylor series and the relationship between β and η equal to 30, in condition as β= [0.62, 0.7], we get good agreement between the model (2), and the assumed data. Regarding to the rate function of the model(2), the function tend to infinite

according to the second order of the model(2), in the opposite way the basic equation of the depth the corrosion goes to zero, when the time tend to infinie the inverse of the exponential tend to zero. Then we substitute the next expression of the two limits the rate function of the model (2), and the basic equation:

$$\lim_{t\to\infty} r(t) = \lim_{t\to\infty} d_\infty \frac{\beta}{\eta}\left(\frac{t-T_{st}}{\eta}\right)^{\beta-1} \text{Exp}\left[-\left(\frac{t-T_{st}}{\eta}\right)^{\beta}\right] = 0 \quad (4.8)$$

$$\lim_{t\to\infty} r(t) = \lim_{t\to\infty} d_\infty \frac{\beta}{\eta}\left\{\left(\frac{t-T_{st}}{\eta}\right)^{\beta-1} - \left(\frac{t-T_{st}}{\eta}\right)^{\beta}\right\} \to \infty \quad (4.9)$$

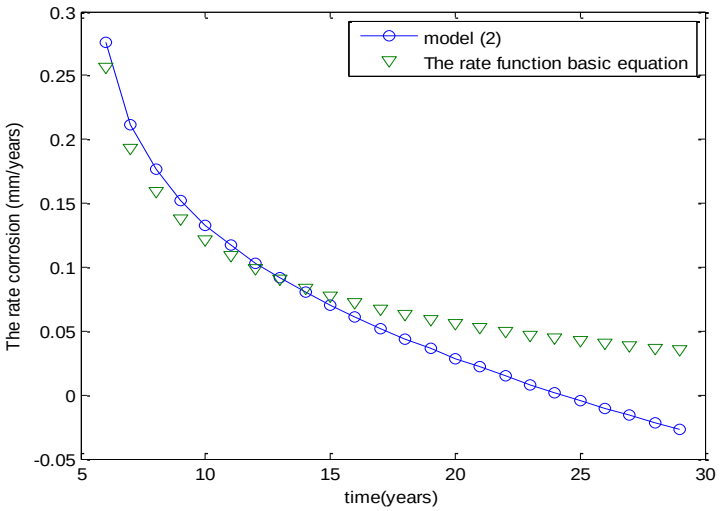

Figure.4.13. The flexibility of the basic equation, and the model (2).

By study the flexibility of the model (2), regarding to the basic equation of the depth corrosion, when time tend to infinite the speed of corrosion will be negligible as we can see the rate function the basic equation goes to zero. For that reason we fix the validity of the model (2) until 25 years as we have the speed of corrosion zero.

4.7. Effect the Corrosion to Reduce the Ratio the Section Modulus and the Section Area of the Deck Cargo

To define the model describing the variation of the ratio the section modulus versus ship service, subject to the uniform corrosion, we follow the next steps.

We consider the section (J) as presented in the drawing Fig.4.6 the cargo deck.

The section modulus is calculated as follow the formula:

$$Z = \frac{I}{\mathrm{y}} \quad (4.10)$$

We define the ratio of the section modulus by the formula $\mathrm{RSM} = \frac{Z}{Z_0}$, and the ratio the section area following the formula: $RSA = \frac{SA}{SA_0}$ (4.11).

where *I*: is the total inertia of the amidships section, and y: is the distance from the neutral axis to deck.

For the tanker ship VLCC, as our model in this present thesis, we have such details:

The initial inertia equal 9.43 10^{14} mm^4, and the position of the neutral axis equal 14.35 m.

Then the initial section modulus was Z_0=58732492940.4847 mm^3.

Basic to the evolution the depth the corrosion of the cargo deck, using the assumed data, and the model (2), we calculate at selection year the lost of the section modulus, and the section area. Then, we get the result presented in Fig.4.14, as we can observe the model of the lost the section modulus and the section area versus ship service, track the polynomial function the order six. To simplify the polynomial model of the ratio section modulus versus time, it is important to predict easy function to define the variation of the section modulus due to the uniform corrosion, by fitting the curve (cf. Fig4.15) after 5 years following cubic function.

Then, the evolution the section modulus versus time follows the formula:

$$RSM = 1 - 7.610^{-6}t^3 + 4.810^{-4}t^2 - 0.01t \quad (4.12)$$

Similar, the section areas vary follow the formula:

$$RSA = 1.1 - 1.210^{-5}t^3 + 9.210^{-4}t^2 - 0.023t \quad (4.13)$$

We summary the results, we lost 5% the section modulus of the deck during 15 years the ship service, and for the mean section area we lost 9.3% during 25 years.

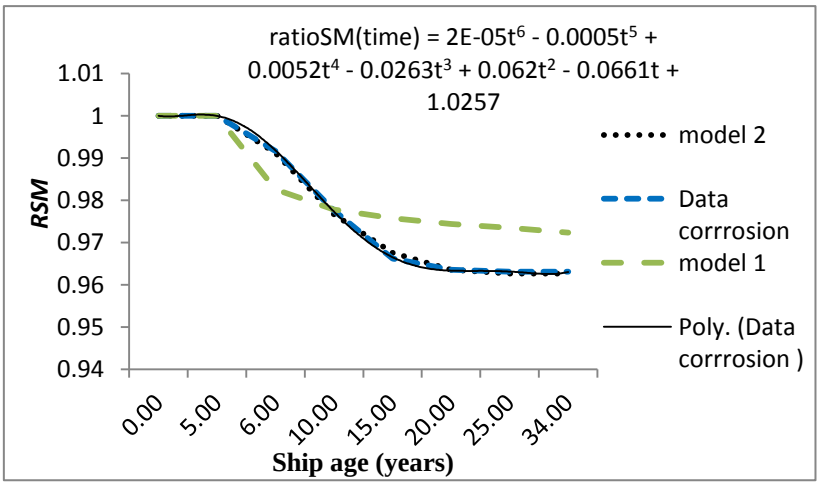

Figure.4.14.The section modulus versus ship age, subject to the uniform corrosion.

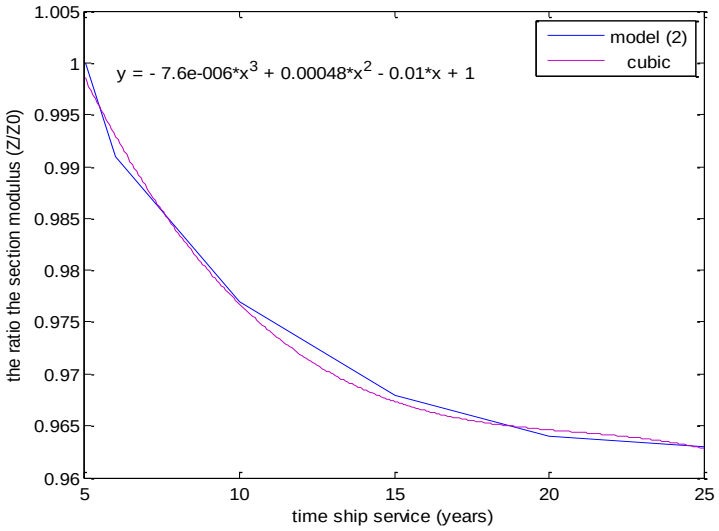

Figure.4.15. The fit the curve section modulus versus ship age, subject to the uniform corrosion.

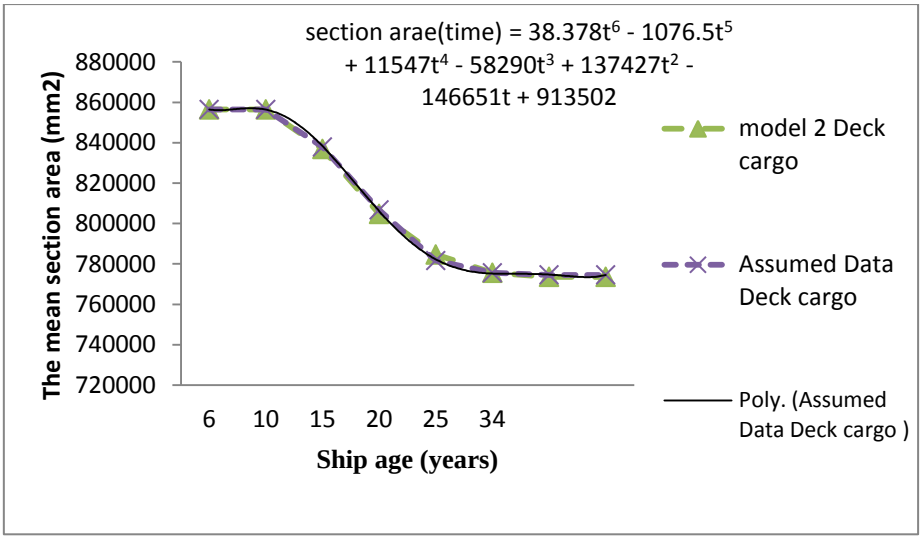

Figure.4.16. The mean section area of the deck versus ship age, subject to the uniform corrosion.

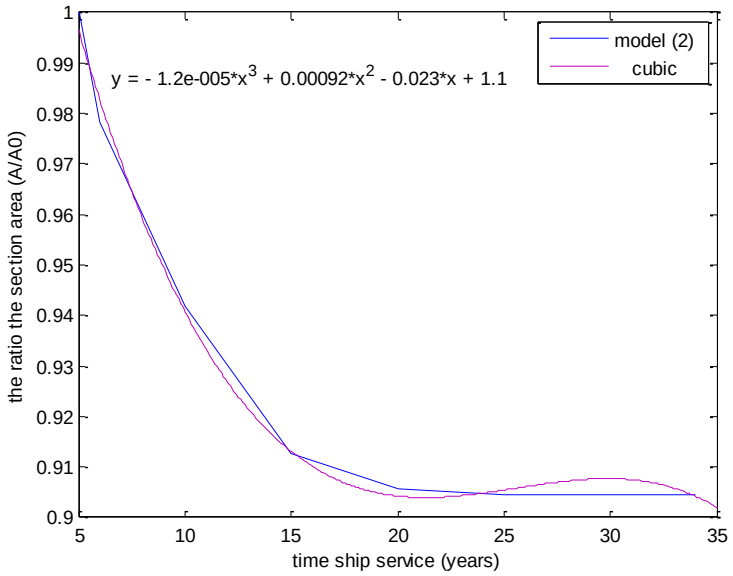

Figure.4.17. The fit the curve section area versus ship age, subject to the uniform corrosion.

To assume the weight the structure of the deck, we propose the standard steel material has the density equal 7850 Kg/m^3; and the yielding stress equal 320 MPa, the details are presented in Table.4.4:

Table.4.4. Mechanical properties of some typical structural steels. Available from http://nptel.iitm.ac.in/courses/IITMADRAS/Design_Steel_Structures_I/1_introduction/3_properties_of_steel.pdf.Design of Steel Structures Prof. S.R.Satish Kumar and Prof. A.R.Santha Kumar.

Type of steel	**Designation**	**UTS(MPa)**	**Yield strength (MPa)**			**Elongation Gauge 5.65(s0)^0.5**	**Charpy -notch values joules (min)**
			Thickness (mm)				
			<20	20-40	>40		
standard structural steel	Fe4 10A	410	250	240	230	23	27
	Fe4 10B	410	250	240	230	23	27
	Fe4 10C	410	250	240	230	23	27
Micro alloyed high strength steel	Fe440	440	300	290	280	22	
	Fe540	540	410	390	380	20	
	Fe590	590	450	430	420	20	

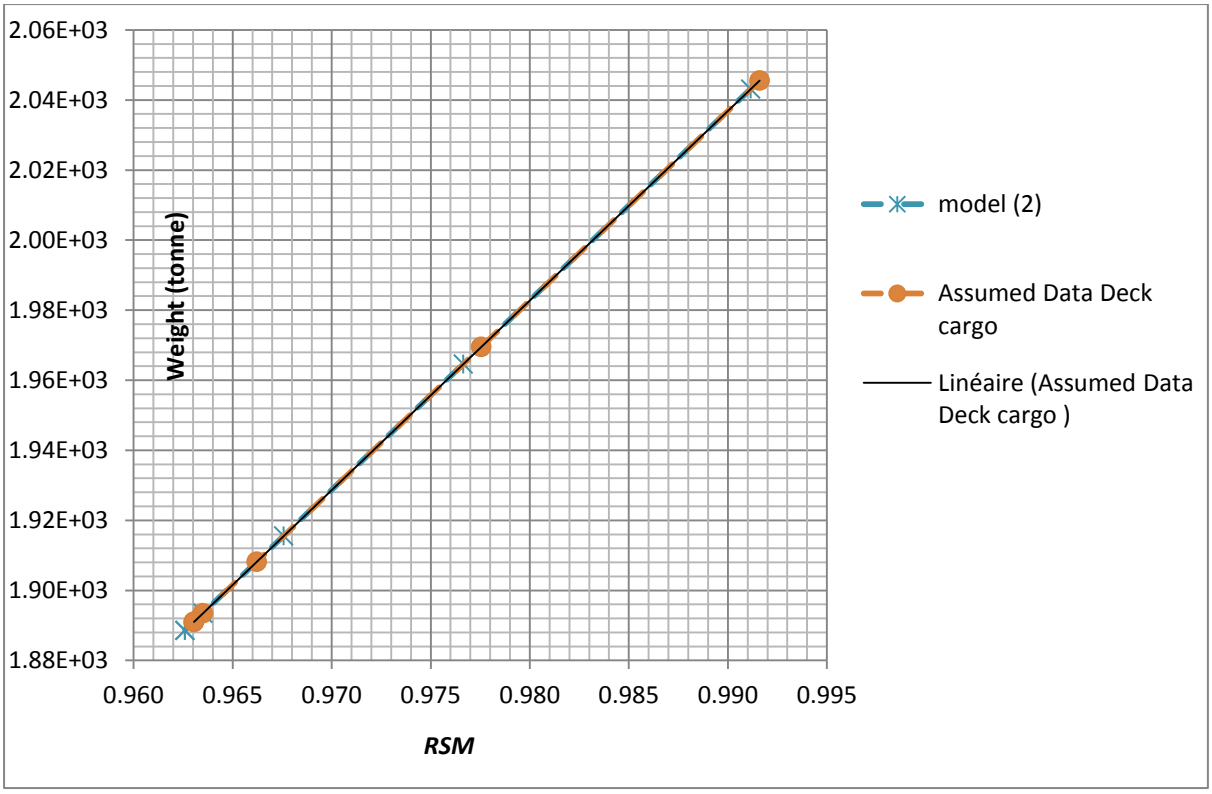

Figure.4.18. The relationship between weight and ratio section modulus of the deck tanker SHVLCC.

From the Fig.4.18 above, the weight is linear with the ratio the section modulus of the deck touched by uniform corrosion. Then, we describe the model weight versus the section modulus follow the formula:

$$Weight\ (tonne) = 5410.9 * RSM - 3319.9 \quad (4.14)$$

The analysis of the corrosion model, have large point to touch. In fact, the initial work is to define the model (2), to obtain the depth of the corrosion, comparing with the assumed data.

Using model (2) we get good prediction to assumed data. Since, we find the reduction of the section modulus and the section area follow polynomial model the order six. Finally we lost 5% the section modulus of the deck during 15 years the ship service, and for the mean section area, we lost 9.3% during 25 years.

From point of view engineer, the critical area can be check by inspection is the side at draft level, where the shear forces very high at position 0.3L and 0.7L from aft part.

5. APPLICATION: ULS CAPACITY THE SINGLE HULLVLCC TANKER SHIP SUBJECT TO THE EFFECT THE CORROSION

5.1 Introduction

This chapter discusses the ultimate strength of the ship tanker, regarding to the effect the general corrosion.

For that reason, we follow the procedure of the CSR to touch all the point of analysis, such as the subject is to define the reduction the ultimate strength capacity of the vessel.

In the other way, is to make computation between the different candidates model, presented in the Chapter one, comparing with as getting by CSR.

In the beginning, we identify the external loading, to describe the design bending moment requirements.

Second point, is to examine the ultimate strength of the plates, stiffened panels, and the progressive collapse of the hull girder.

Using the ABS data, we acquire the thickness of the corrosion in the each zone the ship in the deck, in the bottom, and in the side after 25 years service.

Reducing the section modulus of the element structure by effect of the corrosion, decrease the ultimate bending moment, in the hogging and sagging, with influence of the neutral axis position to reach the collapse of the structure.

5.2. Design Loading Condition

Using a small script on Matlab we define the longitudinal bending moment, following the DNV Rules and we get the next results:

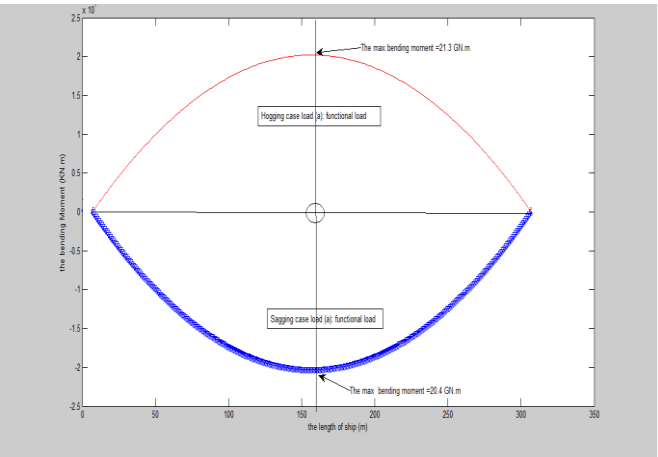

Figure.5.1. The bending moment case (1).

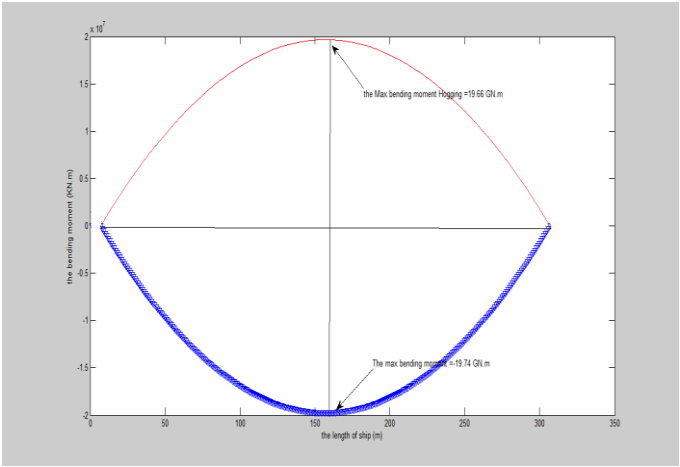

Figure.5.2. The bending moment case (2): the functional +environmental load.

Such as the case (1) is the functional load, the second case (2) recommended by DNV rules is the functional and environmental load. In this present thesis we consider the case (1).

In sagging, the oil cargo tanks will be full, and the ballast tanks are empty, the draught is 20 m. In hogging, the draught is 8 m, the oil cargo tanks will be empty, and the ballast tanks should be full.

Following the DNV Rules, we substitute the static pressure at bottom and lower side, and the design stress getting by Nauticus Hull DNV software. In sagging the total pressure at bottom 200 KN/m^2 and in the lower side is 27.8 KN/m^2, and in hogging the total pressure at bottom 65 KN/m^2 and in the lower side is 237.1 KN/m^2.

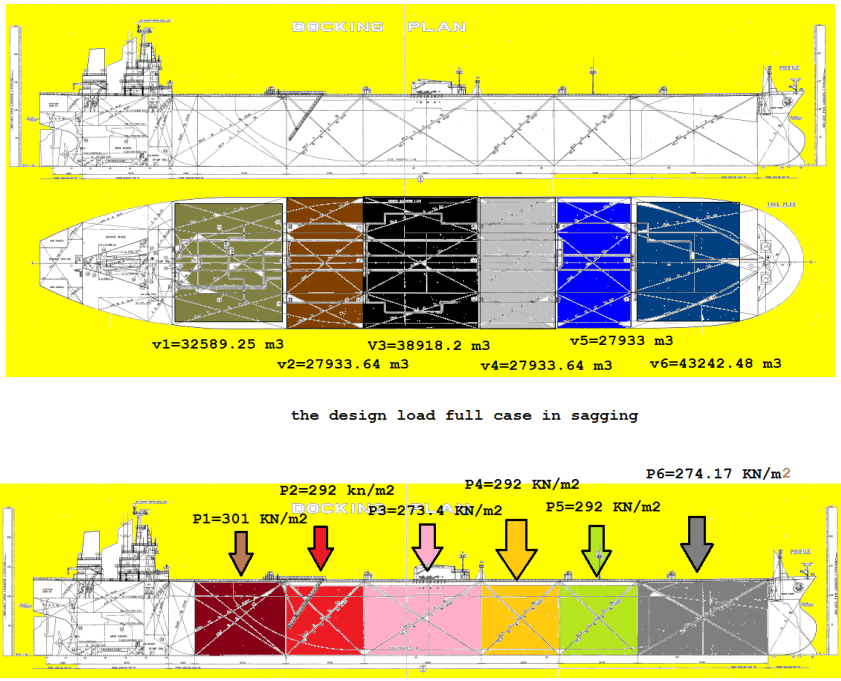

Figure.5.3. Design internal load of tanker ship in sagging.

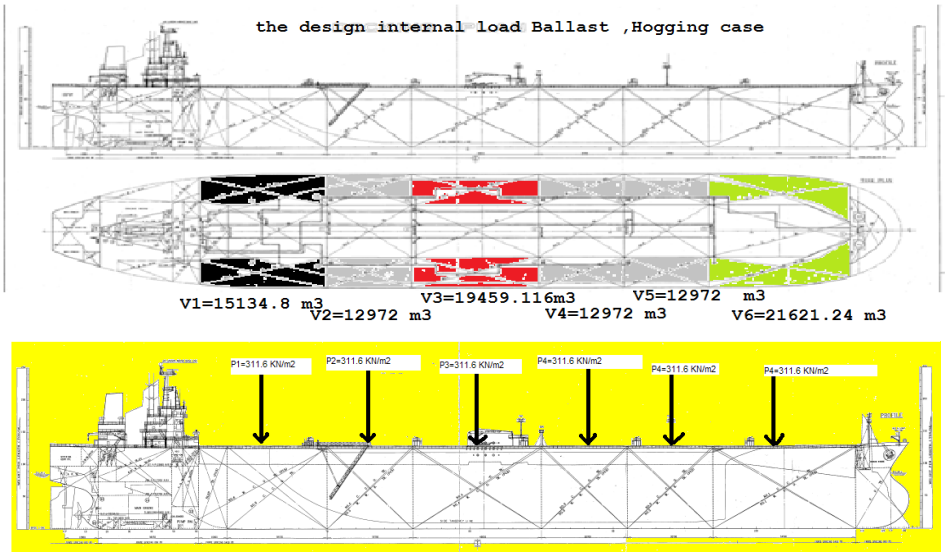

Figure.5.4. Design internal load of tanker ship in hogging.

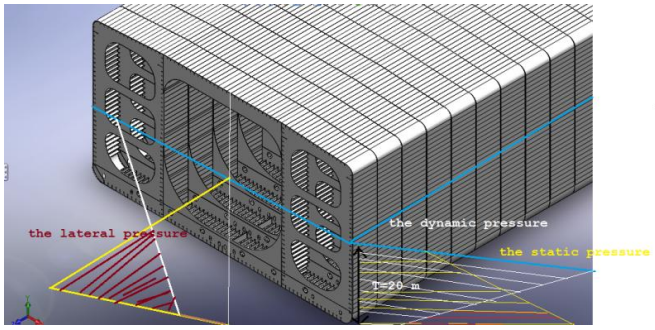

Figure.5.5. Distribution of the lateral pressure in sagging (full load).

In case the sagging we have high draught ,in fact the static pressure will be primordially than dynamic, since the bottom applied load resulting between the dynamic and static is 200 KN/m^2 ,and in the lower side equal 27.8 KN/m^2 (cf. Fig.5.5) .

In the hogging case, the more effect of pressure will be the dynamic pressure, because the draught was small (draft=8m), for that reason we search out the difference between dynamic and static applied load in the bottom equal 65 KN/m^2,and in the lower side equal to 237.1 KN/m^2.

5.3. Results of the Design Stress, Shear Forces, and von Mises Stress Criteria

After done all the data, we present the design stress, shear stress, and the von Mises stress for the mid ships section as showing in Figs.5.6, 5.7:

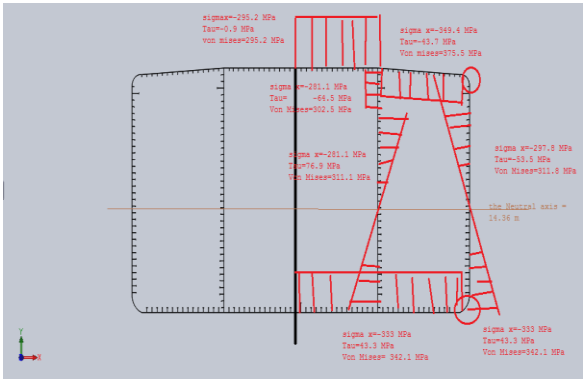

Figure.5.6. Distribution of the global stress, the shear stress and the von Mises stress in sagging.

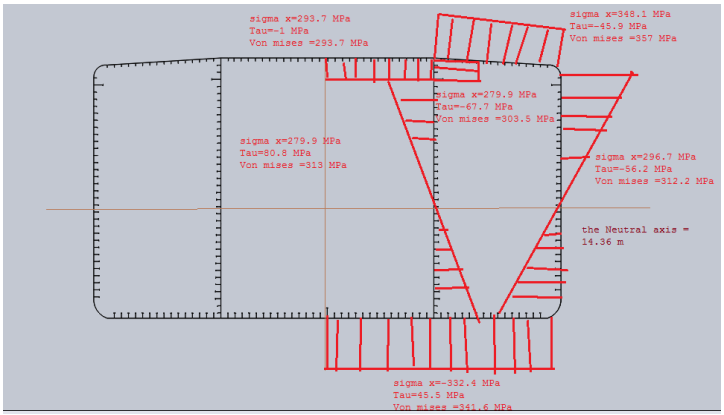

Figure.5.7. Distribution of the global stress, the shear stress and the von Mises stress in hogging.

5.4. The Ultimate Limit State of Plate

Starting by Case (2) (ballast condition, hogging), for test buckling the strength analysis for stiffened panels in compression is evaluated (bottom, lower longitudinal bulkhead, and lower side).

Considering ship as beam, the working stress is described. In hogging the longitudinal stress in the bottom equal -332.4 MPa, and the transverse stress equal -99.72 MPa.

The stiffeners spacing is 870 mm and the frame spacing was 5450 mm.

In hogging the plate bottoms was in compression, and for test buckling the plate is take-off between two stiffeners and two frames.

After fixing the parameters of simulation to run DNV PULS, the boundary condition was clamped supports, and the input value of model imperfection was calculated.

Following the DNV Rules the total pressure in the bottom 1 equal 65 KPa and the internal pressure due to the liquid ballast was 20.55 KPa, then the lateral pressure apply in the plate bottom 1 was 0.044 MPa.

In fact the lateral pressure applying in the lower side equal to 0.216 MPa. We consider as well the quality of imperfection the plate.

Table.5.1.The working stress using to assess ULS and buckling under PULS software

	Working stress	σ_x(Mpa)	σ_y(Mpa)
Hogging	Bottom 1	332,4	99,72
	Bottom 2	332,4	99,72
	Lower longitudinal bulkhead	279,9	0
	Lower side	312,2	0
Sagging	Deck 1	295,2	88,56
	Deck 2	349,4	104,82
	Upper side 1	281,1	0
	Upper side 2	297,8	0

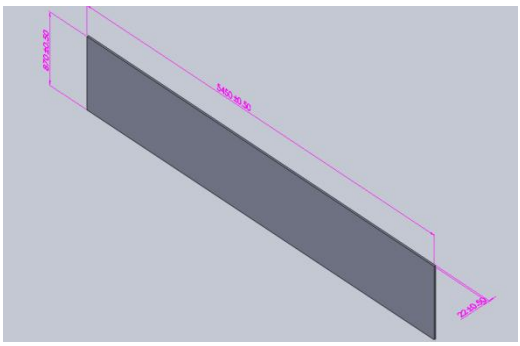

Figure.5.8. The dimension the plate bottom 1.

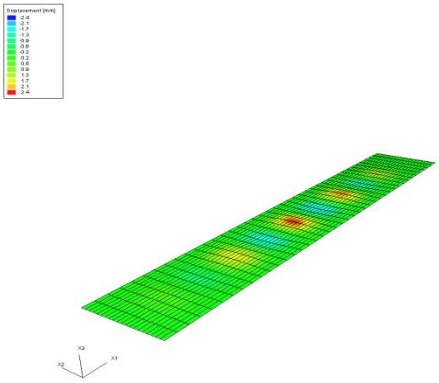

Figure.5.9. Ultimate stress capacity the plate bottom1, with lateral pressure (P=0.044 MPa; and the initial deflection the plate=1.48 mm), the maximum displacement 2.4 mm.

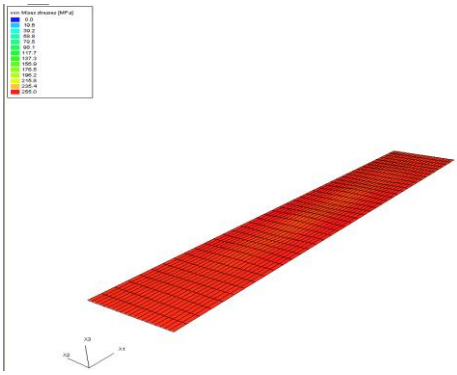

Figure.5.10. The von Mises stress the plate bottom1, with lateral pressure (P=0.044 MPa; the initial deflection the plate =1.48 mm), the maximum stress 255 MPa.

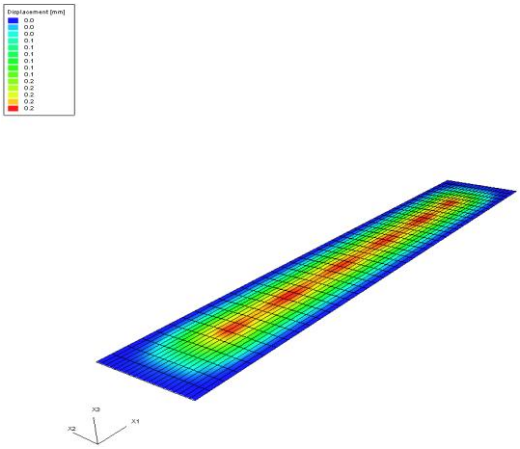

Figure.5.11.Distribution the pressure of the plate bottom1, with lateral pressure (P=0.44 MPa; and the initial deflection the plate =1.48 mm), the maximum displacement 0.2 mm.

According to the results the DNV PULS, the plate cannot support the entire load applied, and then the net scantling of the thickness bottom plate will be not acceptable to avoid the buckling is confirmed.

The factor usage of the plate after analysis was 1.17 greater than 1, as we take like allowable usage factor. The allowable usage factor according to the definition received by DNV Rules should be 1 the defaults value proposed by DNV PULS.

Table.5.2. ULS computation of the plate bottom 1 by Paik model, and DNV PULS

			DNV PULS with (P=0,044 Mpa)		**DNV PULS without Lat,pressure**	
Wp0	β	Paik	σ_U(Mpa)	Usage Factor	σ_U(Mpa)	Usage Factor
1.48	1.38	222.05	284	1.17	285	1.17

In Table 5.2 above, the effect of the lateral pressure to decrease the ultimate strength of the plate is described, for thickness plate 22 mm the ultimate stress equal 284 MPa with lateral pressure, but in case without lateral pressure we obtained 285 MPa. The gap between ultimate stress evaluated by Paik model and the PULS DNV software is large; it was 60 MPa, maybe the Paik model under estimate the initial imperfection.

Following the same step to study ultimate strength of the plate bottom1, the summary results the plates of the tanker ship, during the five years of the service, as showing in Table 5.3.

Table.5.3. The summary results the ultimate capacity the plate at amidships section of the tanker ship, for 5 years the ship service, using DNV PULS

					DNV PULS	
	Plate (less than 5 years service)	W_{p0} (mm)	β	Paik model	σ_U(Mpa)	Difference between Paik and DNV PULS (%)
Hogging	Bottom 1	1.48	1.38	222.05	284	21.81%
	Bottom2	1.71	1.60	213.40	281	24.06%
	lower longitudinal bulkhead	1.55	1.48	218.03	253	13.82%
	Lower side	1.72	1.65	211.38	245	13.72%
Sagging	Deck1	1.76	1.64	211.65	281	24.68%
	Deck2	1.67	1.55	215.06	283	24.01%
	upper longitudinal bulkhead	2.00	1.91	200.61	246	18.45%
	Upper side	1.72	1.65	211.38	251	15.79%

Table.5.4. The ultimate capacity collection the test buckling the plate at amidships section of the tanker ship

		Bottom1 plate (p=0.044 Mpa); W_{p0} =1.48 mm					
Hogging	$\sigma_{U,x}$(Mpa)	254	283	290	245	151	58
	$\sigma_{U,y}$(Mpa)	0	79	176	262	292	277
	$\sigma_{U,x}/\sigma_Y$	1,00	1,11	1,14	0,96	0,59	0,23
	$\sigma_{U,y}/\sigma_Y$	0,00	0,31	0,69	1,03	1,15	1,09
		Plate bottom 2 (p=0.044 Mpa); W_{p0}=1.71 mm					
	$\sigma_{U,x}$(Mpa)	252	281	287	243	149	57
	$\sigma_{U,y}$(Mpa)	0	79	175	260	287	273
	$\sigma_{U,x}/\sigma_Y$	0,99	1,10	1,13	0,95	0,58	0,22
	$\sigma_{U,y}/\sigma_Y$	0,00	0,31	0,69	1,02	1,13	1,07
		Plate lower long bulkhead ; W_{p0}=1.55 mm					
	$\sigma_{U,x}$(Mpa)	253	282	289	244	150	56
	$\sigma_{U,y}$(Mpa)	0	79	176	262	290	271
	$\sigma_{U,x}/\sigma_Y$	0,99	1,11	1,13	0,96	0,59	0,22
	$\sigma_{U,y}/\sigma_Y$	0,00	0,31	0,69	1,03	1,14	1,06
		plate lower side (P=0.216 MPa); W_{p0}=1.72 mm					
	$\sigma_{U,x}$(Mpa)	251	279	286	242	148	56
	$\sigma_{U,y}$(Mpa)	0	78	74	260	285	271
	$\sigma_{U,x}/\sigma_Y$	0,98	1,09	1,12	0,95	0,58	0,22
	$\sigma_{U,y}/\sigma_Y$	0,00	0,31	0,29	1,02	1,12	1,06
Sagging		**Plate deck1; W_{p0}=1.76 mm**					
	$\sigma_{U,x}$(Mpa)	251	279	286	242	148	56
	$\sigma_{U,y}$(Mpa)	0	78	174	260	285	271
	$\sigma_{U,x}/\sigma_Y$	0,98	1,09	1,12	0,95	0,58	0,22
	$\sigma_{U,y}/\sigma_Y$	0,00	0,31	0,68	1,02	1,12	1,06
		Plate deck2 ; W_{p0}=1.67 mm					
	$\sigma_{U,x}$(Mpa)	252	281	288	244	150	57
	$\sigma_{U,y}$(Mpa)	0	79	175	261	289	274
	$\sigma_{U,x}/\sigma_Y$	0,99	1,10	1,13	0,96	0,59	0,22
	$\sigma_{U,y}/\sigma_Y$	0,00	0,31	0,69	1,02	1,13	1,07
		Plate upper long bulkhead; W_{p0}=2.1mm					
	$\sigma_{U,x}$(Mpa)	246	270	274	230	133	52
	$\sigma_{U,y}$(Mpa)	0	76	167	246	257	249
	$\sigma_{U,x}/\sigma_Y$	0,96	1,06	1,07	0,90	0,52	0,20
	$\sigma_{U,y}/\sigma_Y$	0,00	0,30	0,65	0,96	1,01	0,98
		Plate upper side ; W_{p0}=1.81 mm					
	$\sigma_{U,x}$(Mpa)	251	280	286	242	148	56
	$\sigma_{U,y}$(Mpa)	0	78	174	260	285	271
	$\sigma_{U,x}/\sigma_Y$	0,98	1,10	1,12	0,95	0,58	0,22
	$\sigma_{U,y}/\sigma_Y$	0,00	0,31	0,68	1,02	1,12	1,06

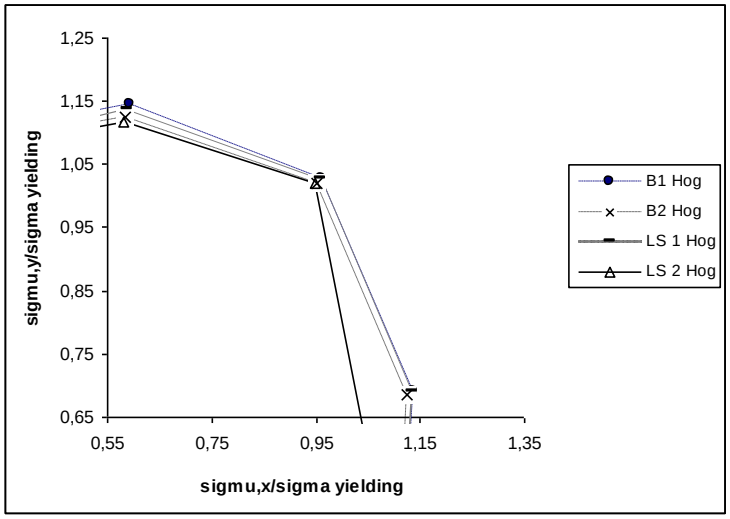

Figure.5.12. The ultimate capacity of the plate bottom and side in hogging (ballast case).

According the above curve (cf. Fig.5.12), the plate of the lower side cannot support all the longitudinal stress, but the plate bottom and plate the longitudinal bulkhead can be resistive. In hogging the plate of the lower side and plate bottom 2 can be buckled faster in the beginning because have small strength capacity to support the longitudinal stress in the ballast load.

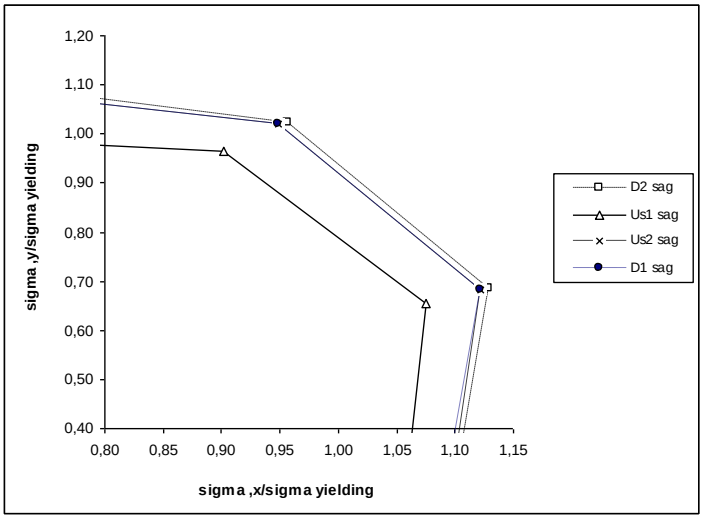

Figure.5.13. The ultimate capacity of the plate deck and side in sagging (full load).

The above curve (cf. Fig.5.13) the ultimate capacity of the plate upper longitudinal bulkhead very lower than the plate of the side, the deck1 and the deck 2.

In fact, the plate of the upper longitudinal bulkhead, and plate the deck1 can be buckled in the beginning in case the full load (sagging).

Finally we conclude, in the hogging (ballast load) the ultimate capacity of the plate lower side, and the plate bottom 2 have small strength and then the risk to buckle is higher.

In sagging (full load), the plate of the upper longitudinal bulkhead, and deck 1 can be lost the strength and will be buckled faster than the other plate.

However, comparing the ultimate stress of the plates, getting by PULS using non-linear theory, with the Paik model, we set up the results presented in Table 5.5, with assessment of the error between the PULS and Paik model. The large error was 24%, then we can consider the results getting by PULS are quite close to the analytical results using Paik model to evaluate the ultimate capacity of the plate.

By considering the effect of the general corrosion, the reduction the ultimate strength the plate after 25 years of the ship service is discussing. According to the results getting in Table5.5, we describe at different area the single hull tanker the gap the lost the ultimate strength, since to define the critical area has been the risk to be failure faster.

The difference between Paik model and PULS results, not so higher, since the gap smaller than 20%, and according to the Table 5.6 including effect the general corrosion ,the ultimate strength of the plate reduce by 8% for the bottom ,the lower side, and the lower longitudinal bulkhead ,in case the hogging.

However, in sagging the ultimate strength of the plate reduces by 8% for the deck and the upper side, except for upper longitudinal bulkhead the ultimate strength reduces by 10%.

The critical area for the tanker ship is the longitudinal bulkhead; as we conclude the ultimate strength reduce by 10 %, because the thickness the longitudinal bulkhead decrease in the two sides, the first side the oil cargo, and the second is the water ballast.

Table.5.5. The summary results the ultimate capacity the plate at midships section of the tanker for 25 years the ship service, using DNV PULS

	Plate (after 25 years service)	$\boldsymbol{W_{p0}}$ (mm)	β	Paik model	$\boldsymbol{\sigma_{U,x}}$ (MPa)	Difference between Paik /DNV PULS (%)
Hogging	Bottom 1	1.64	1.53	216.23	261	17.15%
	Bottom2	1.83	1.71	208.92	257	18.71%
	lower longitudinal bulkhead	1.66	1.58	213.95	233	8.18%
	Lower side	1.84	1.75	207.02	223	7.16%
Sagging	Deck1	1.93	1.80	205.13	256	19.87%
	Deck2	1.79	1.67	210.26	259	18.82%
	upper longitudinal bulkhead	2.18	2.08	193.73	223	13.13%
	Upper side	1.84	1.75	207.02	231	10.38%

Table.5.6. The summary results the reduction the ULS of the plate

		Reduction the ultimate strength the plate
Hogging	Bottom 1	8.10%
	Bottom2	8.54%
	lower longitudinal bulkhead	7.91%
	Lower side	8.98%
Sagging	Deck1	8.90%
	Deck2	8.48%
	upper longitudinal bulkhead	9.35%
	Upper side	7.97%

5.5. The Ultimate Limit State of Stiffened Panel

The target is to assess the ULS of the stiffened panels, by four methods, namely DNV PULS, Hughes, Paik model, and Rahman progressive collapse algorithm.

The Fig.5.14 show the dimension of the stiffened panels bottom1 under study, and Table.5.7 show the different dimensions of the stiffeners and the plates.

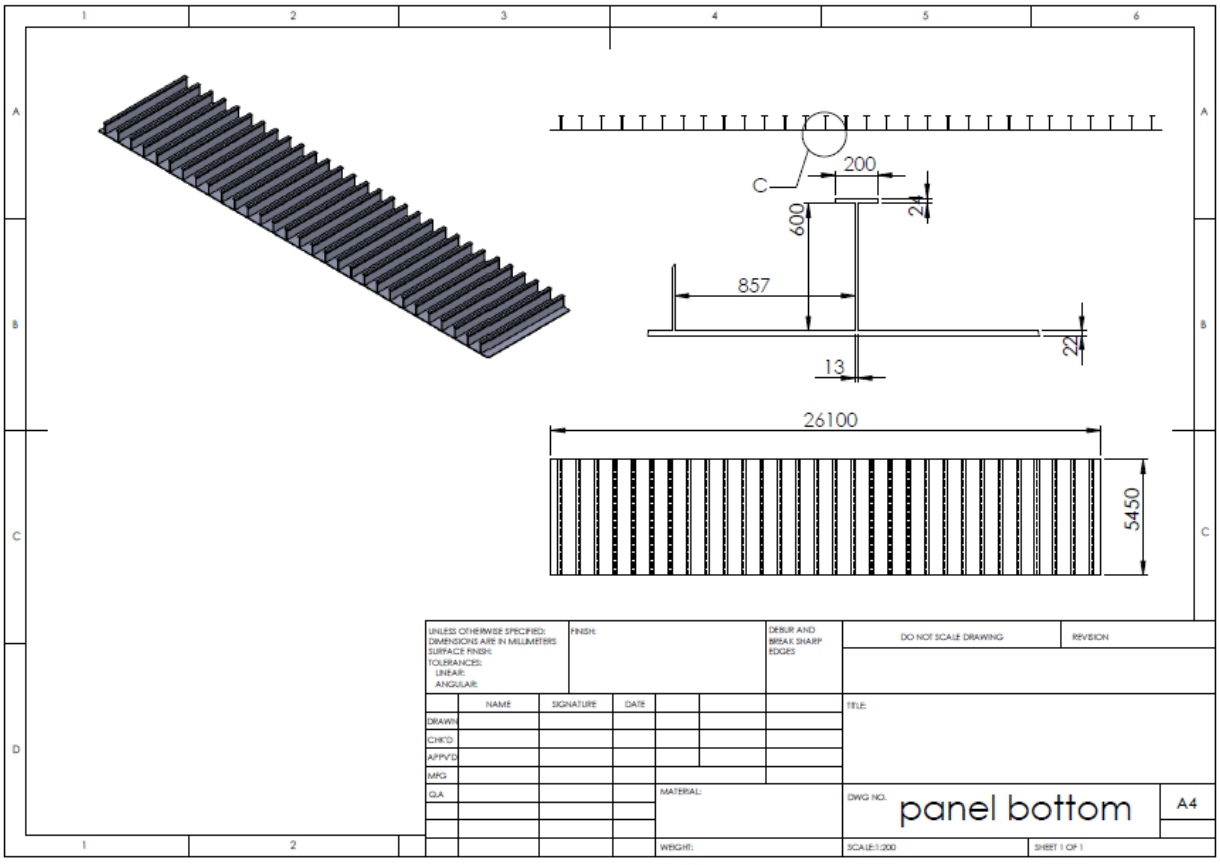

Figure.5.14.The plan the stiffened panel bottom 1.

Table.5.7. The dimension the stiffened panel bottom 1

Element	e_i(breath) mm	b_i(height) mm
Effective plating	870,00	22
Web	13	600
Flange	200	24
The neutral axis	181,64	mm
λ	0,25	
β	1,38	
b_e (effectif width)	0,804	m

For the purpose of the present comparison ,welding residual stress are not considered, in fact we consider the initial imperfection of the stiffeners proposed by defaults in DNV PULS (υ_{0s}=5.45 mm, W_{0s}=5.45 mm, and W_{p0} =4.35 mm).

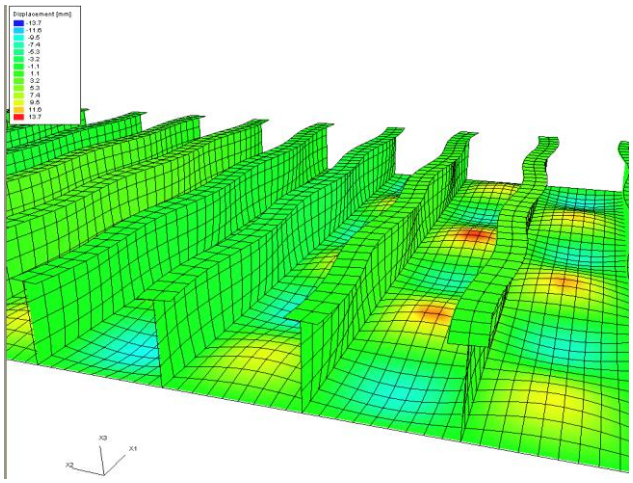

Figure.5.15. The ultimate local capacity stress of the panel bottom, with lateral pressure (P=0.044 MPa), (the initial deflection of stiffeners=5.45 mm and 4.35 mm for plate), the maximum displacement 13.7 mm.

The stiffened panels were buckled, because the applied load more higher than the ultimate strength of the panel (cf. Table 5.10), the usage factor equal 1.38, as the load design equal 1.38 times the ultimate stress of the panels. In hogging, the bottom panel will be in compression and the stress reach faster to the stress of buckling and then firstly the plate collapse , and the maximum displacement in the middle the plate in buckling was 13.7 mm, as we can see the effect of the lateral pressure to increase the deformation of plate.

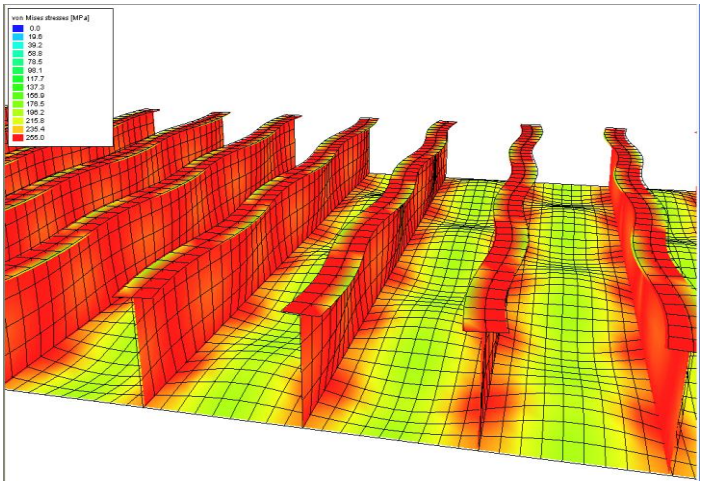

Figure.5.16. The von Mises stress of the panel bottom, with lateral pressure (P=0.044 MPa) load (the initial deflection of stiffeners =5.45 mm, 4.35 mm for plate and the ultimate load was 220 MPa), the maximum stress 255 MPa.

The critical area was the junction web/plate and the junction web/flange as explained by the maximum von Mises stress criteria of the stiffened panels bottom.

The plate deformed until cannot support the biaxial compression, the stress propagate to web/flange junction, as we can see the flange start to be in plastic mode, since is presented by mode 4 ,web buckling, and mode 5 tripping phenomena (cf. Fig.5.16).

By acting the lateral pressure the stiffened panels can be in tripping, if there is no bracket, to focus about strength of the plate connected to stiffener different thickness set up to describe the evolution of the ultimate strength versus the reduced slenderness of local plate.

By following the same procedure, we study ULS and buckling for the others panels in two cases hogging and sagging.

The Table.5.8 shows the dimension of the stiffened panels under analysis using DNV PULS, to get at the end the computation between Paik, Hughes, and Rahman models.

Table.5.8. The dimension the stiffened panels in sagging

		Dimension	breath(mm)	height(mm)	Nbre Stiffeners	spacing stiffeners (mm)	Spacing frame (mm)
Sagging	Deck 1,2	Deck1 flat bar	28	400	14	870	5450
		Deck 2 flat bar	24	330	16		
	Upper side	side 2 web	313	12	3	850	
		side 2 flange	36	62			
		side 2 web	1100	11.5	1		
		side 2 flange	18.5	180			
		side 2 web	403	11.5	3		
		side 2 flange	46	77			
		side 2 web	450	12	5		
		side 2 flange	21.5	150			

		side 2 web	500	12	3	
		side 2 flange	21.5	180		
	Upper Long bulkhead	side 1 web	403	21.5	2	850
		side 1 flange	46	77		
		side 2 web	1100	11.5	1	
		side 1 flange	12.5	180		
		side 1 web	400	12	4	
		side 1 flange	42	70		
		side 1web	403	11.5	6	
		side 1 flange	46	77		
		side 1 web	450	12	2	
		side 1 flange	20	150		

Table.5.9. The dimension the stiffened panels in hogging

		Dimension	breath(mm)	height(mm)	Nbre Stiffeners	spacing stiffeners (mm)	Spacing frame (mm)
Hogging	Bottom 1,2	bottom stif web1	13	600	B1 : 14	870	5450
		bottom stif flange1	200	24	B2 : 14		
	lower Long bulkhead	side 1 web	600	12	3	850	
		side 1 flange	20	180			
		side 1 web	650	12	2		
		side 1 flange	20	200			
		side 1 web	360	12	2		
		side 1 flange	12	64			
	lower side	side 2 web	600	12	2	850	
		side 2 flange	21.5	180			
		side 2 web	650	12	6		
		side 2 flange	21.5	150			

Table.5.10. The summary results the ULS of the stiffened panels in two cases (sagging and hogging)

	Panels	Width (mm)	Thickness (mm)	Lateral pressure(Mpa)	σ_U (Mpa)	usage factor	statuts of Buckling
Hogging	Bottom 1	13050,00	22,00	0,04	241,00	1,38	Not Ok
	Bottom2	13050,00	19,00	0,04	229,00	1,45	Not Ok
	Lower Long Bulkh	6000,00	20,00	0,00	218,00	1,28	Not Ok
	Lower side	6000,00	18,00	0,22	208,00	1,50	Not Ok
Sagging	Deck1	13050,00	18,50	0,00	192,00	1,54	Not Ok
	Deck2	13920,00	19,50	0,00	155,00	2,25	Not Ok
	upper Long Bulkh	6800,00	15,50	0,00	187,00	1,50	Not Ok
	Upper side	6800,00	18,00	0,00	207,00	1,43	Not Ok

The summary results presented in Table.5.10 above, we conclude the stiffened panels bottom buckle even if we use the large thickness of the plate as showing in the curve.

The panel will be buckled by collapse of the plate, in the beginning under the transversal compression, because the ultimate capacity of panel depends of the reduced slenderness of local plate (the more results of buckling test are presented in the appendices).

In Figs.5.17, 5.18 we found in hogging the stiffened panels lower side, lower longitudinal bulkhead and the bottom 2 had the lower zone strength. We obtained the large zone strength in the panel bottom1, and to summarize in the case the ballast condition more probability of collapse will be from failure the structure the lower side panel. In fact in case the sagging the risk of collapse will be from deck 2 and uppers longitudinal bulkhead panels.

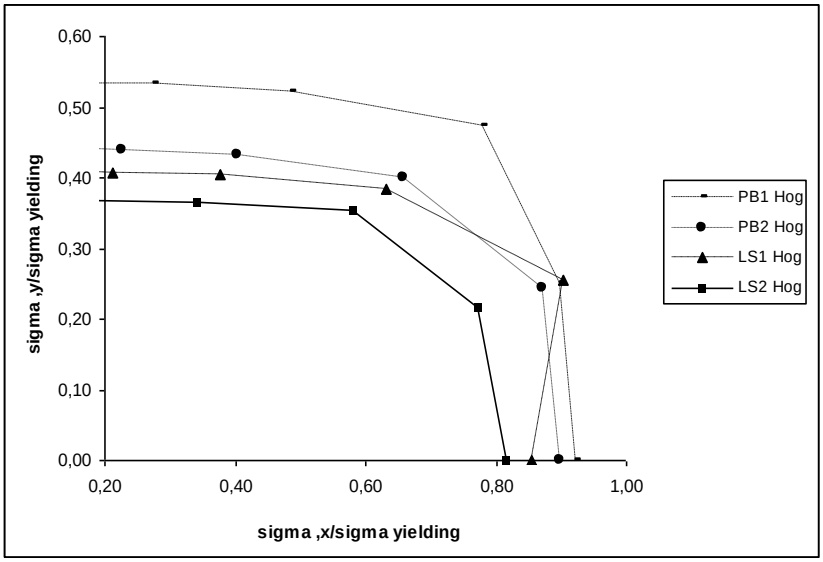

Figure.5.17.The ULS capacity of the stiffened panels in hogging.

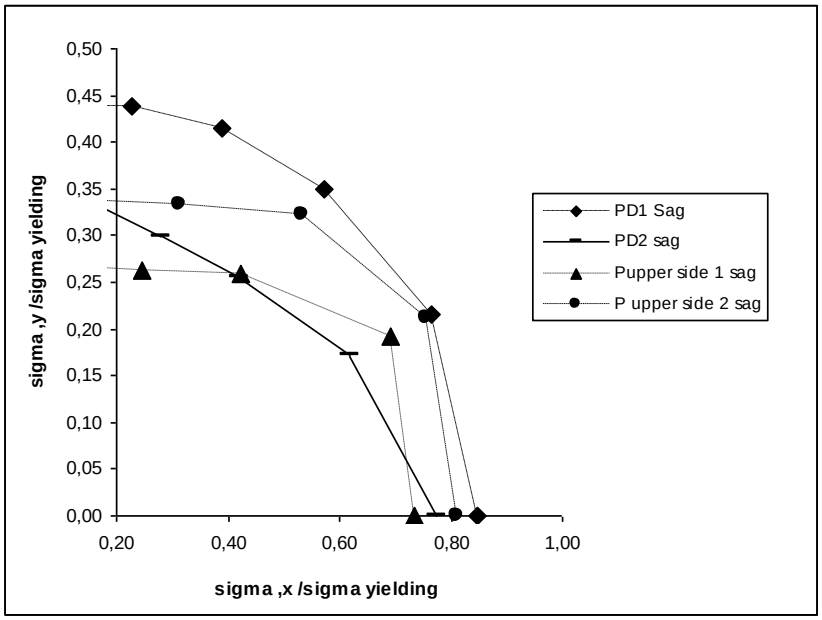

Figure.5.18.The ULS capacity of the stiffened panels in sagging.

To obtain more marge safety and to avoid the buckling effect, take account the bracket to assess the ultimate strength interaction between biaxial compressive loads. The bracket had good aim to avoid the tripping effect occur by interaction of the plate and lateral pressure. To make more accuracy analysis, we check the results getting by PULS software and the other candidate models, Rahman, Hughes, and Paik.

By running the code of Rahman, we obtain the next results of the ultimate strength of the full panels in hogging and sagging (cf. Figs.5.19, 5.20).

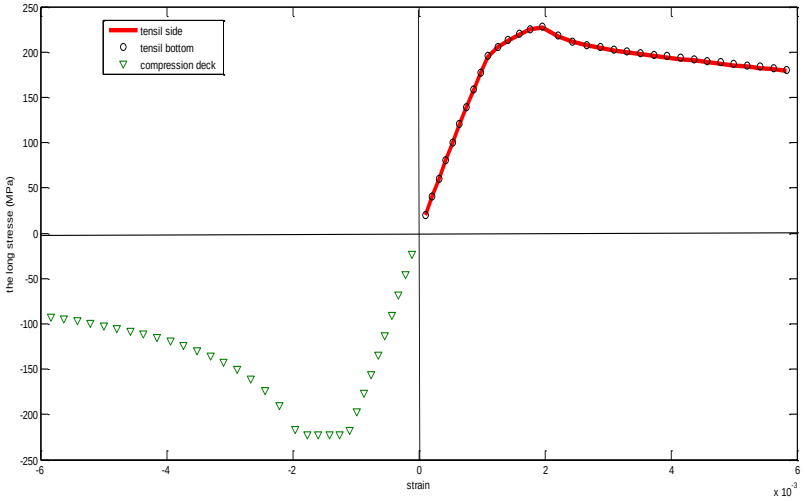

Figure.5.19.The strain-stress curve in sagging (Rahman code).

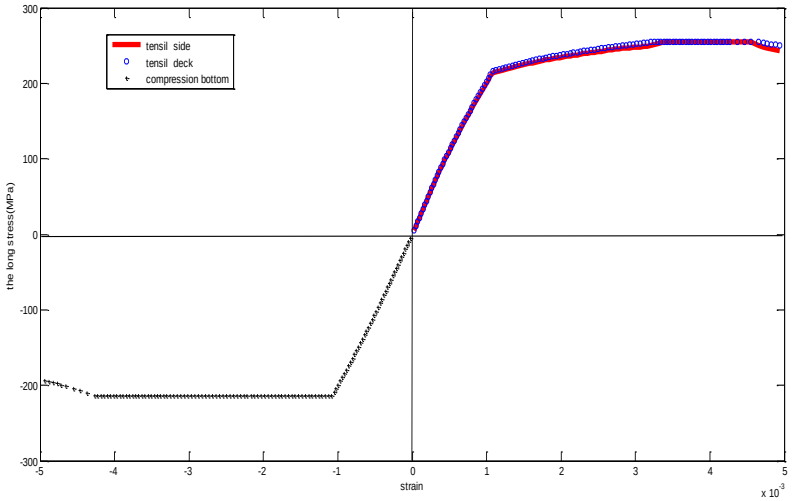

Figure.5.20.The strain-stress curve in hogging (Rahman code).

Table.5.11.The summary computation between PULS and other candidate model (ULS of panel for ship service less than 5 years)

		σ_U(Mpa)				Difference between models /DNV PULS (%)		
	Panels (less than 5 years service)	DNV PULS	Paik model	Rahman model	Hughes	Rahman model	Hughes	Paik model
Hogging	Bottom 1	241.00	215.87	235.98	170.37	2.08%	29.31%	10.43%
	Bottom2	229.00	215.87	213.56	176.2	6.74%	23.06%	5.73%
	lower longitudinal bulkhead	218.00	211.44	----	------	----	-------	3.01%
	Lower side	208.00	205.74	147.34	186.33	29.16%	10.42%	1.09%
Sagging	Deck1	192.00	189.78	221.66	201.72	-15.45%	-5.06%	1.16%
	Deck2	155.00	182.37	220.96	199.29	-42.55%	-28.57%	-17.66%
	upper longitudinal bulkhead	187.00	187.06	201.61	152.29	-7.81%	18.56%	-0.03%
	Upper side	207.00	200.42	-----	------	-----	-------	3.18%

In Table 5.11 we conclude the Rahman code, and Paik model have not bad prediction to reach the ultimate stress received by PULS. The error in two cases sagging and hogging less than 30%. In the opposite way, Hughes still have large gap to reach the exact results of the PULS software. However, the subject is to assess the gap the reduction the ultimate strength of stiffened panels under effect the general corrosion. By reducing the thickness the plate, the slenderness plate and the column slenderness increase, then the stiffness of the structure reduces. In this present thesis is to evaluate the decline the ultimate stress in the panel, regarding to the computation between the DNV PULS, and the candidates models.

Table.5.12. The summary computation between PULS and other candidates model (ULS panel for ship service 25 years)

		σ_U (Mpa)				Difference between candidate models /DNV PULS (%)		
	Panels(after 25 years service ,effect the uniform corrosion)	DNV PULS	Paik model	Rahman model	Hughes	Rahman model	Hughes	Paik model
Hogging	Bottom 1	214.00	207.24	228.54	164.91	-6.79%	22.94%	3.16%
	Bottom2	206.00	210.40	201.7	159.08	2.09%	22.78%	-2.14%
	lower longitudinal bulkhead	198.00	204.77	----	------	----	-------	-3.42%
	Lower side	190.00	197.57	125.53	168.52	33.93%	11.31%	-3.98%
Sagging	Deck1	173.00	181.60	211.3	185.66	-22.14%	-7.32%	-4.97%
	Deck2	141.00	175.19	212.23	185.93	-50.52%	-31.87%	-24.25%
	upper longitudinal bulkhead	164.00	175.87	179.53	132.9	-9.47%	18.96%	-7.24%
	Upper side	183.00	192.17	-----	------	-----	-------	-5.01%

Table.5.13. The summary results the reduction the ULS the panel (effect the uniform corrosion after 25 years ship service)

		Bottom 1	Bottom 2	Lower longitudinal bulkhead	Lower SIDE	Average (%)
Hogging	DNV PULS	11.20%	10.04%	9.17%	8.65%	5.39%
	Paik model	4.00%	2.53%	3.15%	3.97%	5.33%
	Rahman model	3.15%	5.55%	----------	14.80%	6.16%
	Hughes	3.20%	3.20%	----------	9.56%	9.25%
		Deck1	Deck2	upper longitudinal bulkhead	Upper side	Average
Sagging	DNV PULS	9.90%	9.03%	12.30%	11.59%	6.71%
	Paik model	4.31%	3.94%	5.98%	4.12%	5.91%
	Rahman model	4.67%	3.95%	10.95%	----------	10.49%
	Hughes	7.96%	6.70%	12.73%	----------	7.86%

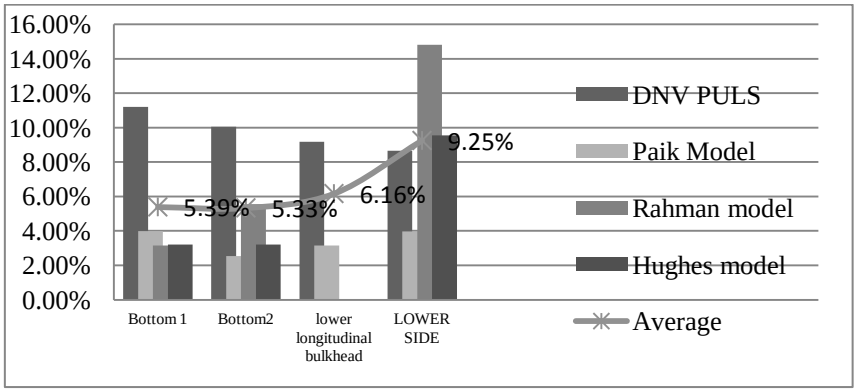

Figure.5.21.The reduction the ULS the panel (effect the uniform corrosion) in hogging.

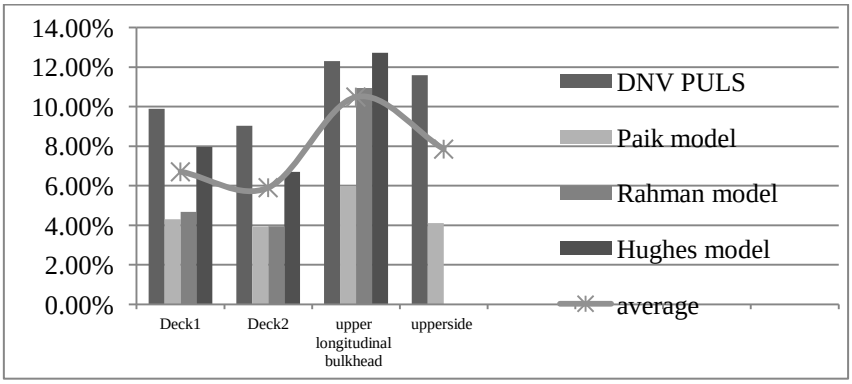

Figure.5.22. The reduction the ULS the panel (effect the uniform corrosion) in sagging.

The Hughes model has large gap to evaluate the ultimate strength of the stiffened panels bottom in hogging, regarding to the results the DNV PULS.

Discussing the accuracy of the results, the different models are compared, and we arrived to describe the reduction the ultimate strength of the stiffened panels, subject to the uniform corrosion.

From the diagram (cf. Fig.5.21), the gap of the reduction the ultimate strength the panels in hogging was 10%, as we remark, the stiffened panels bottom not lost much strength than lower side.

According to the gap the ultimate strength, the speed the corrosion in the bottom very slow, comparing to that for lower side. Physically in hogging, the draft very close to the lower side area, at that zone the interface water air create electrolyte reaction, adding the effect the atmospheric corrosion, then the depth the corrosion is higher ,the consequence will be the section modulus the lower side goes down, and the ultimate capacity become lower.

Especially, at 0.3L and 0.7 L from aft part ,the shear forces is very higher ,without repair and maintenance in the side at this position, where the stiffness the structure become lower ,the risk the failure of the vessel will be higher .

However, in sagging the gap the reduction the ultimate strength was 11%, and the critical area have very large gap the reduction of the ultimate strength is the upper longitudinal bulkhead. At that zone in full load, the depth the corrosion very important ,since the oil cargo contact to the wall of the upper longitudinal bulkhead, where the air exist ,the electrochemical reaction touch the wall and the thickness the structure decrease. In fact the probability to get the crack and failure of the structure is very important, in the upper longitudinal bulkhead.

5.6. The Progressive Hull Girder Collapse Analysis

The ULS of the hull girder is assessed following the geometry details of the hull girder (cf. Fig.5.23). However, the subject is to measure the gap the reduction the ultimate bending moment, in two cases sagging and hogging regarding to the computation between the CSR and the candidates models, hence the Chapter one confer philosophy and methodology the candidates model to assess the ultimate bending moment.

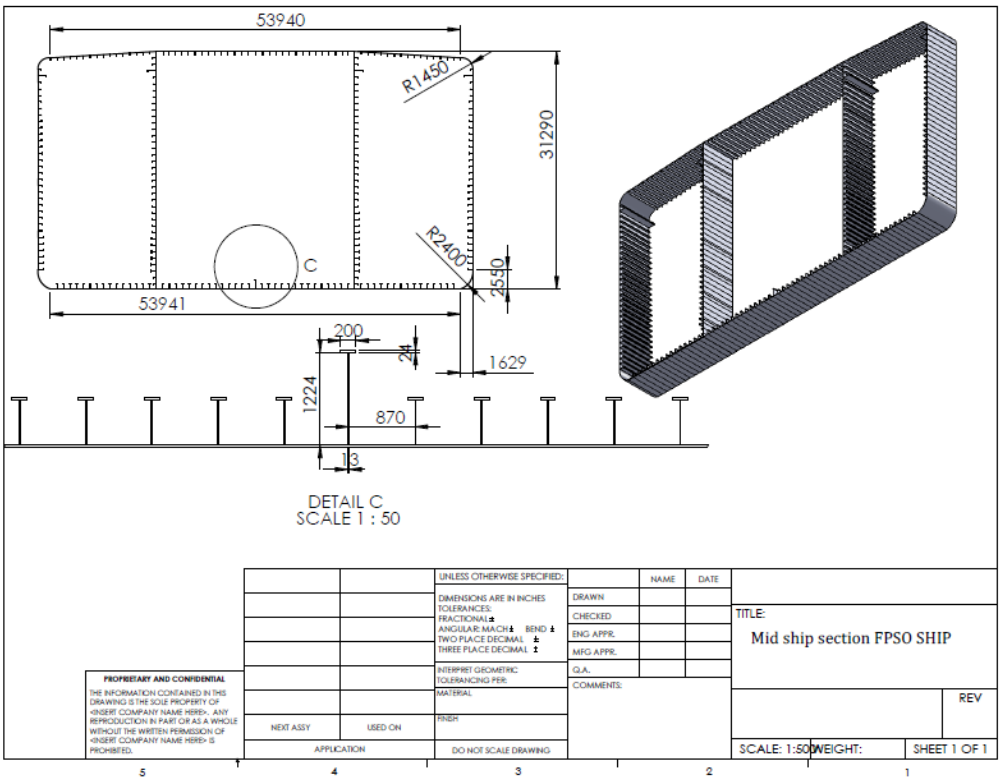

Figure.5.23.The details geometry of the hull girder.

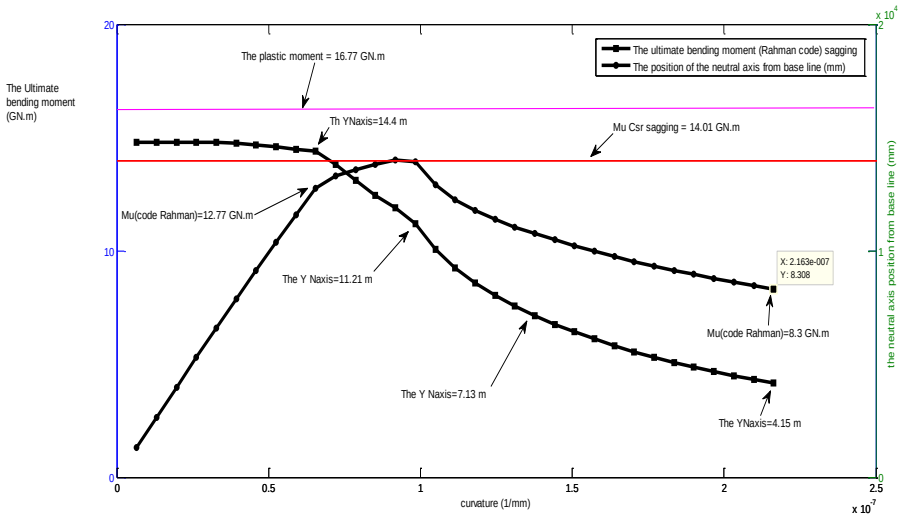

Figure.5.24. Curve of bending moment and position of neutral axis in sagging ignoring corrosion.

In Fig.5.24 show when the bending moment increase the deck structures start buckling collapse and progressively lose their effectiveness when the ultimate bending moment reach the maximum value 14.01 GN.m ,and subsequently the neutral axis moves downward rapidly from 11.21 m until 4.15 m. Since, when the ultimate limit state of hull is reached as the bending moment sagging growing, the bottom structures fail by gross yielding and then the axis neutral change position. On the other side, in Fig.5.25 show the evolution the ultimate

bending moment and the neutral axis position versus curvature, with effect of the uniform corrosion, the ultimate bending moment the deck structures reach the maximum value 11.8 GN.m ,and subsequently the neutral axis moves downward rapidly from 11.62 m until 1.5 m. By considering the uniform corrosion, after 25 years the ship service of the single hull tanker, the gap the reduction the ultimate bending moment in sagging was 15.62%, and the neutral axis position move by 4% to reach the failure of the deck structure (cf. Fig.5.25), according the results getting by Rahman code.

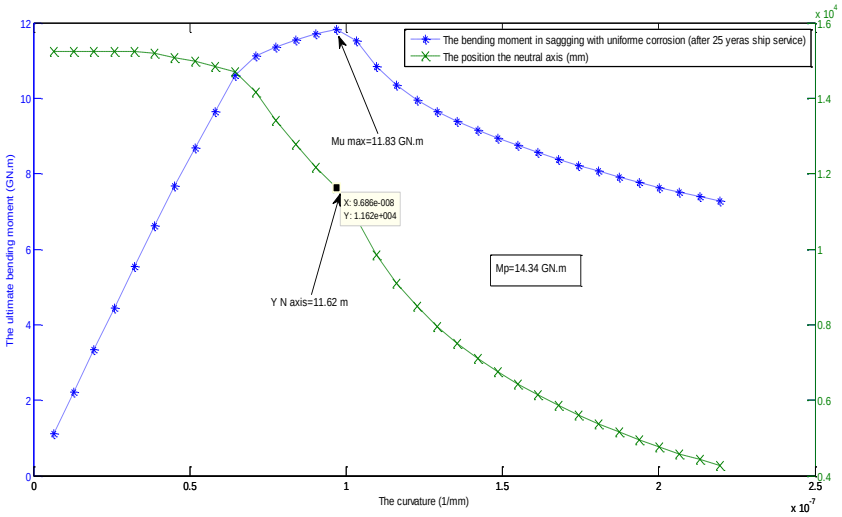

Figure.5.25. Curve of bending moment and position of neutral axis in sagging with corrosion.

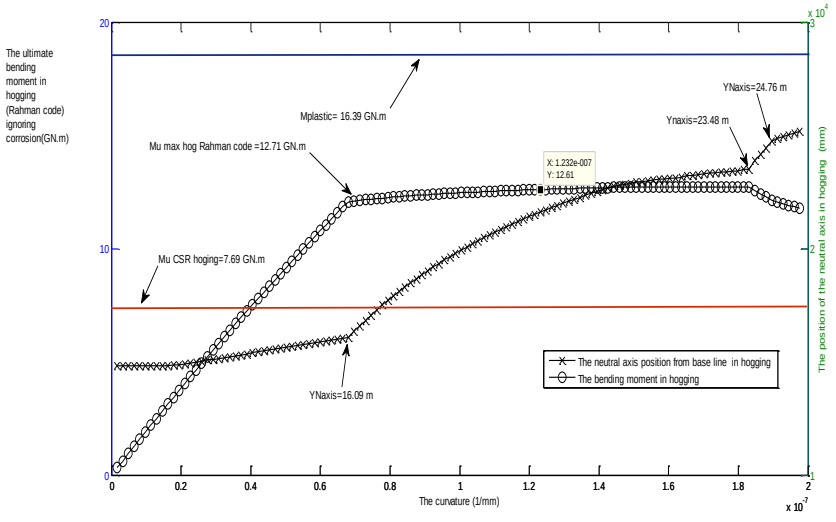

Figure.5.26. Curve of bending moment and position of neutral axis in hogging ignoring corrosion.

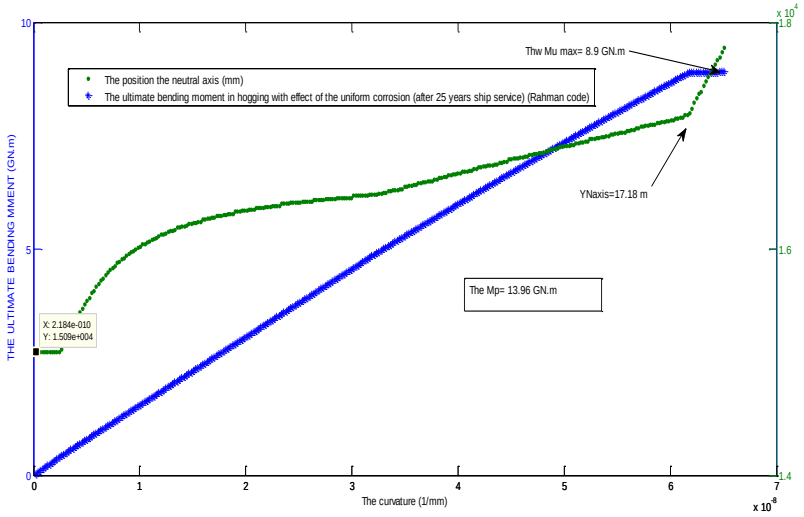

Figure.5.27. curve of bending moment and position of neutral axis in hogging with corrosion.

In the other way, in Fig.5.26 show when the bending moment increase in hogging, the bottom structures start to be collapse, when the ultimate bending moment reach the maximum value 12.71 GN.m, and subsequently the neutral axis goes up rapidly from 16.09 m to 23.48 m. When the ultimate limit state of hull girder is reached as the bending moment hogging growing, the deck structures fail by gross yielding and then the neutral axis change position. Regarding to the effect of the uniform corrosion, the gap the reduction the ultimate bending moment in the hogging is 30%, and the gap the reduction the position the neutral axis is 26% (cf. Fig.5.27).

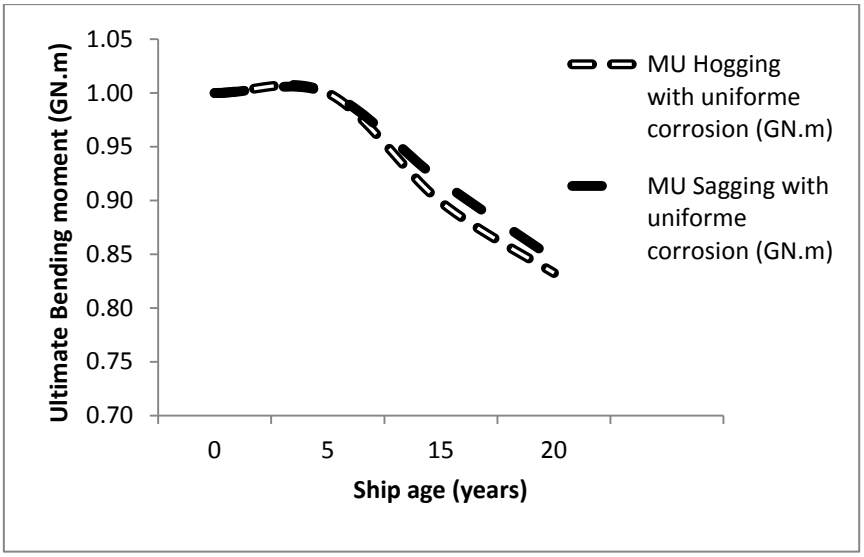

Figure.5.28.Mean value the variation of ultimate bending moment under hogging and sagging condition.

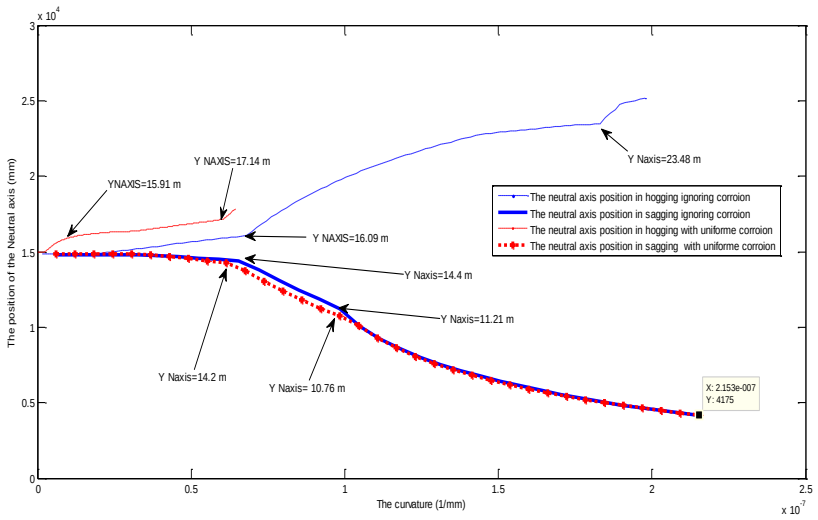

Figure.5.29.The evolution of the neutral axis in hogging and saging.

According to the results showing in Table 5.15, the comparisons the results getting by DNV software (using the CSR) and others candidates models was very large. The Rahman model in the sagging was similar as the Nauticus Hull, in fact in case the hogging was bigger gap as we can see two times the difference.

Looking to the others candidate's models, the Valsgaad/Steen, and Faulkner/Sadden models reach same value the ultimate bending moment in hogging and sagging, but very large difference compared to that of DNV software (CSR), and the difference was 60% . hence , the Paik/Mansour and modified Caldwell model tend to the same results assessing the ultimate bending moment in hogging and sagging ,with difference less than 40% compared to that the DNV software .

In fact, to consider the effect of the uniform corrosion and after 25 years of the ship service the average gap the reduction the ultimate bending moment in hogging was 18% (cf. Fig.5.30), and in sagging was 16 %, such as the average the gap defined by the results getting by the candidates models.

To summary the discussion the results, the scantling of the hull girder the single hull VLCC cannot support the bending moment designed in sagging and hogging.

Table.5.14. The ultimate bending moment (Mu GN.m) with effect of the corrosion (after 25 years ship service) /Difference (*): the reference the difference CSR Rules

Mu (The ultimate bending moment GN.m) with effect of the corrosion(after 25 years ship service) /Difference (*): the reference the difference CSR Rules								
Model	**condition**	**Paik/Mansour**	**Modified Caldwell**	**Vinner**	**Faulkner/Sadden**	**Valsgaad/steen**	**Rahman**	**CSR Tanker**
Ship tanker	**Sagging**	9,9/15%	9,96/15%	3,65/69%	4,52/61%	4,18/64%	11,83/-0,1%	11.81
	Hogging	10,75/-69%	12,5/-96%	8,92/40%	10,8/-69%	10,2/-60%	8,9/-39%	6.36
(*): the reference the difference CSR rules								

Table.5.15. The ultimate bending moment (Mu GN.m) (less than 5 years ship service) /Difference (*): the reference the difference CSR Rules

Model	**condition**	**Paik/Mansour**	**Modified Caldwell**	**Vinner**	**Faulkner/ Sadden**	**Valsgaad/steen**	**Rahman**	**CSR Tanker**
Ship tanker	**Sagging**	11,69/30%	11,7/40,83%	4,4/68,59%	5,4/61,46%	5,08/63,74%	14.02/0.07%	14.01
	Hogging	12,76/49,54%	15,2/18.21%	10,76/69.05%	13/69.05%	12,32/60.21%	12.71/65.28%	7.69
(*): the reference the difference CSR rules								

Table.5.16. Reduction the ultimate bending moment (Mu GN.m) by effect of the uniform corrosion

Model	condition	Paik/Mansour	Modified Caldwell	Vinner	Faulkner/Sadden	Valsgaad/steen	Rahman	CSR Tanker
Tanker FPSO	**Sagging**	15.31%	14.87%	17.05%	16.30%	17.72%	15.62%	15.70%
	Hogging	15.75%	17.76%	17.10%	16.92%	17.21%	29.98%	17.30%
	Average Sag	**16.08%**	**16.08%**	**16.08%**	**16.08%**	**16.08%**	**16.08%**	**16.08%**
	Average Hog	**18.86%**	**18.86%**	**18.86%**	**18.86%**	**18.86%**	**18.86%**	**18.86%**

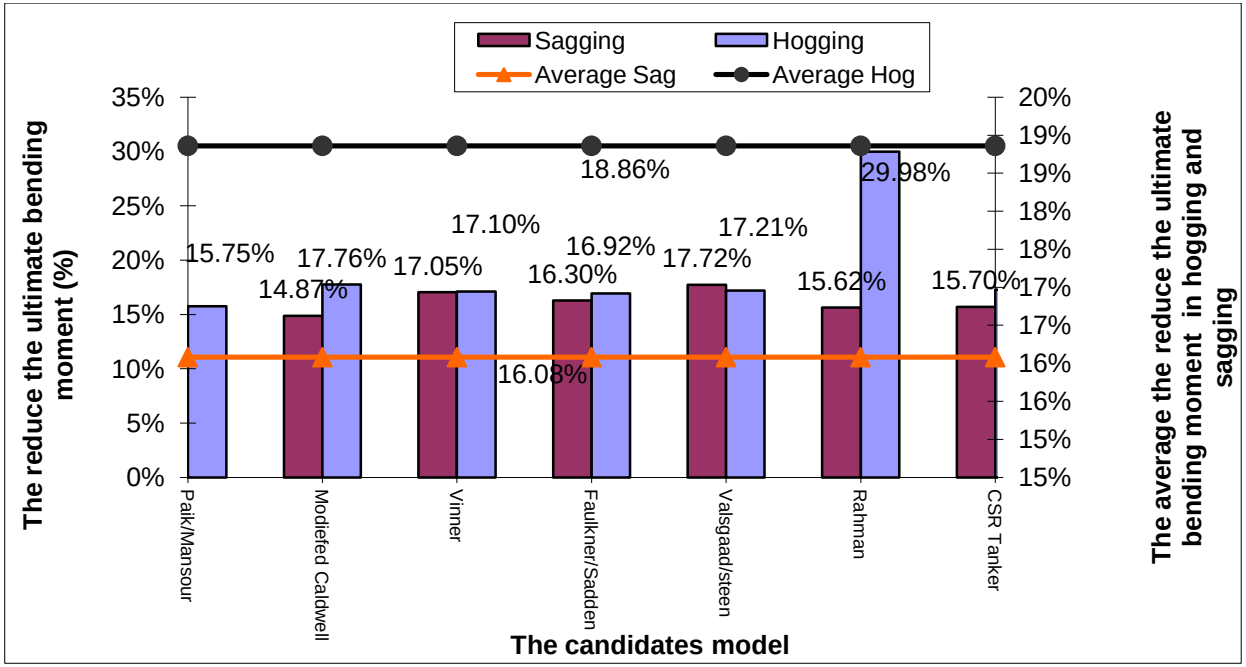

Figure.5.30.The results the average the ultimate bending moment of the computation models.

5.7. Finite Element Analysis of Single Hull Tanker VLCC

5.7.1. Introduction

This chapter gives guidance on how to perform finite element calculations for the girder system within the midship area of tankers. In general the finite element model shall provide results suitable for evaluating the strength of the girder system .This may be done by using a 3D finite element model of the midship area. Several approaches may be applied; ranging from a detailed 3D-model of the cargo tanks to a coarse mesh 3D-model.
Coarse mesh models can be used for calculating deformations and stresses typically suited for buckling control. The model extend are in general to comprise two tank lengths (1/2+1+1/2).

5.7.2. Elements and Mesh Size

The performance of the model is closely linked to the type, shape and aspect ratio of elements, and the mesh topology that is used. The mesh described here is adequate for representing the cargo tank model and frame and girder model as defined in the DNV Rules Pt.3 Ch.1 Sec.13. The following guidance on mesh size is based on the assumption that 4-noded shell or membrane elements in combination with 2-noded beam or truss elements are used.
In general the mesh size should be decided on the basis of proper stiffness representation and load distribution of tank and sea pressure on shell or membrane elements (DNV Rules Classification Notes No. 31.3).

5.7.3. Boundary and Loading Conditions

The boundary conditions to be applied at the ends of the cargo tank FE model are given in Table 5.17 the analysis may be carried out by applying all loads to the model as a complete load case or by combining the stress responses resulting from several separate sub-cases.
Loading conditions as given in Table 5.18 apply LC-A10 is for vessels with cross ties in centre tanks. Such as the model study is single hull tanker VLCC, in the other way the rules apply to assess the finite element for double hull. In fact by approach the similar procedure are apply to assess the strength of single hull.

Table.5.17. Boundary constraints at model end (Recommended Practice DNV-RP-CN31-3, 1999)

location	Translation			Rotation		
	δx	δy	δz	θx	θy	θz
Aft End						
aft end (all longitudinal elements)	RL	-	-	-	RL	RL
independent point aft end	Fix	-	-	-	Mv.end	Mh.end
Deck,inner bottom and outer shell	-	springs	-	-	-	-
side ,inner skin and longitudinal bulkheads	-	-	springs	-	-	-
Fore End						
Fore end (all longitudinal elements)	RL	-	-	-	RL	RL
independent point fore end	-	-	-	-	Mv.end	Mh.end
Deck,inner bottom and outer shell	-	springs	-	-	-	-
side ,inner skin and longitudinal bulkheads	-	-	springs	-	-	-

Where: - : no constraint applied (free)

RL : nodal point of all longitudinal elements rigidly linked to independent point at neutral axis on centreline

Table.5.18. Rule loading conditions for tankers of type A (Recommended Practice DNV-RP-CN31-3, 1999)

LC	Draught	Condition	External pressure	internal pressure
A1	T	sea	Dynamic	Static
A2	T	sea	Dynamic	Static
A3	TA	sea	Dynamic	Static
A4	TA	sea	Dynamic	Static
A5	TA	sea	Dynamic	Static
A6	0.25D	Harboour	Static	Static
A7	0.25D	Harboour	Static	Static
A8	0.35D	Harboour	Static	Static
A9	TA	sea	Sea	Static
A10	0.25D	Harbour	Harbour	Static

5.7.4. Result Evaluation

Starting by building the model in the software engineering (Genie DNV software), and the boundary, loading conditions are applying showing in Fig.5.31, such as in this analysis the case A2 taking in consideration.

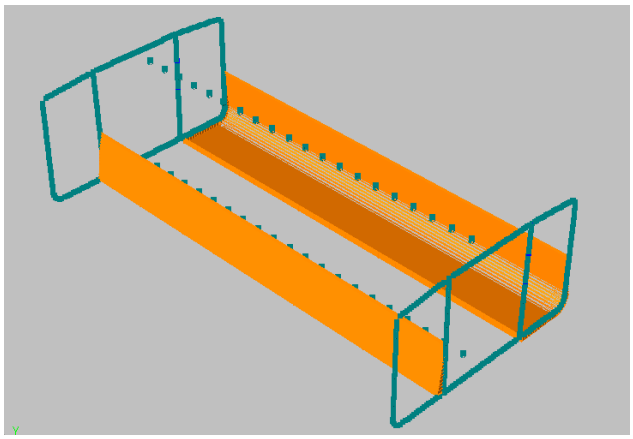

Figure.5.31.The boundary and load conditions applying in the single hull VLCC.

Wherever, the size the mesh is stiffeners spacing (stiffeners spacing =870 mm). By running the program, the results the analysis is showing in the beginning as deformation of mesh of the full model.

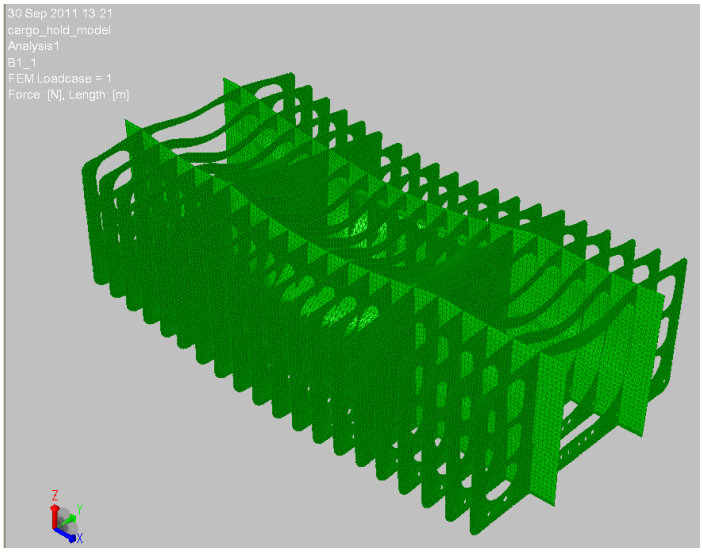

Figure.5.32.The deformed web frame-mesh case A2.

According to the results the finite element analysis of the single hull VLCC in the case A2, the quality of mesh and adjust load is important to describe good results and satisfy accuracy. Regarding to the size the memory of computer, and time consuming of the analysis the full model it was interesting to start by bigger size of mesh, and to decrease step by step until get enough results. From the Figs.5.33, 5.34, 5.32, the deformed shape of the outer shell the hull, the stiffeners and the transverse, longitudinal frame are presented.

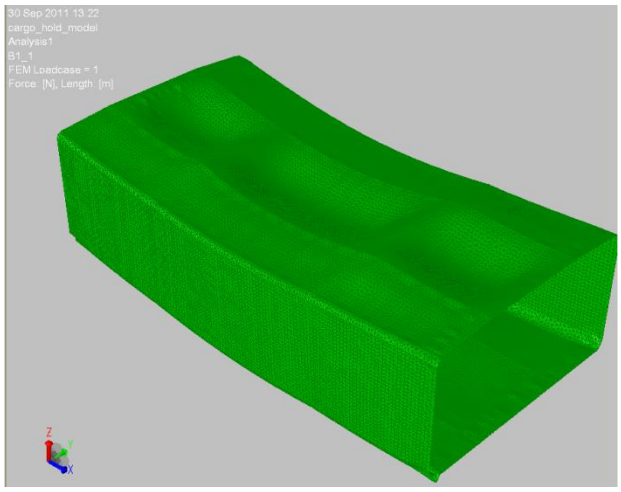

Figure.5.33.The deformed out shell-mesh case A2.

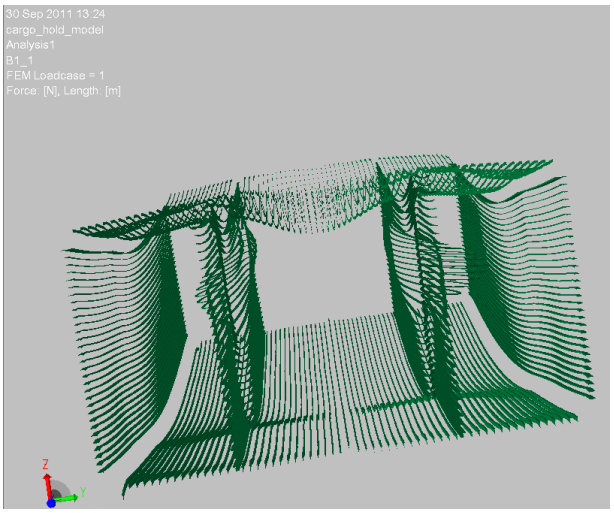

Figure.5.34.The deformed Stiffeners-mesh.

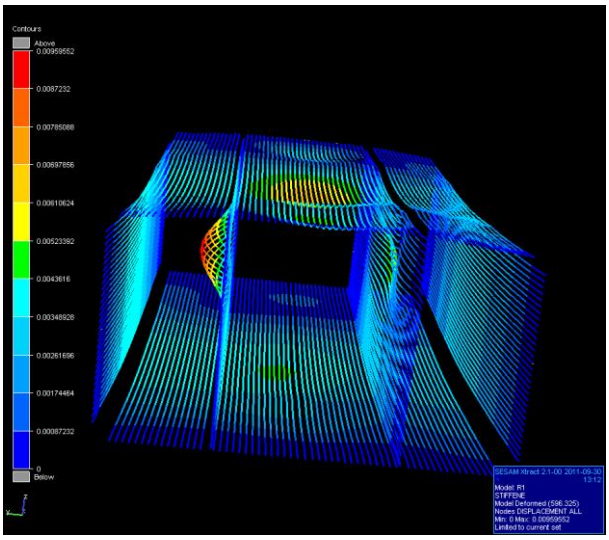

Figure.5.35. All displacement the stiffeners case: A2, Max displacement=9.5 mm.

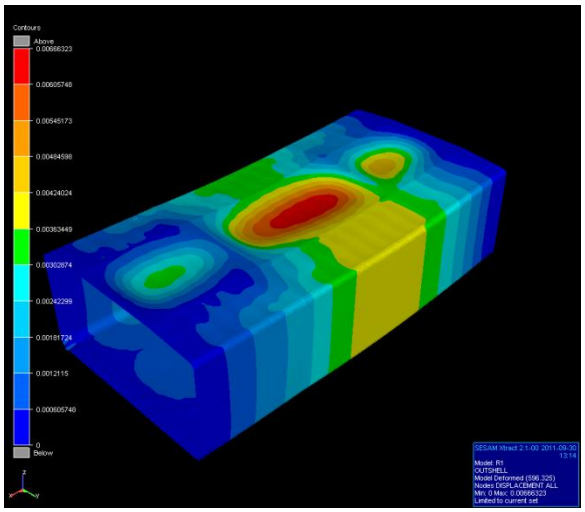

Figure.5.36. All displacement out shell case: A2, Max displacement =6.6 mm.

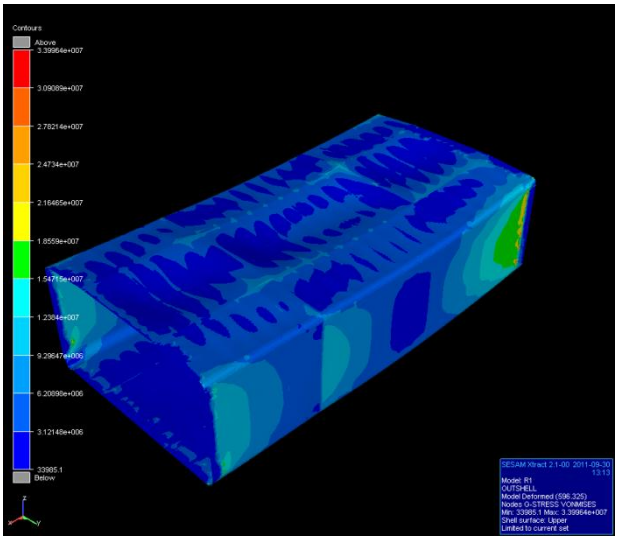

Figure.5.37.The von Mises stress of out shell case: A2, Max stress=40 MPa.

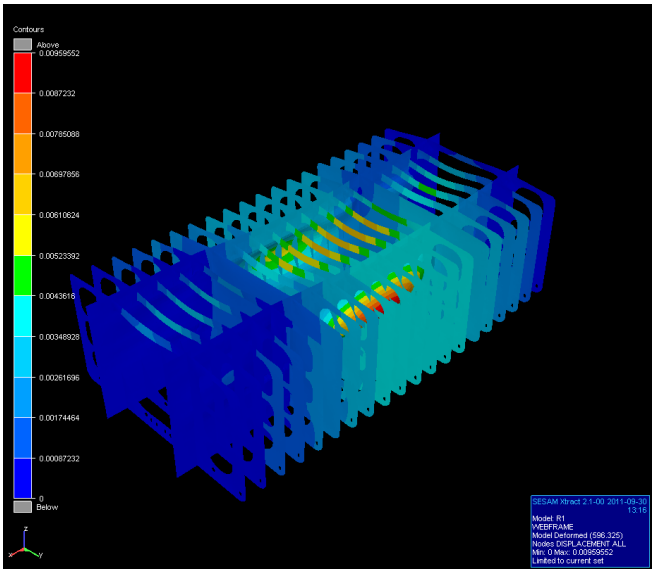

Figure.5.38. All displacement web frame case A2, Max displacement=9.5 mm.

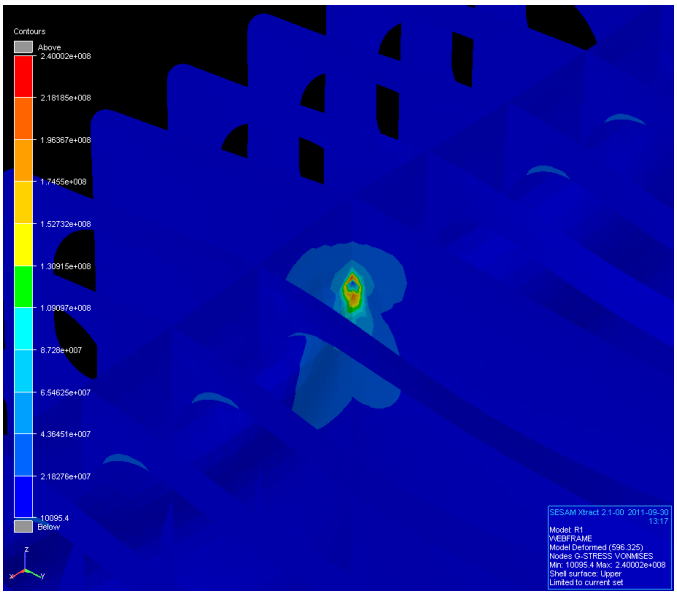

Figure.5.39. The von Mises stress of web frame case A2, Max stress =240 MPa.

The interesting results of the analysis, showing in Fig.5.36 are presented.

In case A2 (full load), the maximum displacement of the full model was 6.6 mm. In fact the stiffeners and transverse frame had very large displacement 9.5 mm.

According to the results showing in Fig.5.39, the corner connect the longitudinal and transversal bulkhead set up the critical area, following the high value the von Mises stress criteria equal to 240 MPa.

To come back, to the subject of the present finite element analysis by describing the effect the general corrosion after reducing the thickness of the geometry, to assess the gap the reduction the ultimate strength .

Following similar procedure the finite element analysis for initial scantling, second run for final dimension after reducing the thickness the full model.

Regarding to the result presented in Fig.5.40, the total displacement of the model was 1.03 cm , in fact the difference the displacement between first and second model was5 mm, and to summary, reducing the thickness of the geometry by effect of the general corrosion reduce the section modulus (see Chapter 4) and the structure lost the ultimate strength capacity.

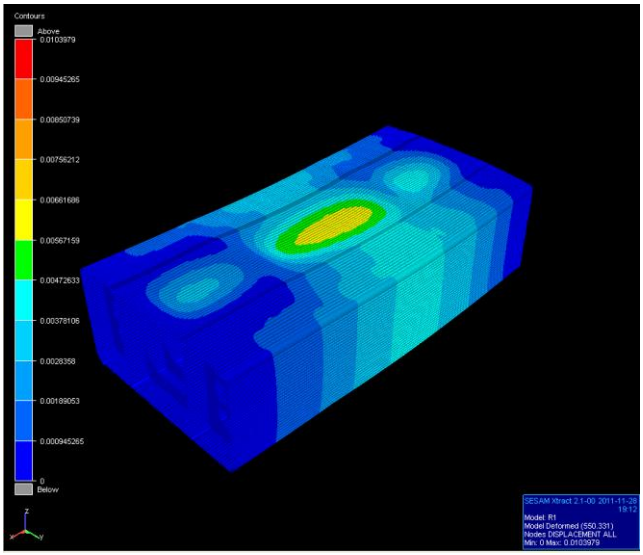

Figure.5.40.All displacement single hull tanker VLCC (with effect the corrosion)

The max displacement =1.03 cm.

6. CONCLUSION

As Common Structure Rules (CSR) comes into effect, the ultimate state assessment has been recognized as an important field in ship structural analysis.
This report describes the results of comparative studies on ultimate limit state assessment of ship plates, stiffened plates, and hull girders, using some candidate methods subject to the corrosion.

DNV PULS, Paik, Hughes, and Rahman codes are employed for the assessment of plating and stiffened plates.

For the ultimate strength of hull girder, IACS CSR, and Rahman codes are used. The assessment is applied to a single hull oil VLCC tanker structure. The ultimate limit states of bottom plates, deck plates, deck stiffened panels, and bottom stiffened panels are analyzed.

The ultimate vertical bending moment capacity of the hull structure is also assessed by IACS CSR, Rahman code, Modified Caldwell, Vinner, Faulkner/Sadden, and Valsgaad/Steen and their results are compared.

The analysis of the corrosion model, have large point to touch. In fact, the initial work is to define the model (2) (see Chapter 4), to describe the depth of the corrosion (atmospheric corrosion), comparing with the assumed data.

Using model (2) we get good prediction to assumed data. Since, we found the reduce of the section modulus and the section area of the deck cargo follow polynomial model the order six. Finally we lost 5% the section modulus of the deck cargo during 15 years the ship service, and for the mean section area, we lost 9.3% during 25 years.

From point of view engineer, the critical area attacked by corrosion, can be check by inspection is the side at draft level, where the shear forces very high at position 0.3L and 0.7L from aft part. In fact should be care about the pitting corrosion, is dangerous to get failures of the tanker.

By considering the effect the general corrosion, the aim for this work is to define the reduction the ultimate capacity of the plate, panel and hull girder.

The ultimate strength the plate reduces by 8% in the bottom, in the lower side plates, and in the lower longitudinal bulkhead, in case the hogging.

However, in the sagging, the ultimate strength the plate is reduced by 8% in the deck and in the upper parts of the sides, except for upper longitudinal bulkhead where the ultimate strength is reduced by 10%.

In fact, the difference between the results the Paik model and the DNV PULS, not so high, and the difference is smaller than 20%.The critical area for the tanker ship is the longitudinal bulkhead; as we conclude the ultimate strength is reduced by 10 %, because the thickness the longitudinal bulkhead decrease in the two sides, the first side the oil cargo, and the second one the water ballast.

The reduction the ultimate strength of the panels in hogging was 10%, and in sagging was 11%. The critical area has very large reduction is the upper longitudinal bulkhead. Discussing the comparisons the results the reduction getting by DNV software (using the CSR) and others candidates models, the difference was very large, and the results of the Rahman model in sagging were similar to those obtained using the Nauticus Hull (DNV software), in fact in case the hogging was bigger reduction the ultimate strength of the panels as we can see in the chapter 5, two times the difference.

Looking to reduction the ultimate bending moment, the Valsgaad/Steen, and Faulkner/Sadden models reach the same value in hogging and sagging, but very large difference compared to that of DNV software (CSR Rules); the difference being 60%. Hence, the Paik/Mansour and modified Caldwell model tend to the same results in hogging and sagging, with difference less than 40% compared to that the DNV software .

Considering the effect of the uniform corrosion, and after 25 years of the ship service, we conclude the average the reduction the ultimate bending moment in hogging was 18%, and in sagging is 16%, such as the average the reduction defined by the results getting by the candidate models.

7. ACKNOWLEDGEMENTS

First of all, I would like to express my warmest appreciation to all my professors who gave me lots of knowledge during my study in naval construction in ANAST, University of Liege (Belgium), Ecole Centrale de Nantes (France), and West Pomeranian University of Technology, Szczecin (Poland).

Furthermore, I would be grateful to Prof. Dr. Maciej Taczala for providing me the necessary tools and the comfortable conditions to prepare this work.

I would like to thank responsible Tomasz Msciwujewski from DNV Company in Gdynia for his support and advice during my internship.

Finally, I would like to express my whole-hearted gratitude to my family for all their love and support.

8. REFERENCES

Book	S.Tanaka, Y.Okada, Y.Ichikawa, 2005, offshore Drilling and production Equipment.
	Philippe Rigo and Enriso Rizzuto, 2003, analysis and design of ship.
	Owen F.Hughes, 1983, Ship structural Design: A rationally-Based, computer-Aided optimization
	Mansour, Alaa, Liu, Donnald, 2008, Principles of naval architecture series: Strength of ships and ocean structures.
Internet document	http://www.marinecorrosionforum.org/explain.htm.
	http://nptel.iitm.ac.in/courses/IITMADRAS/Design_Steel_Structures_I/1_introduction/3_properties_of_steel.pdf.Design of Steel Structures Prof. S.R.Satish Kumar and Prof. A.R.Santha Kumar.
News paper article	JEOM K.Paik and Alaa, E.Mansour, 1995, A simple formulation for predicting the ultimate strength of ships.
	Recommended Practice DNV-RP-C102, Appendix D, February 2002.
	Yao T. et al. (2000). Ultimate Hull Girder Strength: Report of Committee VI.2 Proc. 14thInternational Ship and Offshore Structure Congress, Ohtsubo H. and Sumi Y. (Eds), Elsevier, 2,321, 391.
	Cui WC, Mansour AE. Effects of welding distortions and residual stresses on the ultimate strength of long rectangular plates under uniaxial compression. MarStruct 1998; 11:251–69.
	Faulkner D. A review of effective plating for use in the analysis of stiffened plating in bending and compression. J Ship Res 1975; 19(1):1-17.
	M.A.Shama, 2005, The problem of corrosion of ship structure.
	Shengping Qin and Weicheng Cui School of Naval Architecture and Ocean Engineering, Shanghai Jiao Tong University, Shanghai, 200030, China, 2002.
	Offshore Technology Conference, 5 May-8May 2003, Houston, Texas.
	Recommended Practice DNV-RP-CN31-3 strength analysis of hull structure in tankers, January 1999.
	Smith, C.S., Davidson, P.C., Chapman, J.C. and Dowling, P.J.: Strength and Stiffness of Ship Plating under In-plane Compression and Tension, The Royal Institution of Naval Architects, W6, 1987, pp.277-296.
Journal article	Emi H, Yuasa M, Kumano A, Arima T, Yamamoto N, Umino M. A study on life assessment of ships and offshore structures (3rd report: Corrosion control and condition evaluation for a long life service of the ship). Journal of the Society of Naval Architects of Japan 1993; 174:735-744.

APPENDICES

A.1. The Detail Plans of the Single Hull Tanker VLCC

A.2. The Results the Test Buckling for Stiffened Panels the Tanker Ship Using DNV PULS Software

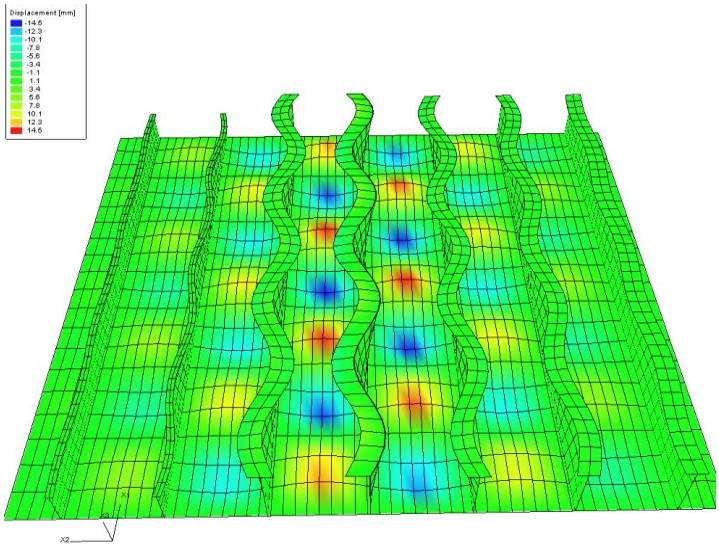

Figure.A.1. Buckling mode of the lower longitudinal bulkhead panel (max displacement of plate at buckling strength 7.24 mm).

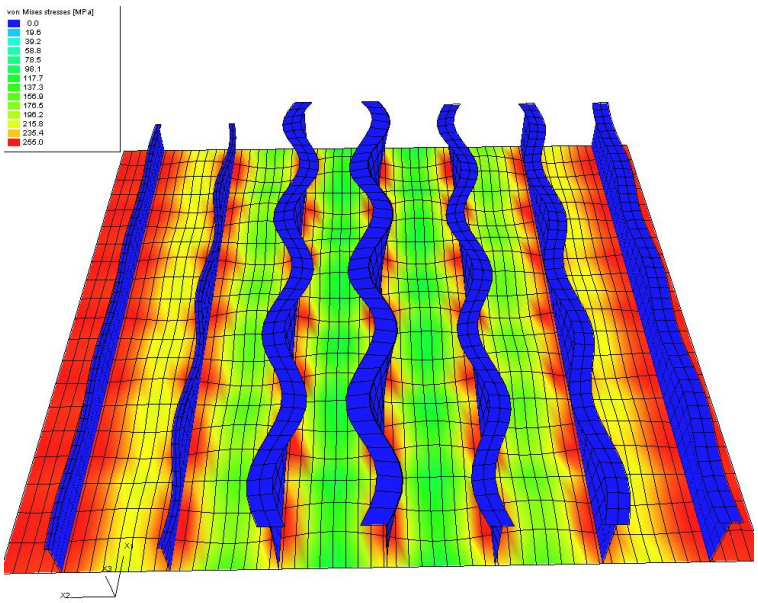

Figure.A.2. The von Mises stress of the lower longitudinal bulkhead panel.

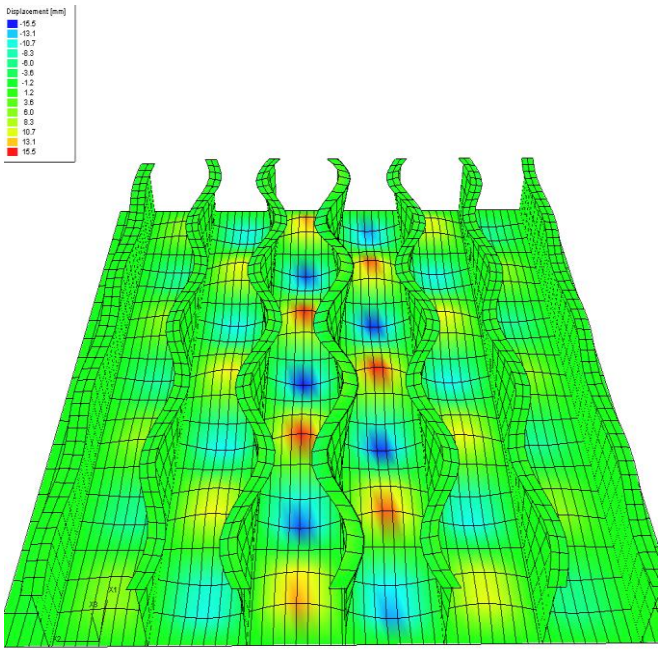

Figure.A.3. Buckling mode of the lower side panel (max displacement of plate at buckling strength 9.08 mm).

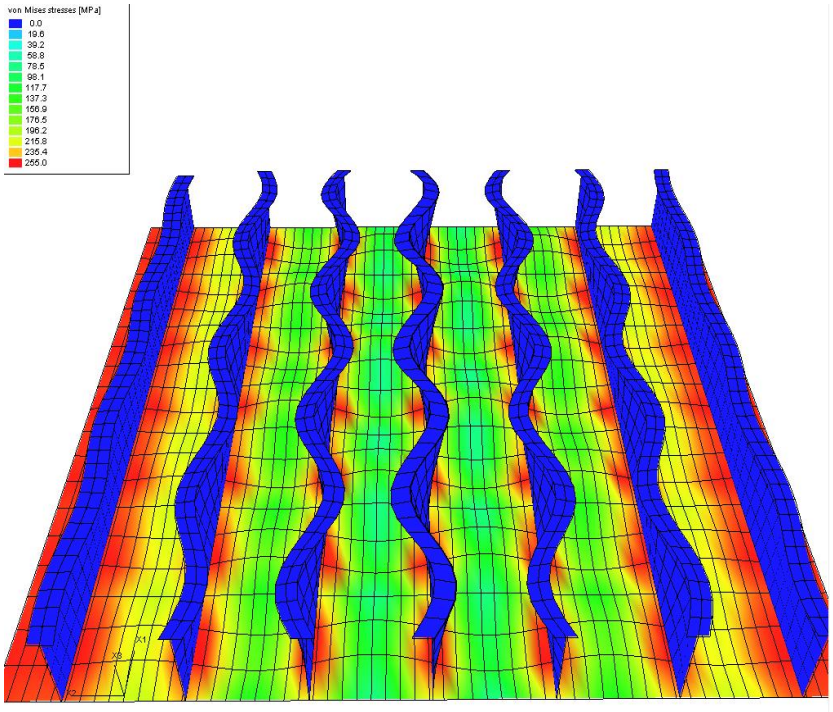

Figure.A.4. The von Mises stress of the lower side panel.

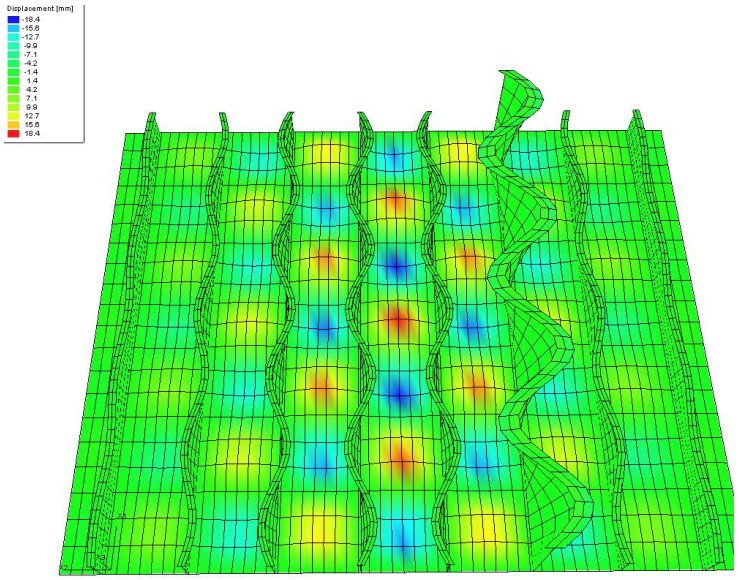

Figure.A.5. Buckling mode of the upper longitudinal bulkhead panel (max displacement of plate at buckling strength 13.16 mm).

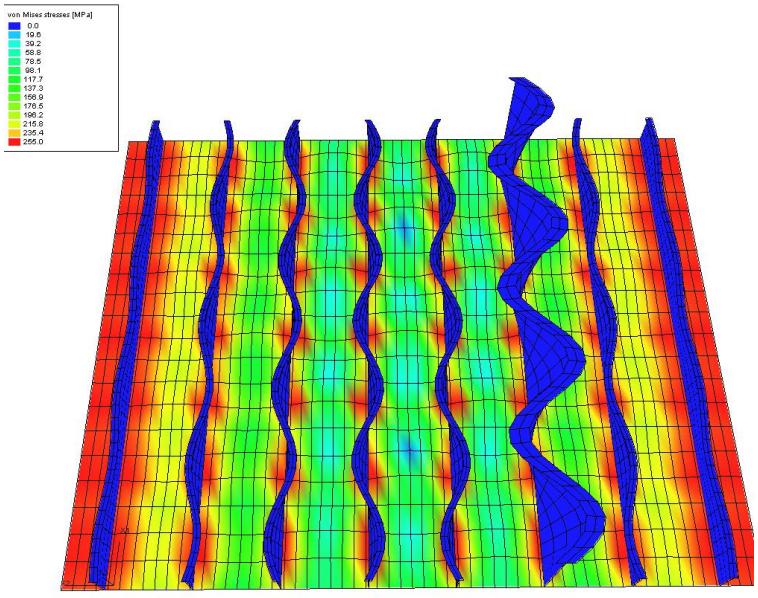

Figure.A.6. The von Mises stress of the upper longitudinal bulkhead panel.

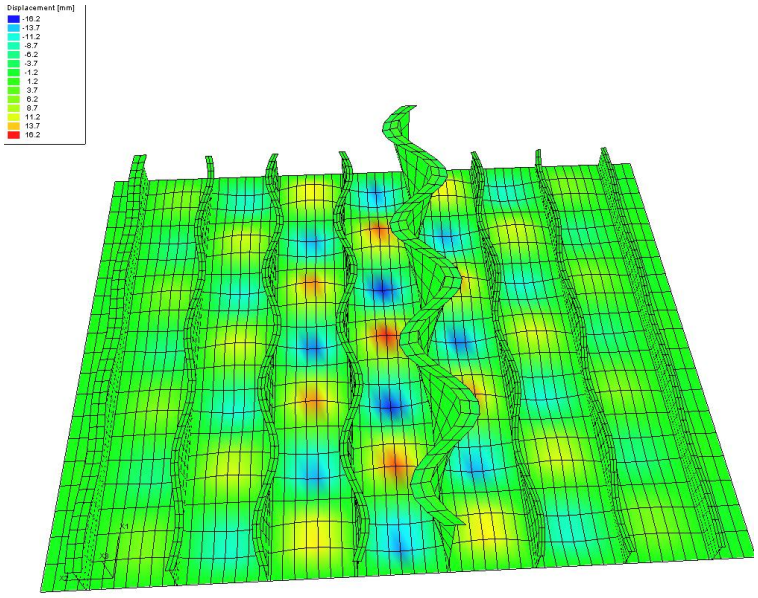

Figure.A.7. Buckling mode of the upper side panel (max displacement of plate at buckling strength 9.5 mm).

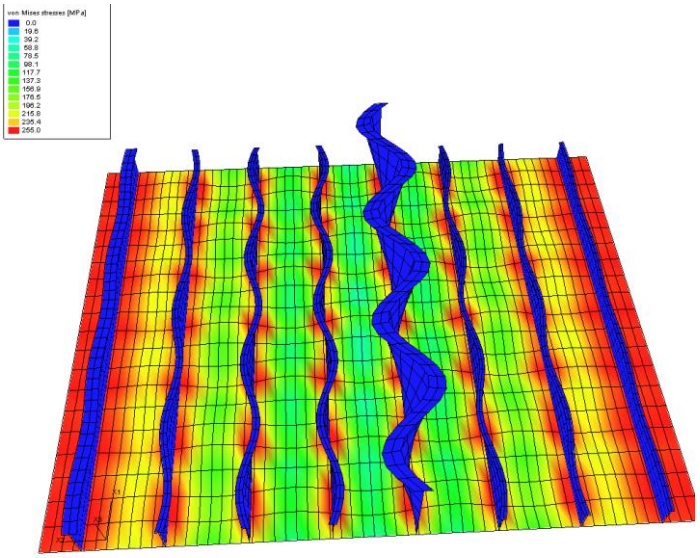

Figure.A.8. The von Mises stress of the upper side panel.

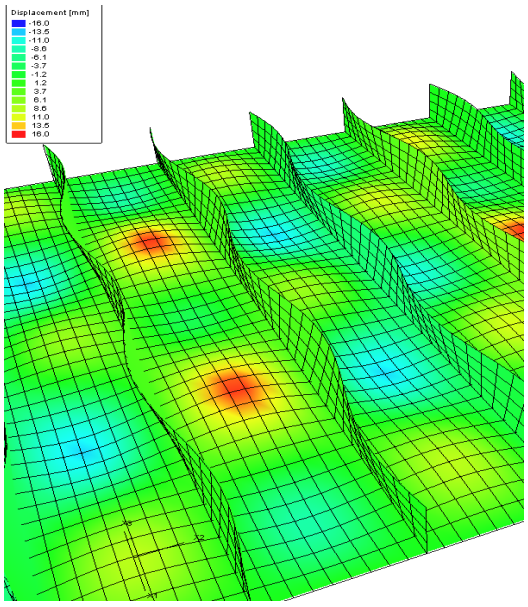

Figure.A.9. Buckling mode of the deck 1 panels (Max displacement=16 mm).

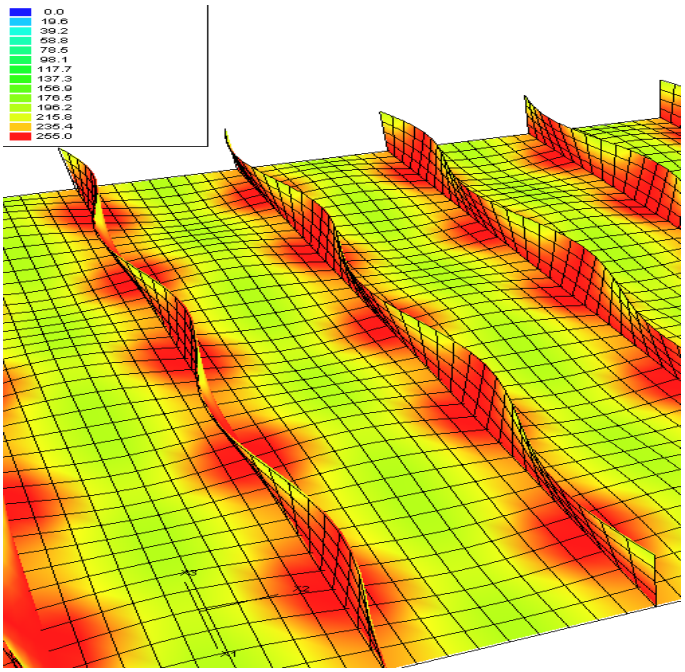

Figure.A.10. The von Mises stress of the deck 1 panel.

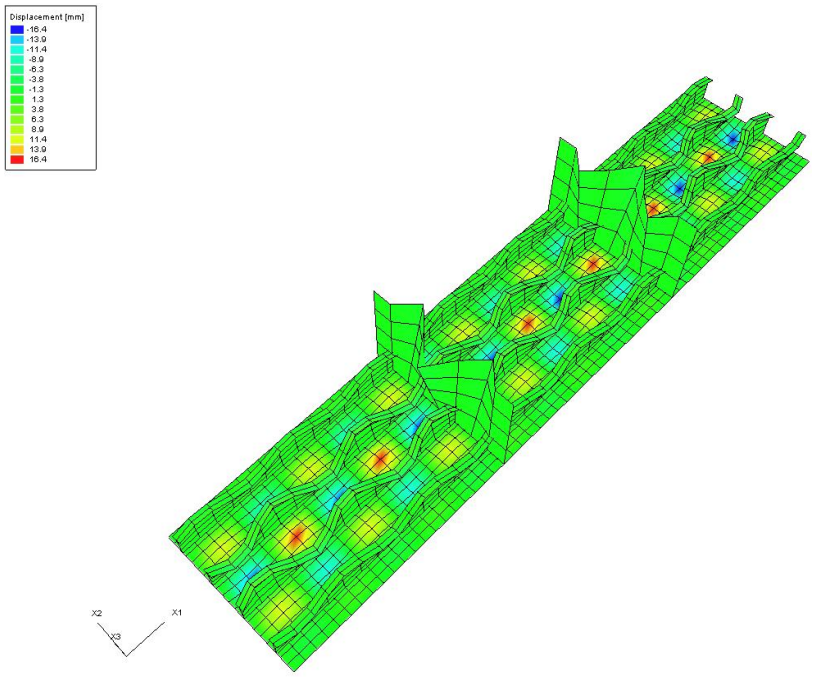

Figure.A.11. Buckling mode of the frame panel bottom (Max displacement of the plate at buckling strength equal to 13.76 mm).

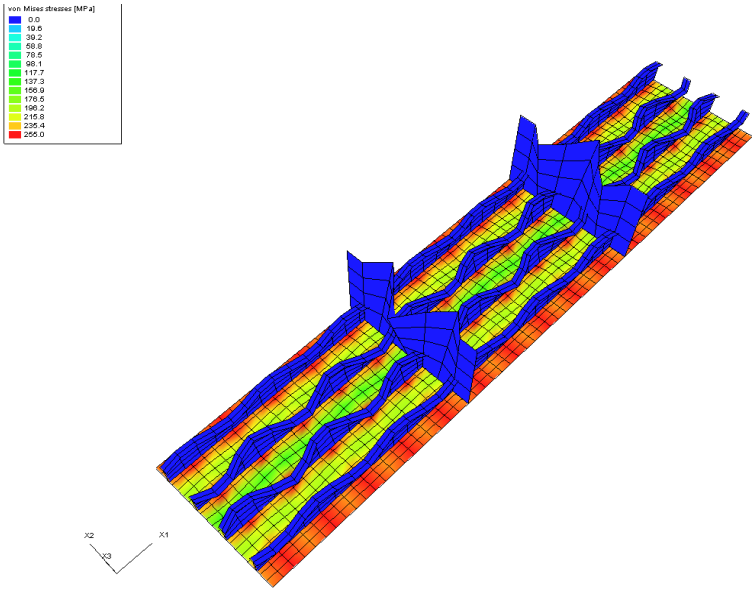

Figure.A.12.The von Mises stress criteria of the frame panel bottom.

The ultimate strength of the frame equals 249 MPa and the usage factor equal to 1.33.

A.3. The Results the Finite Element Analysis of the Single Hull Tanker VLCC

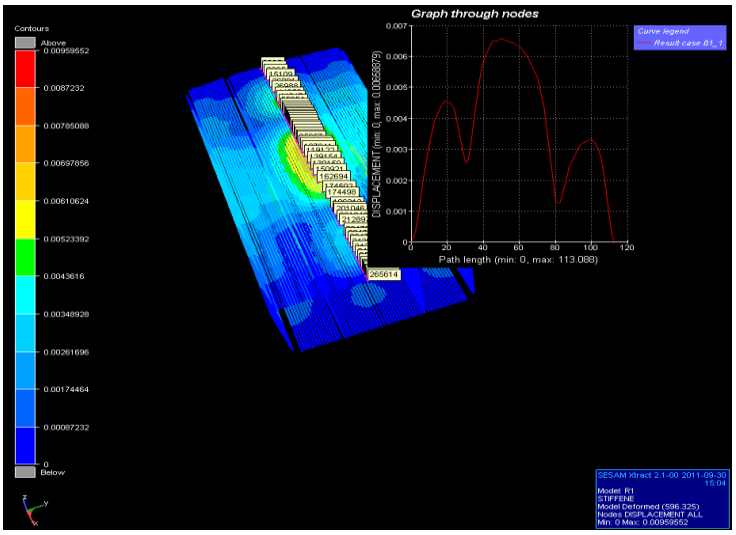

Figure.A.13 The displacement curve the deck of the tanker case A2 (sagging).

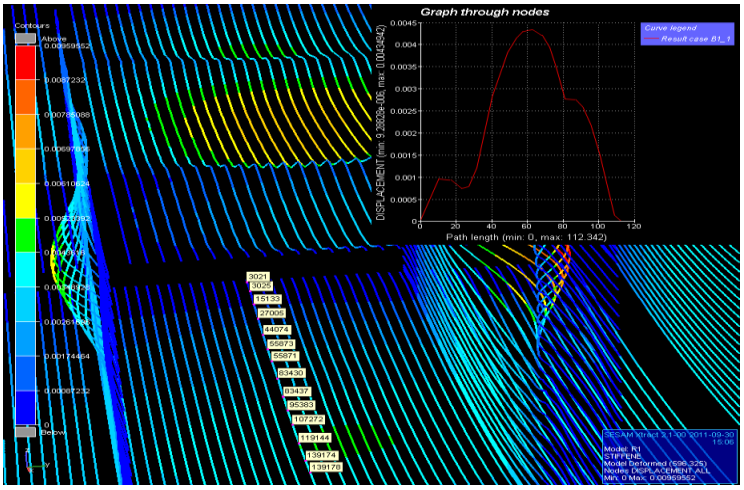

Figure.A.14 7The displacement curve the bottom of the tanker case A2 (sagging).

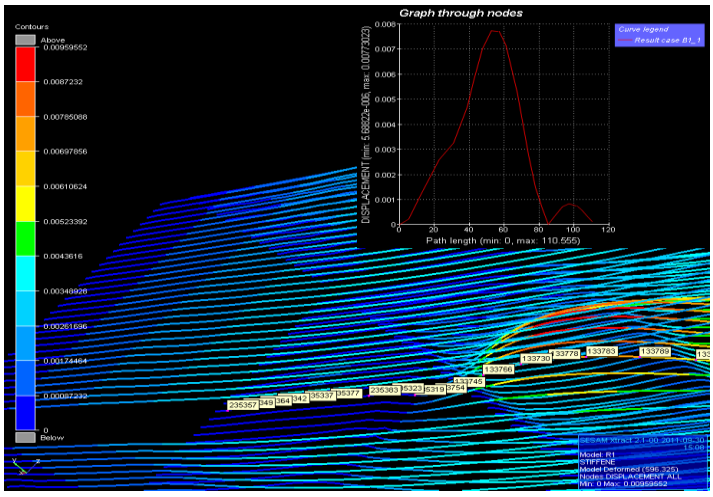

Figure.A.15 The displacement curve the long bulkhead of the tanker case A2 (sagging).

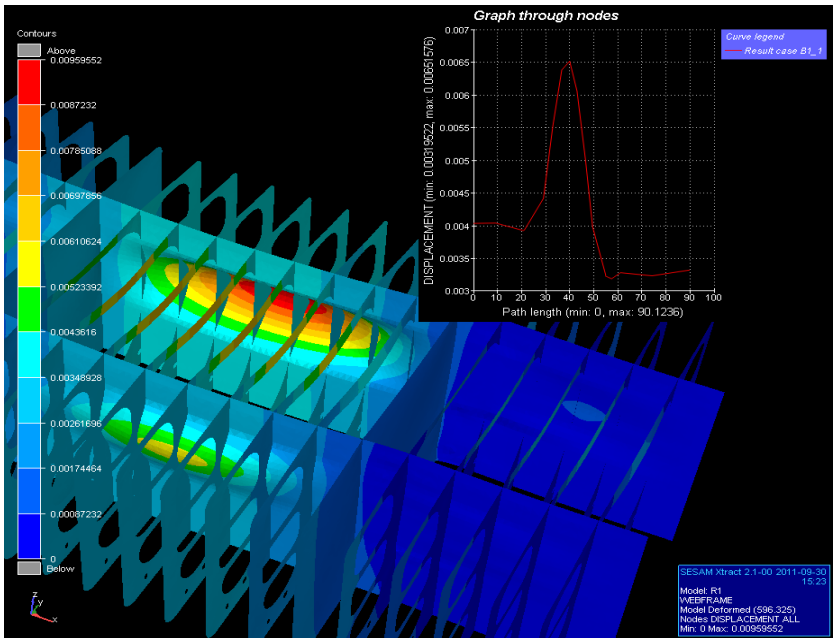

Figure.A.16 The displacement curve the Web frame of the tanker case A2 (sagging).

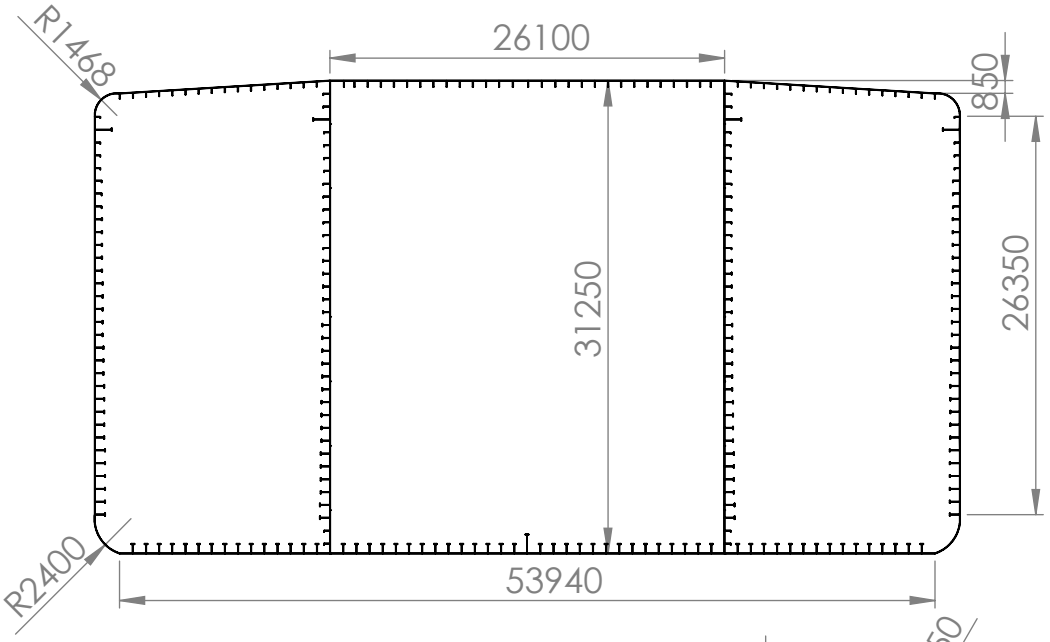

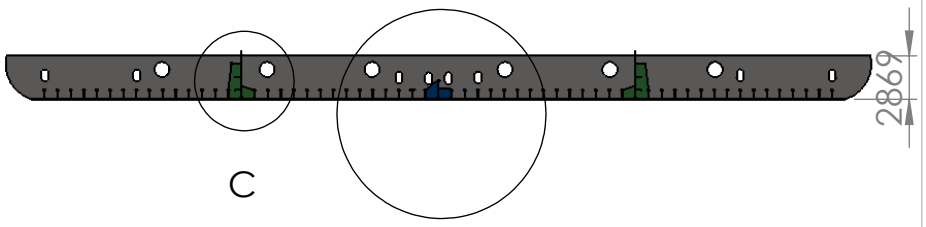

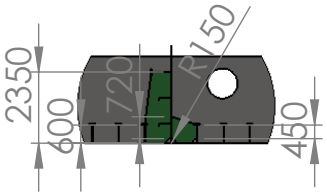

DETAIL C
SCALE 1 : 250

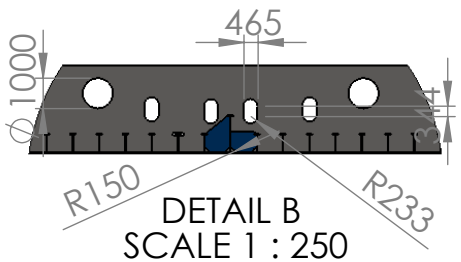

DETAIL B
SCALE 1 : 250

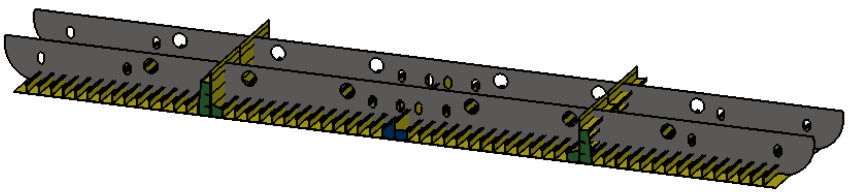

TITLE:
Amidship section details of SH VLCC

SIZE	By : DAMI RACHID	REV
SCALE: 1:500	WEIGHT:	SHEET 1 OF 1

5 4 3 2 1

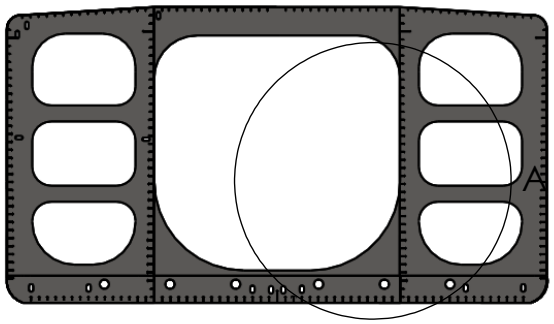

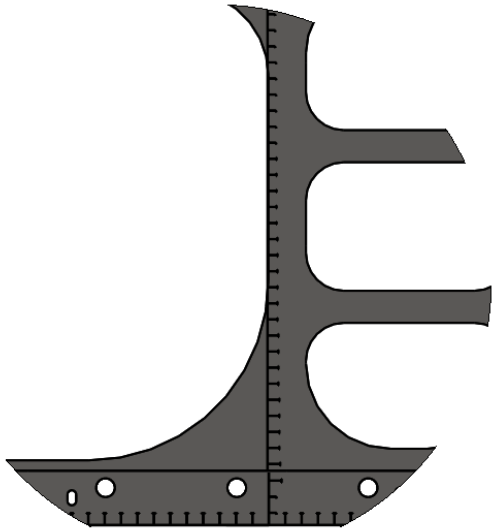

DETAIL A
SCALE 1 : 400

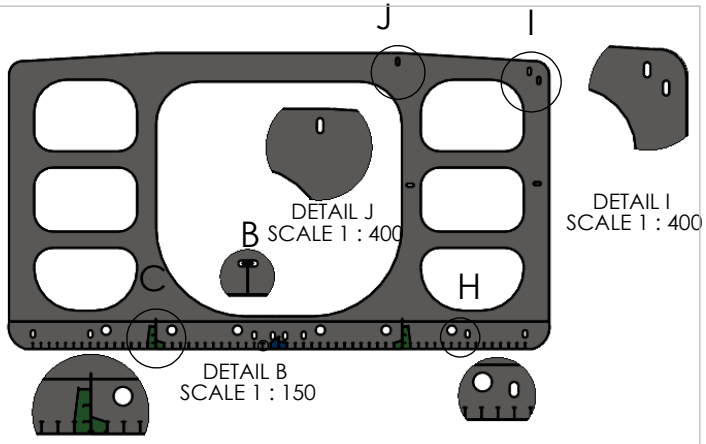

DETAIL J
SCALE 1 : 400

DETAIL I
SCALE 1 : 400

DETAIL B
SCALE 1 : 150

DETAIL C
SCALE 1 : 400

DETAIL H
SCALE 1 : 400

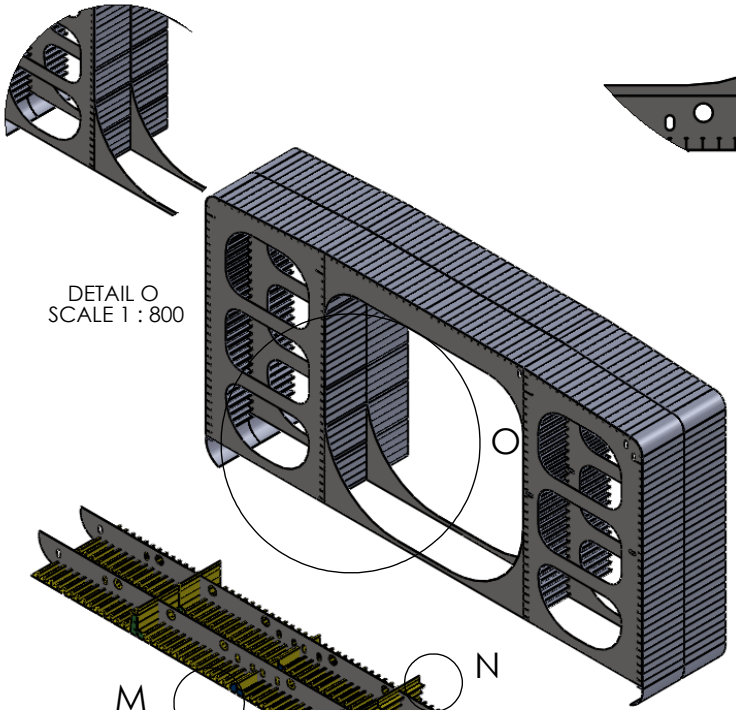

DETAIL O
SCALE 1 : 800

DETAIL M
SCALE 1 : 350

DETAIL N
SCALE 1 : 350

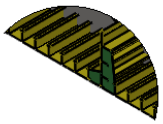

DETAIL K
SCALE 1 : 350

DATE:18/09/2011

TITLE:

Detail criticals areas

SIZE **A**

created by : DAMI RACHID

SCALE: 1:1000

SHEET 1 OF 1

5 4 3 2 1

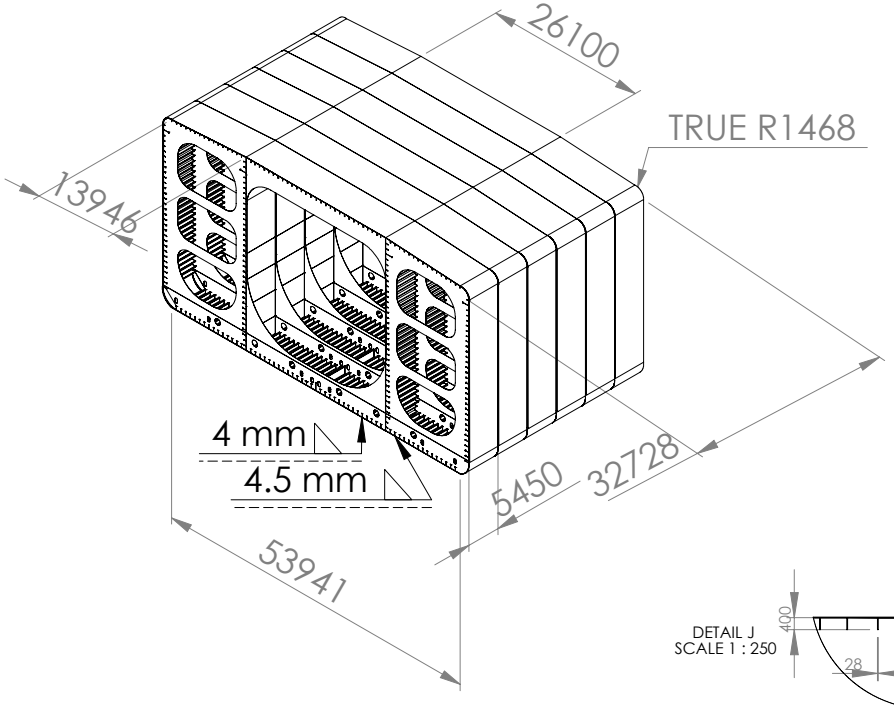

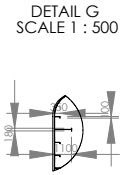
DETAIL G
SCALE 1 : 500

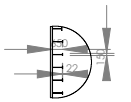
DETAIL D
SCALE 1 : 500

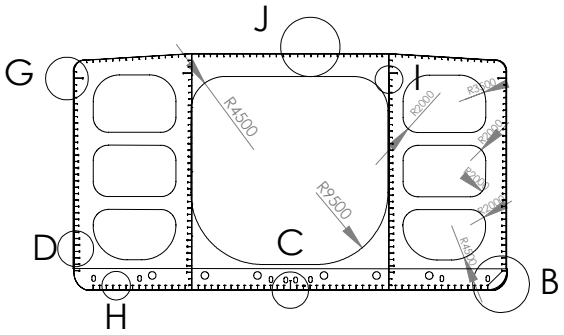

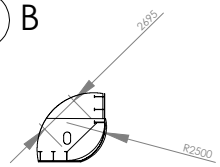

DETAIL B
SCALE 1 : 500

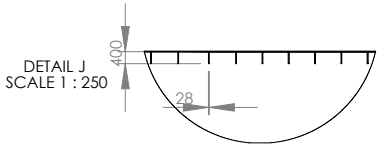

DETAIL J
SCALE 1 : 250

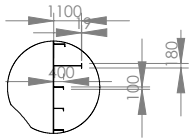

DETAIL I
SCALE 1 : 300

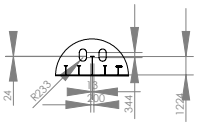
DETAIL C
SCALE 1 : 500

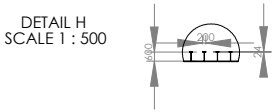

DETAIL H
SCALE 1 : 500

		MATERIAL Steel AH32	Speed:15.4Knots DWT:284497	DATE: 18/09/2011 TITLE: Hull girder detail ULS and FLS SHVLCC tanker
			Supervisor: Dr.Maciej Taczala WPUT Szcecin Poland	SIZE A Created by : DAMI RACHID REV
NEXT ASSY	USED ON	FINISH		
APPLICATION		DO NOT SCALE DRAWING		SCALE: 1:1000 SHEET 1 OF 1

5 4 3 2 1

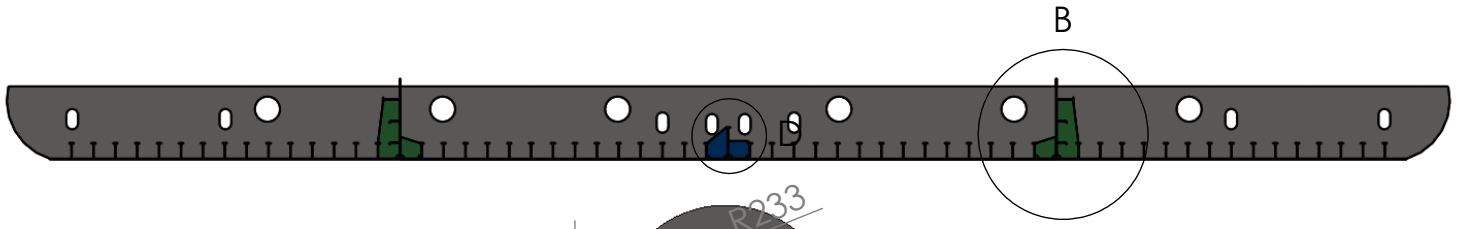

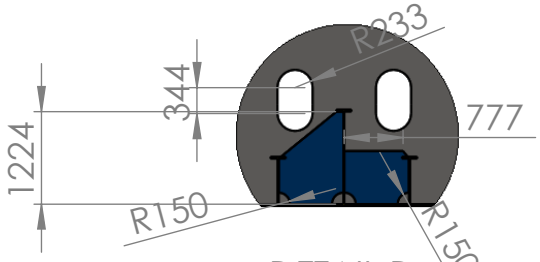

DETAIL D
SCALE 1 : 100

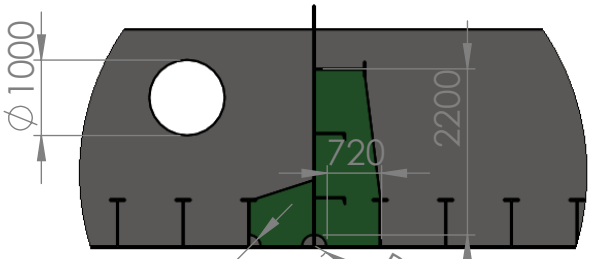

DETAIL B
SCALE 1 : 100

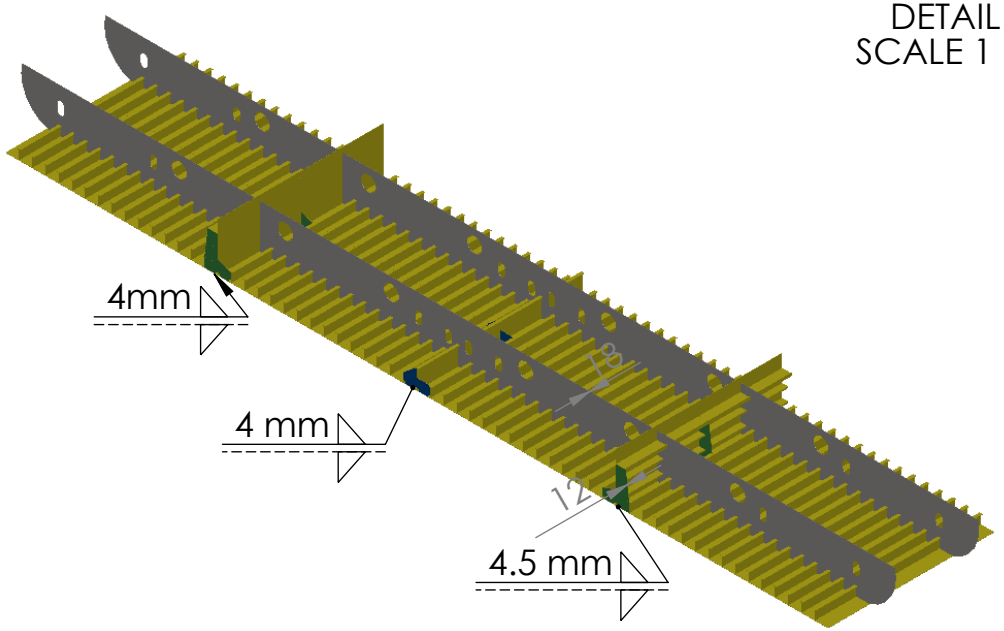

APPROVED
By DAMI RACHID at 7:37 pm, Jan 13, 2012

		UNLESS OTHERWISE SPECIFIED:	NAME
			DRAWN DAMI RACHID
			CHECKED
			ENG APPR.
			MFG APPR.
		INTERPRET GEOMETRIC TOLERANCING PER:	Q.A.
		MATERIAL : steel	COMMENTS: the details drawing explain the bracket conexion to the stiffeners plate panel and the type of welding fill the thicknes was 4 mm for oil wing ,and 45 for water ballast
NEXT ASSY	USED ON	FINISH	
APPLICATION		DO NOT SCALE DRAWING	

Date : 10/09/2011

TITLE:
Detail of the stiffened panels bottom

Developed at West Pomeranian University of Technology, Szczecin Poland

SCALE: 1:500 | SHEET 1 OF 1

5 4 3 2 1